Assessing Technology for Detection, Mitigation, and Simulation of Concussive Rugby Impacts

Danyon Stitt

A thesis presented for the degree of Master of Engineering

In Mechanical Engineering

At the University of Canterbury,

Christchurch, New Zealand

2020

Acknowledgments

I would like to acknowledge the support of my supervisors during my studies. A special thank you goes to Dr Natalia Kabaliuk for providing funding, expertise, guidance, encouragement and proofreading of this thesis. I would also like to give a special thank you to Professor Keith Alexander for funding and practical guidance throughout the early stages of the project. Last but not least, a special thankyou to Professor Nick Draper for presenting some of the results of my work at the 2020 SESNZ conference and for continued encouragement and support throughout the project.

The technical staff within the mechanical engineering workshops: Tony Doyle, Gary Cotton, and the rest of the workshop staff, Julian Phillips, and Zac Perston contributed invaluable work, advice, encouragement, and practical knowledge throughout the entire study. A special thank you goes to Bill Mohs for allowing me to use the space in the aerodynamics laboratory for various testing.

I would like to express my gratitude to my mates and my partner for the support throughout the year, without whom, this study would not have been possible. I thank my mother, father and sister for the encouragement and support throughout all my years at the university finishing my studies. None of this work would have been possible without any of these people.

Abstract

Traumatic brain injury (TBI) represents a major health issue for children and adolescents. Neuroimaging techniques in concordance with animal models have suggested the developing brain has a different response to concussive injury than the mature brain (Shrey, Griesbach et al. 2011, Choe, Babikian et al. 2012). Children exposed to TBI's can face long-term developmental, health, and quality of life difficulties extending into adulthood (Anderson, Brown et al. 2009, Jones, Prah et al. 2019). Even a single TBI may disrupt the neurological mechanisms underlying ongoing development (Graham, Rivara et al. 2014). Furthermore, the risk of sustaining repeated injuries while recovering from a prior TBI is higher for children and adolescents than adults (Harmon, Drezner et al. 2013). Other studies of contact sport players found they were up to 60% more likely to sustain injuries following a concussive injury (Nordstrom, Nordstrom et al. 2014, Burman, Lysholm et al. 2016, Cross, Kemp et al. 2016) . One study of high school athletes found those with a history of concussion (3 or more) were more likely to suffer loss of consciousness, anterograde amnesia, mental changes lasting more than 5 minutes, and were 9.3 times more likely to demonstrate abnormal markers of injury severity (Collins, Lovell et al. 2002). Since concussions can be difficult to diagnose at the time, and symptoms can take up to 24 hours to manifest (ACC 2015), many players are likely to continue playing when they should be off the field.

A study based in Canterbury shows that rates of child and youth TBI in their Christchurch cohort were also higher than previously reported and contact sport-related concussions were one of the leading injury causes among 15-25 year olds (McKinlay, Grace et al. 2008). Additionally, there is evidence to suggest that outcomes are poorer for female players who are also at a higher risk of TBI (Zuckerman, Lee et al. 2012, Harmon, Drezner et al. 2013). In spite of the acknowledged high incident rates of TBI important gaps in the research remain evident especially for junior rugby players. While protective headgear is used in a number of sports such as snow sports, cycling and American Football, until recently, rugby headgear was designed only to protect against cuts and damage to the ears rather than to mitigate against concussion. Given the complexity of interaction between brain injury and brain development, understanding, monitoring, and mitigating the impacts of sporting TBI is critical. In the past few years especially, there has been increased attention on possible concussion mitigation through using protective headgear, with World Rugby introducing new testing standards for headgear as a medical device (Rugby 2019). This allows innovative headgear designs to be tested for medical benefits such as potential concussion mitigation.

In recent years, rugby headgear has seen significantly advancement in design and technology, with N-Pro and Gamebreaker releasing their headgear onto the market, claiming head impact force reduction. These claims, though currently unconfirmed by external researchers, if true, could mark the start of a new era of concussion awareness and mitigation in rugby.

The claims made by these new headgear manufacturers about impact force reduction are currently unsubstantiated by in published literature. This study therefore aimed to investigate the impact force reduction capabilities of new headgear types compared to headgear that has been widely used and approved by World Rugby. This provided a detailed assessment of the linear acceleration reduction achieved by the most common types of rugby headgear. A new

rugby headgear testing protocol was designed providing a far more in depth analysis of headgear properties.

This headgear testing used a Hybrid III headform rigidly mounted to a drop carriage. This only allows for linear accelerations to occur. To more accurately recreate head impacts in a laboratory, a neckform should be used in conjunction with the headform. This allows for rotational motions of the head around a fixed point (representing the torso) and therefore allows rotational accelerations to be induced. Rotational kinematics have been widely theorised as more damaging to the brain tissues than linear kinematics through animal studies. The Hybrid III neck was been developed for the automotive industry based on early published data of various volunteers and cadavers (Humanetics 2019). Cadaver head and neck motions during impacts differ significantly from that of a living human. Additionally, the data used to develop these necks is outdated and has questionable reliability. Therefore, a basic validation model has been developed based on more recent published data for living humans. In addition, a new neckform was designed based on the Hybrid III design. This was assessed using the newly developed validation criteria.

The ability to accurately simulate sporting head impacts in the laboratory depends largely on how well impact conditions can be measured and reported during gameplay. Wearable sensor technology provides real time information about head impacts on the field. Some of these systems however demonstrated high error rates both in the laboratory and on the field demonstrating the need for validation (McCuen, Svaldi et al. 2015, Nevins, Smith et al. 2015, Schussler, Stark et al. 2017, Tyson, Duma et al. 2018). With a new instrumented mouthguards on the market showing promising preliminary results, a validation study was carried out in a controlled laboratory environment to assess the accuracy of the HitIQ Nexus A9 instrumented mouthguard. This was chosen as it displayed promising preliminary results for accuracy and detection rate. A new impact method was developed to recreate impact conditions previously measured on the field.

Publications arising from this research

Journal papers

1. Draper, N., **Stitt, D**., Alexander, K., Kabaliuk, N., Potential of soft shelled rugby headgear to reduce linear impact accelerations. Sports Engineering. (*Accepted for review, re-submitted with reviewer comments addressed*)
2. **Stitt, D**., Draper, N., Kabaliuk, N., Laboratory validation of instrumented mouthguard for use in sport. Journal of Biomechanics. (*Under review*)

Conference presentations

1. **Stitt, D**., Draper, N., Kabaliuk, N., Laboratory validation of instrumented mouthguard for use in sport. SESNZ 2020 conference. *Presented By Danyon Stitt (Won the Best Student Presentation Award)*.
2. Draper, N., **Stitt, D**., Alexander, K., Kabaliuk, N., Potential of soft shelled rugby headgear to reduce linear impact accelerations. Should Rugby be restricted for Children under 12? SOBI symposium, SESNZ 2020 conference. *Presented By Nick Draper*.

Contents

Acknowledgments 3
Abstract 4
Publications arising from this research 6
Journal papers 6
Conference presentations 6
List of figures 9
1 Introduction 11
1.1 Mild Traumatic Brain Injury (mTBI) in contact sports 11
1.2 Concussions in rugby 13
1.3 Impact testing standards 15
1.4 Injury metrics 16
1.5 The human and Hybrid III neck 19
1.6 Response of the human and Hybrid III head and neck to accelerations 21
2 Experimental investigation into the potential of soft-shelled rugby headgear to reduce linear impact forces 26
2.1 Rugby headgear 26
2.2 Drop test rig 27
2.3 Headgear drop testing methods 29
2.4 Headgear drop testing results 31
2.4.1 Composite behaviour 31
2.4.2 Location specific behaviour 32
2.5 Discussion 34
2.6 Conclusion 37
3 Developing a biofidelic alternative to the Hybrid III ATD neck 38
3.1 Development of a neckform validation criteria 38
3.2 Neckform impact testing method 41
3.3 Data collection and processing 43
3.4 Neck design 46
3.4.1 First design 46
3.4.2 Improved neckform design 48
3.4.3 Further neckform design modifications 50
3.4.4 Final neckform design 51
3.5 Neckform impact test results 52
3.6 Discussion 56
3.6.1 Neck performance 56

3.6.2 Alternative solutions 58
3.7 Conclusion 58
4 Laboratory validation of instrumented mouthguard for use in sport 59
4.1 Mouthguard drop testing method 60
4.2 Data acquisition 62
4.3 Post processing 63
4.4 Statistical analysis 64
4.5 Mouthguard accuracy 64
4.6 Discussion 68
4.7 Conclusion 70
5 Conclusions and Future Work 71
6 References 72

List of figures

Figure 1 Impact sites specified in the World Rugby standards for impact testing of headgear 15
Figure 2 Human cervical neck showing the bone structure on the left (Ornstein 2019) and the ligament structure on the right (Barnes 2020) 20
Figure 3 Motions of the head and neck (LeBlanc 2016) 20
Figure 4 The Hybrid III neck showing the steel cable that goes through the centre of the neck and the upper instrumentation mounting (Foster, Kortge et al. 1977) 21
Figure 5 Two pivot linkage mechanism used for relative head motion description, taken from (Wismans, van Oorschot et al. 1986) 22
Figure 6: Response corridors for the acceleration input, accelerations and rotation angles for 9 volunteer experiments taken from (Thunnissen, Wismans et al. 1995) 23
Figure 7: The applied T1 acceleration and the frontal H3 response (solid line) compared with proposed frontal performance requirements based on experimental data (dotted line) taken from (Thunnissen, Wismans et al. 1995) 23
Figure 8: Impact behaviour of the hybrid III neck compared to the BioRID and human corridor taken from (Walsh, Kendall et al. 2018) 24
Figure 9 Drop test rig used in this study 28
Figure 10 headgear included in the testing, from top left to bottom right: CCC Ventilator, Kukri, 2nd Skull, Gamebreaker blue, Gamebreaker Black, Npro 30
Figure 11 Impact locations, and locations on the MEP pad. From top left to bottom right: rear boss, rear, side, front, front boss 31
Figure 12 Mean (SD) peak linear acceleration for each headgear unit in each orientation at A. 238mm, B. 300mm, C. 610mm and D. 912mm 33
Figure 13 Mean (SD) max HIC scores for all headgear units in each orientation from drop heights of A. 238mm, B. 300mm, C. 610mm and D. 912mm 33
Figure 13: test setup showing head and neck orientation for flexion testing (top left) and extension testing (top right). Pendulum dimensions and requirements for the neck validation (bottom), taken from (Administration 1997) 38
Figure 14 Humanetics Hybrid III T1 accelerations compared to those used in the literature (Ewing, Thomas et al. 1969, Ewing, Thomas et al. 1978, Thunnissen, Wismans et al. 1995) (Wismans, van Oorschot et al. 1986, Wismans, Philippens et al. 1987, Van den Kroonenberg, Philippens et al. 1998) 39
Figure 15 A - D: Validation corridors created using the published data (Ewing, Thomas et al. 1969, Ewing, Thomas et al. 1978, Thunnissen, Wismans et al. 1995) (Wismans, van Oorschot et al. 1986, Wismans, Philippens et al. 1987, Van den Kroonenberg, Philippens et al. 1998) 41
Figure 16 Peak accelerations at the base of the neck for the impact velocities measured 42
Figure 17 impact surface for the pendulum showing the alternating foam slabs with those on the left associated with testing Round 1, and those on the right for Round 2 43
Figure 18 tracking dots on the base of the neck (T1) showing the horizontal velocity of each point .. 44
Figure 19 typical angle used for evaluation of the rotations of the head and neck 46
Figure 20: molding process for the individual pieces of the neck rubber (left). Complete first attempt of the neck (right) 47
Figure 21: Video image of the validation carried out on the first neck showing the separation of the rubber and aluminium along the back of the neck (left). Second attempt at validating the neck showing failure of the neck internal cable and separation of the discs (right) 48
Figure 22: single layer of the mold showing the asymmetrical shape. Complete mold showing the inside cavity to be cast with urethane rubber (right) 49

Figure 23 Second design of the neck showing the failure during rear end impacts 50
Figure 24 Attempt at casting the silicone neck 51
Figure 25 maximum rotation angle of the neck for flexion (left) and extension (right) 52
Figure 26 Peak head rotation angle with the first round of testing (round 1) shown in red and the second shown in yellow (round 2) 53
Figure 27 Peak neck rotation angle with the first round of testing shown in red and the second shown in yellow 53
Figure 28 Peak rotational velocity of the head round of testing shown in red and the second shown in yellow 54
Figure 29 Peak rotational acceleration of the head round of testing shown in red and the second shown in yellow 54
Figure 30 acceleration of the closest matching impact to the Humanetics standard compared to the requirements set in the standard 55
Figure 31 Head rotation for the two closest matching impact to the Humanetics standard compared to the requirements set in the standard 56
Figure 32 Peak accelerations of the pendulum during testing compared to those reported in past studies and those in the Humanetics validation standard (Ewing, Thomas et al. 1969, Ewing, Thomas et al. 1978, Thunnissen, Wismans et al. 1995) (Wismans, van Oorschot et al. 1986, Wismans, Philippens et al. 1987, Van den Kroonenberg, Philippens et al. 1998) 56
Figure 33: Impact locations from top left to bottom right: Front/Forehead, Front Boss, Side, Rear, and Rear Boss. The mouthguard and dentition are both shown rigidly fixed to the upper jaw of the ATD headform 61
Figure 34: HitIQ headform with a rigidly mounted top jaw for the mouthguard to attach to through testing 61
Figure 35: Time periods considered for RMS calculations with impact (A and C) defining a 20% of the peak threshold either side of the peak. Full (B and D) defines the same time duration for both based on linear and rotational 20% thresholds 64
Figure 36: Correlation (A and C) and Bland-Altman (D and D) plots for PLA and PRA 65
Figure 37: Normalised RMS values calculated over two different time periods for both linear and rotational acceleration 66
Figure 38: Probability of any single impact producing a NRMS error based on both rms durations used. The red line shows the mean NRMS error for each type of rms calculation 67
Figure 39: each impact in the 20g 15ms front boss scenario with the outlier marked 67

1 Introduction

1.1 Mild Traumatic Brain Injury (mTBI) in contact sports

Concussion is an inherent risk of participating in contact, combat or collision sports. Some of the most studied sports include American Football, Ice hockey, Rugby union and boxing. All attract high numbers of participants with 8.5 million rugby players internationally (Rugby 2017), 7.3 million participating in combat sports in the U.S and U.K (Lock 2018, Lange 2019), over 5 million American football players in the U.S (Lock 2020), and 1.5 million playing ice hockey globally (Gough 2019). Given the high intensity of these sports, injuries are common, with concussions being one of the most common. One Study estimates as many as 300,000 sports related concussions occur annually in the U.S alone (Sosin, Sniezek et al. 1996). A large number of researchers have investigated the incidence rates of concussion, and report varied rates of concussive injury with 0.5 - 4.35/1000 athlete exposures (AE) in American football (Powell and Barber-Foss 1999, Schulz, Marshall et al. 2004, Gessel, Fields et al. 2007, Lincoln, Caswell et al. 2011, Kontos, Elbin et al. 2013, Willigenburg, Borchers et al. 2016), 0.4 - 46/1000 AE in rugby (Schick, Molloy et al. 2008, Moore, Ranson et al. 2015, Ma, Lopez et al. 2016, Fuller, Taylor et al. 2017, Hecimovich and King 2017, Silver, Brown et al. 2018, King, Hume et al. 2019), 0.2 - 14.93/1000 AE in ice hockey (Schick and Meeuwisse 2003, Agel, Dick et al. 2007, Agel, Dompier et al. 2007, Rishiraj, Lloyd-Smith et al. 2009), and 11.4 - 250.6/1000 AE for boxing and kickboxing (Porter and O'Brien 1996, Zazryn, Finch et al. 2003, Zazryn, Finch et al. 2003, Bledsoe, Li et al. 2005, Buse and Wood 2006, Estwanik, Boitano et al. 2016). This range encompasses both male and female athletes of all levels of play (youth, high school, collegiate, professional).

When the head experiences impact accelerations, the difference in density and mechanical properties of the various brain tissues causes parts of the brain to accelerate at different rates, causing stresses and strains to develop within the brain tissue (Graham, Rivara et al. 2014). This was shown to lead to neuronal and axonal damage (Graham, Rivara et al. 2014). The brain can handle some stresses and deformations without injury, however once a certain threshold is surpassed, trauma occurs which can elicit a variety of biological responses (Graham, Rivara et al. 2014). These may be structural (torn vessels and axons) or functional (changes in blood flow or neurological status), and may be immediate or delayed (Graham, Rivara et al. 2014). This gives rise to the short term symptoms of concussion such as loss of balance and memory (Table 1). Concussions and other head injuries can result in changes to the integrity of gray and white matter (Graham, Rivara et al. 2014).

The developing brain is more susceptible to concussion than the adult brain and may require more time to recover (Baillargeon, Lassonde et al. 2012). Impacts over 10g that do not result in a participant presenting with acute symptoms of concussion, have been identified to be sub-concussive impacts (Bailes, Petraglia et al. 2013). Repetitive sub-concussive impacts may have negative long-term effects (Spiotta, Shin et al. 2011). It has been suggested that concussions, or combinations of concussions and sub-concussive head impacts, may result in long-term conditions such as chronic traumatic encephalopathy (Gavett, Stern et al. 2011), mild cognitive impairment (Guskiewicz, Marshall et al. 2005) and depression (Guskiewicz,

Marshall et al. 2007). The exact mechanisms resulting in these conditions is not yet fully understood.

Table 1	Symptoms of a concussive injury	
Physical	**Emotional**	**Mental**
Headache	Irritability	Short term memory difficulty
Nausea/vomiting	Restlessness	Long term memory difficulty
Fatigue	Anxiety	Confusion
Difficulty sleeping	Depression	Slowed processing
	Aggression	Feeling of "Fogginess"
	Lower stress tolerance	Difficulty concentrating

Most concussions go unreported until symptoms start to show, which can be up to a few days (ACC 2015), meaning that a large number of concussions are not identified until 24 hours or more after the injury (Duhaime, Beckwith et al. 2012, McCrory, Meeuwisse et al. 2013), leaving a large amount of time for subsequent head impacts to occur. Additionally, concussive head impacts often do not result in a loss of consciousness, therefore further complicating the diagnosis of a concussive injury on field (ACC 2015). It has been reported that approximately 90% of concussions do not result in a loss of consciousness (Gardner, Iverson et al. 2015). Because of this, the concussion underreporting rates are estimated to be as high as 50%–90% (Gardner, Iverson et al. 2015). For 80 to 90 percent of cases, the individuals' symptoms resolve within 2 weeks (McClincy, Lovell et al. 2006, McCrea, Guskiewicz et al. 2009, Makdissi, Darby et al. 2010, McCrea, Guskiewicz et al. 2013, McCrory, Meeuwisse et al. 2013) although recovery within that period appears to be somewhat slower for adolescents ages 13 years through high school than for college-age athletes (Field, Collins et al. 2003, McClincy, Lovell et al. 2006, Eisenberg, Andrea et al. 2013, Williams, Puetz et al. 2015).

In an ideal case, assessment of an injured player is facilitated by the presence of a certified athletic trainer, team physician, or other health care provider on the side line, however, the vast majority of young athletes practice and play in circumstances where trained personnel are not immediately available. There are currently guidelines imposed on sporting organisations in New Zealand where the players thought to have sustained a concussive injury are removed from gameplay immediately and monitored for typical symptoms (Table 1) (ACC 2015). Additionally, there are various sideline neurocognitive tests which can be performed, however, for most people these are not well known and can be complex. Removal of a player from the game relies upon the player accurately reporting their immediate symptoms, which hinders the effectiveness, as there is a tendency for athletes to underreport their own symptoms (McCrea, Hammeke et al. 2004, Dziemianowicz, Kirschen et al. 2012, Anderson, Gittelman et al. 2016). Studies of high school football players found that 62% of players would continue play after a concussion, with 41% of those players stating they did not want to be removed from the game, and 66% stating they did not think their symptoms were serious enough, therefore did not report their injury (McCrea, Hammeke et al. 2004, Anderson, Gittelman et al. 2016). One epidemiological study of reported traumatic brain injury (TBI) in the US estimated an economic burden of $60 billion annually (Daneshvar, Nowinski et al.

2011). While in New Zealand this number sits between $2 million and $19 million annually (Gaffaney 2014, ACC 2015).

1.2 Concussions in rugby

Rugby Union is a popular contact sport played by approximately 8.5 million people in over 121 countries worldwide (Rugby 2017). Due to the high intensity of the game, some have given rugby the title of a "collision sport" (P McLellan 2013, King, Hume et al. 2017) . Studies conducted into the force experienced by the head during gameplay found average peak linear accelerations (PLA, measured in g force) of 10-38g (P McLellan 2013, King, Hume et al. 2015, King, Hume et al. 2016, King, Hume et al. 2017, Hecimovich, King et al. 2018, King, Hume et al. 2018), with some reaching PLA values of up to 103-165g (Frechede and McIntosh 2009, King, Hume et al. 2015, Hecimovich, King et al. 2018, King, Hume et al. 2018), and a significant number being greater than 80g (King, Hume et al. 2018). Given rugby's high reported impact forces, players are at a much higher risk of injury compared to non-contact sports (Hume, Theadom et al. 2017). Reports indicate that a player receives on average 14-52 impacts to the head over 10g per game (King, Hume et al. 2015, King, Hume et al. 2017, Hecimovich, King et al. 2018). One of the most common injuries in rugby is concussion (Marshall and Spencer 2001, Hendricks, Jordaan et al. 2012, Gardner, Iverson et al. 2015, King, Hume et al. 2019) with incidence rates ranging from 0.4 – 46/1000 match hours (Collins, Micheli et al. 2008, Schick, Molloy et al. 2008, Moore, Ranson et al. 2015, Ma, Lopez et al. 2016, Fuller, Taylor et al. 2017, Hecimovich and King 2017, Silver, Brown et al. 2018, King, Hume et al. 2019).

Only a few studies could be found which investigate the head impacts experienced by youth rugby players. In a junior level rugby league team in New Zealand with a mix of boys and girls, the peak linear acceleration ranged from 10g to 123g (mean 22g, median 16g). Each player received a mean of 13 impacts above 10g per match (King, Hume et al. 2017). Another study found that among 7-17 year olds, the most common area of injury was the head (20.2%) (Sabesan, Steffes et al. 2016), and a third found Junior players had median PLA of 15.1g whereas senior players had median PLA of 15.7g (Hecimovich, King et al. 2018).

A US study found the majority (59.4%) of all rugby injuries occurred in 18-23 year olds and the most common head injury were concussions (40%). The head accounted for 18.5% of all injuries for this cohort (Sabesan, Steffes et al. 2016). For varsity aged rugby teams in the US concussions accounted for 24.6% of all injuries and was responsible for 25.3% of all days lost from participation. Concussion incidence rates were 3.8/1000 AE overall. However, this rate was found to be 11.1/1000 AE for match play, and 1.5/1000 AE for training (Marshall and Spencer 2001). Other studies of senior amateur rugby union (age range 22 ± 4 years old) experienced an average impact PLA of 22.2 ± 16.2g with an average duration of 12ms. These participants had an average of 77 ± 42 head impacts greater than 10g per game (King, Hume et al. 2015). In senior amateur rugby league, players (aged 23.3 ± 4.3 years old) experienced a mean of 52 ± 79 head impacts per player per game. The median PLA of these was 14g (mean of 19g) (King, Hume et al. 2017). In community Australian football, with participants all over 18 years old, concussions made up 3.3% of all injuries. The incidence rate in games was 1.2/1000 participation hours (Fortington, Twomey et al. 2015).

Most of the literature on injury incidence pertains to professional level rugby. A study of the Welsh national rugby team gave a concussion rate of 13.8/1000 match hours with concussion covering 79% of all head injuries (Moore, Ranson et al. 2015). For professional rugby league, 13-17% of players received concussions per season and 16% were repeat injuries. For every 1000 player hours, there were 9.84 concussions in first grade, 7.87 in reserve grade and 5.90 in age-group competitions (Under 21s and Under 19s). The highest rate was seen when an Under 19 team competed, for one season, in a non-age-restricted tournament, playing against older players, yielding a concussion incidence of 18.36/1000 player hours (Hinton-Bayre, Geffen et al. 2004). In Australian football, players received an average of 60 ± 36 impacts per season. (Hecimovich, King et al. 2018). A study of all teams in the 2003 Rugby World Cup (RWC) found that concussion only accounted for 2% of all injuries (four concussions), which is the lowest ever reported in any rugby data. Also, no player missed more than 1 game because of concussion, leading the researchers to the opinion that concussion may be underreported due to concerns by players and team management about the rugby laws. The three week return to play rule in a well monitored tournament may encourage team management, or informed players, to misreport injuries (Best, McIntosh et al. 2005).

In senior women's rugby league (age range 29.2 ± 7.8), the median impact force recorded was 15g (95^{th} percentile was 41g). These impacts lasted 12.4 ± 8ms and each player received average of 14 ± 12 head impacts per game. There was an overall concussion incidence rate of 19.3/1000 match hours (King, Hume et al. 2018). Women were found to be more frequently injured in the head than men were (23% vs 15.9%) (Sabesan, Steffes et al. 2016). At the women's rugby 7's in America (age 23.6 ± 5.2), concussions occurred at a rate of 5.8/1000 player hours for both elite and non-elite. Concussion was the second most common recurrent injury at 3.5/1000 player hours and led to a mean of 52 days absent (Ma, Lopez et al. 2016). In a study of collegiate rugby union in the US, the head and face was the most commonly injured body site for both men and women however this study found men to have higher game incidence of concussion than women (2.16 vs 1.58/1000 player hours), which was lower than elite rugby union (4.4/1000 PGH) (Kerr, Curtis et al. 2008).

Studies reveal that 42-48% of impacts occur to the side of the head, making it the most frequently impacted area of the head (King, Hume et al. 2017, King, Hume et al. 2017). This was followed by the front, then the back of the head. Little has been reported regarding the concussive rate for each impact location. A club rugby study found that up to 33% of concussions were attributed to play that was outside of game rules (Fortington, Twomey et al. 2015). Injuries were found to be more likely to occur during match play than training, of which most were tackle related (Moore, Ranson et al. 2015). The most common mechanism of injury was a high head tackle, or a players head impacting the ground (Hinton-Bayre, Geffen et al. 2004). Concussive injuries were most frequently recognised when the player remained motionless following a tackle (49%). The second most common method of detecting concussion (23%) occurred only after the injured player voluntarily left the field reporting symptoms, despite the presence of certified athletic trainers and medical staff (Hinton-Bayre, Geffen et al. 2004). No statistical difference was found between concussion incidence of the

forwards and backs and no difference in incidence rate was found between the two halves (Hinton-Bayre, Geffen et al. 2004).

An economic study in New Zealand found that Maori recorded significantly more injury claims than any other ethnic group, accounting for 39.8% of all claims and 43.5% of injury entitlement costs. The incidence and costs of concussions is a concern. It was identified that the mean cost of a concussion over the same reporting period was $25,347. The mean cost per concussion over the duration of this study varied by ethnic group. New Zealand European's recorded the lowest mean cost of $2,113 per concussion while New Zealand Maori recorded the highest mean cost per concussion of $38,118, however the reasons for this are still unknown (King, Hume et al. 2009).

1.3 Impact testing standards

The effects of mild to severe brain injury have been investigated for many years (High Jr, Sander et al. 2005, Scurlock and Andersen 2005, Sanchez and Burridge 2007). The specific mechanisms leading to mild traumatic brain injury (mTBI), or concussions, is still not fully understood.

In 1998, the standard for testing rugby headgear was developed by world rugby (Rugby 2014). This standard specifies 3 separate locations for impact testing (Figure 1), with the crown being impacted once, and both forehead and temple areas being impacted twice. The drop height is required to be such that the energy level of the impact is 13.8J, which is defined in the standard as a 4.7kg mass falling from 300mm. This drop height can be adjusted for different mass headforms. The anvil is to be a flat steel surface with diameter 130mm. When tested this way the peak linear acceleration of the impacts shall not be less than 200g, but no more than 550g.

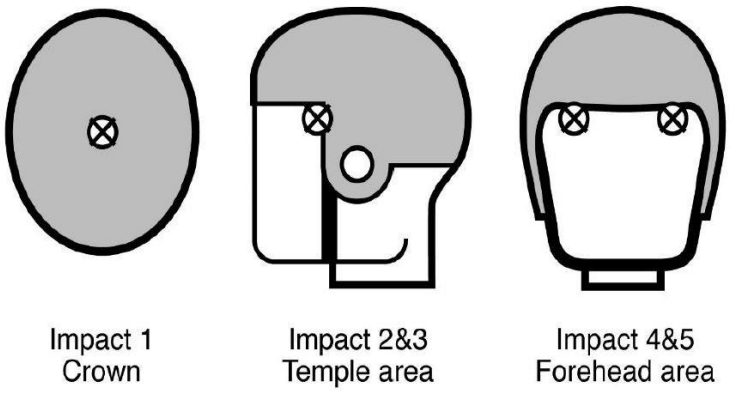

Figure 1 Impact sites specified in the World Rugby standards for impact testing of headgear

This differs from the requirements given by the NOCSAE standard (NOCSAE 2017). This standard pertains more to American football helmets than to the soft shelled rugby headgear. There are 6 impact locations defined in the standard shown in Figure 2. These are: front (forehead), side of the head, front boss (oblique frontal), rear boss (oblique rear), rear and top of the head. For each impact location there are 4 different impact velocities: 3.46, 4.23, 4.88 and 5.46m/s. The requirement of this standard is that the peak severity index (Gadd

Severity Index) shall not exceed 1200 SI, and no impact at 3.46m/s shall exceed 300 SI. It is worth noting that NOCSAE have several different standards for impact testing various headgear, some of which specify drop test rigs, and some use linear impactors. Across all standards however, they all suggest the same few impact velocities be used for testing, across the same impact locations.

Now World Rugby has developed trial processes allowing headgear with proven medical benefits to be used in gameplay, despite breaking the previous material density regulations (Rugby 2019). The 200g limits for impact attenuation defined in the previous standard (Rugby 2014) do not apply for "headgear as a medical device", however all other specifications of regulation 12 must be met. Testing is carried out on the same impact locations (Figure 1), but at a range of drop heights: 0.15, 0.3, 0.45, 0.6, and 0.9m (Rugby 2019). At present, N-Pro is the only headgear to gain WR approval through this change (Rugby 2019). This headgear trial is a very recent development, and as such, many of the past studies into headgear impact attenuation use different methods from each other making comparison difficult.

The NOCSAE and World Rugby standards use different headforms for the impacts. World Rugby specify a metal headform conforming to EN960 (Rugby 2019), whilst NOCSAE specify their own headform be used in conjunction with a Hybrid III 50th percentile neck from Humanetics (NOCSAE 2017).

1.4 Injury metrics

Peak accelerations are the commonly reported measures of the intensity of an impact however, there are several injury tolerance criteria that associate the linear and rotational head acceleration with the degree of head injury severity. The Wayne State Tolerance Curve was developed in the early 1960's to quantify head injury in automotive impacts (Namjoshi, Good et al. 2013). It defines a peak linear acceleration versus impact duration curve, with the onset of serious skull injury lying on the curve boundary (Ransohoff 1970). This injury criteria pertains only to skull fracture rather than brain injury.

The Gadd severity Index (GSI) was an expansion of this, developed using cadaveric and animal data to define limits for tolerance to severe brain injury (Gadd 1966). This equation integrates the acceleration versus time curve for the whole impact duration.

$$GSI = \int_0^T a(t)^{2.5} dt$$

One of the most used methods for assessing the likelihood and severity of brain trauma is the Head Injury Criterion (HIC), used to focus the severity index on the part of the impact most likely to be relevant to the risk of injury to the brain (Versace 1971). This is achieved by averaging the integration of the resultant acceleration vs. time curve over whatever time interval yields the maximum value of HIC. In 1998, the NHTSA introduced HIC_{15}, where t_2 and t_1 are no more than 15 ms apart and the maximum HIC_{15} (hereon referred to as HIC) is not to exceed 700 (Rolf Eppinger, Emily Sun et al. 1998). It was assumed that serious brain and skull injury would result beyond this limit.

$$HIC = (t_2 - t_1)\left[\frac{1}{t_2 - t_1}\int_{t_1}^{t_2} a(t)dt\right]^{2.5}$$

A numerical study by King et al. (King, Yang et al. 2003), estimated that a mild Traumatic Brain Injury (mTBI) tolerance for the HIC, associated with a 25, 50 and 75% likelihood of a concussion to occur, had HIC values of 136, 235 and 333, respectively. Other studies have estimated HIC thresholds of 151, 240 and 369 for a 25, 50 and 80% probability of sustaining a concussion, respectively (King, Hume et al. 2016). It should be noted that these are based on FE analysis of the brain during impact, and these figures have never been validated.

There are a few failings of both the GSI and HIC metrics. They only incorporate linear acceleration and are not specific to impact direction.

Holbourn originally found that the human brain is sensitive to rotational motion in (Holbourn 1943), where shear strain patterns in 2D gel models were used to claim that translational acceleration is not injurious, but rotational accelerations are, due to the incompressibility of the brain tissue. Various animal studies have been performed over the years with different species subjected to linear and rotational head accelerations to see which is more damaging. Generalli et al found squirrel monkeys became concussed only when subjected to purely rotational motion, but not purely translational motion (Gennarelli, Thibault et al. 1972). A seminal study by Denny-Brown and Russell found transient loss of consciousness was induced only when the head was free to rotate but not when the same forces were applied to a fixed head (Denny-Brown and Russell 1941). Further from this, there have been many investigations into the behaviour of the animal (primate or rat) brain in response to rotational accelerations (Gennarelli, Thibault et al. 1982, Gennarelli 1983, Margulies and Thibault 1992, Davidsson, Angeria et al. 2009). A review of non-human primate studies found that loss of consciousness and coma were rarely obtained with impacts causing primarily linear accelerations, but occurred frequently with much lower impact thresholds when the head was free to rotate (rotational accelerations). The same was found for diffuse axonal injury (Cullen, Harris et al. 2016). The same study also suggested that using a porcine model for concussion will produce results that scale to the human brain far more accurately.

These studies have been used to attempt to develop injury risk criteria based on the rotational accelerations, however their reliability is limited due to the differences between the primate, animal, and human brain. Despite these limitations, the results of such studies led to the development of predictive metrics that included rotational head acceleration. In 1986, the Generalised Acceleration Model for Brain Injury Threshold (GAMBIT) was developed by Newnham (Newman 1986), and summed up in one final equation:

$$G = \frac{a_m}{250} + \frac{\alpha_m}{10000} \leq 1$$

Where a_m and α_m are the resultant linear and rotational acceleration peak values respectively. The equation has limits of 0 and 1. This was based on cadaver, monkey, and piglet head impacts, however due to the lack of data, the author concluded the function could not be fully validated with any confidence. Therefore injury thresholds have not been established. Much later, the head impact power was developed which incorporated both linear and

rotational accelerations (Newman, Shewchenko et al. 2000). This has not been as widely employed as HIC as the coefficients must be set to the mass and mass moments of inertia of the head itself. Since these coefficients are not known for each individuals head, it can be difficult to employ in a realistic setting. This, however can be generalised for the population in question. In this particular instance the coefficients have been set to those of the Humanetics Hybrid III 50th percentile male headform. The equation put forward by Newman et al is:

$$HIP = 4.5a_x \int a_x dt + 4.5a_y \int a_y dt + 4.5a_z \int a_z dt + 0.016\alpha_x \int \alpha_x dt + 0.024\alpha_y \int \alpha_y dt + 0.022\alpha_z \int \alpha_z dt$$

Where a (with axial components a_x, a_y, a_z) is the linear acceleration (m/s^2) and α (with axial components α_x, α_y, α_z) is the rotational acceleration (rad/s^2).

Further development of these injury risk functions led to the development of another metric. The Principle Component Score (PCS) is unique as it combines both linear and rotational kinematics, along with the HIC and GSI scores for the impact. This was developed in 2008 by Greenwald et al (Greenwald, Gwin et al. 2008) and found relatively high correlation to data on injurious impacts from American football. The equation is:

$$PCS = 10((0.4718sGSI + 0.4742sHIC + 0.4336sLIN + 0.2164sROT) + 2)$$

Where sX = (X – mean(X))/(SD(X)) (for X = GSI, HIC, etc. SD is the standard deviation), LIN = peak linear acceleration, ROT = peak rotational acceleration, HIC = HIC score, and GSI = GSI score. This was demonstrated to have a low false positive rate when compared to impacts measured from the Head Impact Telemetry (HIT) system in American football. The PCS score can also be weighted for different impact locations. Weighting coefficients are 1.00, 0.95, 0.62, and 0.48 for the side, front, back, and top respectively. This was included to reflect the relative risk of concussive injury from impacts to each of the different regions of the head, measured from gameplay of American football. Weighting the score showed an even lower false positive rate (Greenwald, Gwin et al. 2008). Following from the HIT system being employed, in 2012 Rowson et al proposed an injury risk function based on the accelerometer data collected from American football (Rowson, Duma et al. 2012):

$$Risk = \frac{1}{1 + e^{-(-10.2+0.0433a+0.000873\alpha-0.00000092a\alpha)}}$$

With *a* and α denoting peak linear and rotational accelerations respectively. Based solely on the rotational kinematics (shown in Table 2, taken from Rowson et al., 2012), a nominal injury risk was developed for specific rotational acceleration and velocity. This was based both on data from American football and large animal studies of brain injury.

Table 2	**Rotational accelerations and velocities associated with nominal injury risk values**	
Nominal injury risk	Rotational acceleration (rad/s^2)	Rotational velocity (rad/s)
10%	5260	23.3
25%	5821	25.8
50%	6383	28.3
75%	6945	30.8
90%	7483	33.2

Around the same time, Kimpara et al proposed a rotational version of HIC called the Rotational Injury Criterion (RIC):

$$RIC = (t_2 - t_1)\left[\frac{1}{(t_2 - t_1)}\int_{t_1}^{t_2}\alpha(t)dt\right]^{2.5}$$

With the same variables as the HIC equation, with rotational acceleration used instead (Kimpara and Iwamoto 2012). This is taken over a 36ms time span which, similarly to HIC, leads to the maximum possible value or RIC. This was shown to have limited function on its own, and the authors recommended using RIC in conjunction with HIC. The benefit of using this equation however is its simplicity. RIC can be used without the need for complex head mass moments to be known, and as such, is a very good tool for comparing the intensities of various impacts.

It should be noted that there are a significant number of finite element head models (FEHM), which have aided in developing the risk functions and metrics such as the Brain Injury Criterion (BrIC) (Shugar and Katona 1975, Hosey and Liu 1980, Ward, Chan et al. 1980, Zhou, Khalil et al. 1995, Zhang, Yang et al. 2001). These will not be investigated into any depth, as the present body of work pertains more to real life scenarios and laboratory reconstructions, rather than numerical studies. Additionally, many of the risk functions derived from these models lack accuracy when carried over to the impacts measured during gameplay.

1.5 The human and Hybrid III neck

The human neck is the portion of the body that joins the head to the shoulders and chest. This part of the spinal column is made up of seven vertebra called the cervical spine (C1 – 7) (Figure 2). Below the seventh cervical vertebra the thoracic spine begins. The neck provides support to the head and brain and protects important structures such as the spinal cord, veins and arteries, and the oesophagus, larynx and vocal cords (Britannica 2018). Several muscles such as the trapezius and sternocleidomastoid provide movement of the head and neck in various directions.

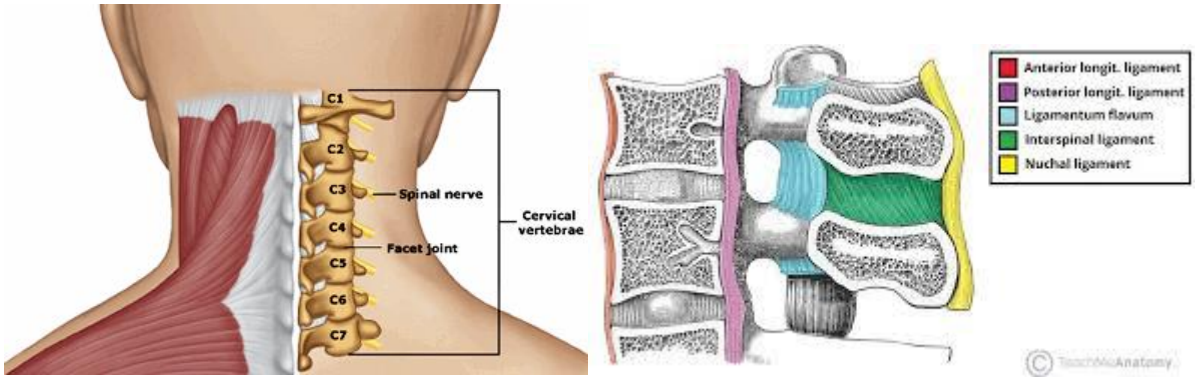

Figure 2 Human cervical neck showing the bone structure on the left (Ornstein 2019) and the ligament structure on the right (Barnes 2020)

The neck also has a number of ligaments that provide stabilisation and limit the motion of the bones (Figure 2). The vertebrae of the neck are comprised of two main materials, the nucleus pulposus and the annulus fibrosus. The structure of the neck allows for flexion, extension, and lateral bending of the neck as well as rotation to the left and right. Flexion and extension describe the forwards and backwards motion of the head respectively (Figure 3), while lateral flexion describes the sideways movement about the base of the neck.

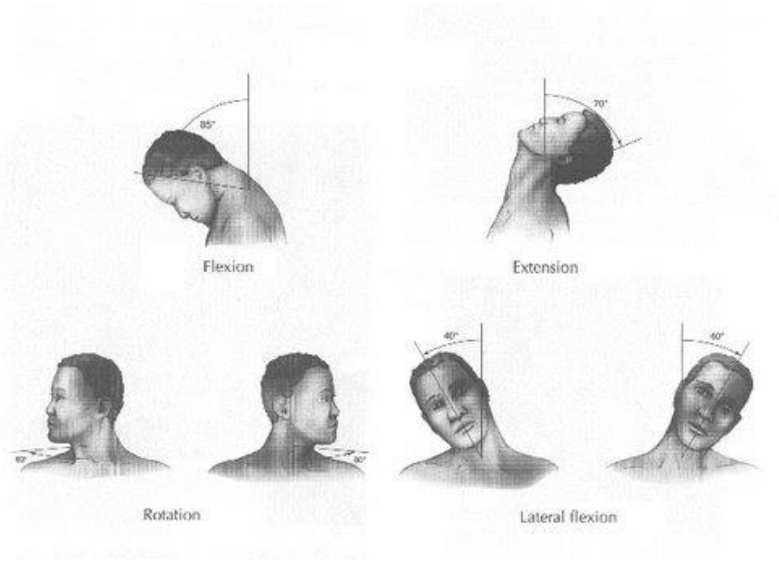

Figure 3 Motions of the head and neck (LeBlanc 2016)

Anthropomorphic test dummies (ATD's) have been widely used to understand how the body reacts to various injurious events since their development by the automotive industry in 1968 (Humanetics 2019). Originally used for crash testing, the Hybrid III (H3) dummy was introduced by general motors in 1976, which had improved features and biofidelity over the previous hybrid II and ATD 502 (Humanetics 2019). Costing upwards of $11,000 USD, the H3 neck uses three rigid aluminium vertebral elements molded in a 75 durometer (shore hardness) butyl elastomer to form the neck structure (Figure 4). The asymmetrical shape is used to provide higher bending resistance to flexion than extension (Foster, Kortge et al. 1977). The H3 is available commercially and is federally mandated for certifying the crashworthiness on frontal impact of all passenger cars sold in the United States and a few other countries (Humanetics 2019). More recently however, H3 components have been used

in studies branching out from automotive crash testing. Laboratory studies of sporting head impacts regularly use the H3 neck and headform. There has, however, been some debate about the biofidelity of the H3 neck, however due to a lack of sufficient data on H3 neck mechanics, it is not clear how well the H3 compares to the living human neck in directional loading.

Figure 4 The Hybrid III neck showing the steel cable that goes through the centre of the neck and the upper instrumentation mounting (Foster, Kortge et al. 1977)

1.6 Response of the human and Hybrid III head and neck to accelerations

Nearly all studies of the response of the living or post mortem human head and neck to impact accelerations were carried out using a sled system. The participants are usually restrained such that minimal movement of the T1 vertebra is observed. This, however, was not always achieved, as stated in a follow up paper by Thunnissen et al, correcting the results for head rotation in their earlier study to account for T1 movement (Thunnissen, Wismans et al. 1995). In the original experiment the head and neck response to frontal acceleration was measured. The data only came from a single participant, and was recorded with a peak sled acceleration of 2.8g. This study yielded a peak head linear acceleration of 7.6g and peak head angular velocity of 550°/s (9.6 rad/s) (Ewing, Thomas et al. 1969). The study fails to report specific values of any other useful variables for comparison such as maximum rotation angles of the head and neck. For simplification of the relative motions produced by the head and neck, the two pivot linkage mechanism was developed (Figure 5). This is still used to this day for reporting head and neck motions.

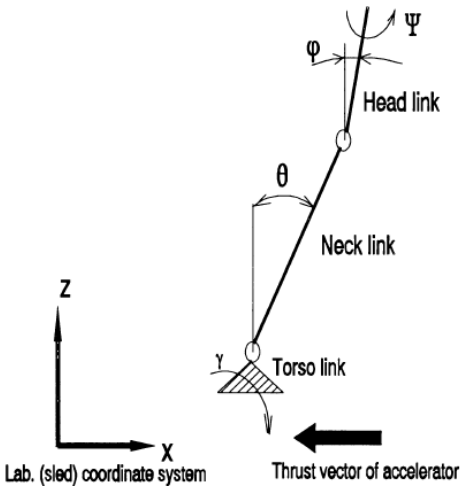

Figure 5 Two pivot linkage mechanism used for relative head motion description, taken from (Wismans, van Oorschot et al. 1986)

The Mertz corridor is commonly referenced for biofidelity tests of ATD's. This corridor describes the head rotation for a given dynamic moment, however, it was created using only one volunteer and some post mortem human data. Wismans et al found that post mortem human subjects (PMHS) had higher head rotation values than living volunteers for a given acceleration through frontal flexion sled tests (Wismans, Philippens et al. 1987). Additionally The PMHS' that were subjected to high level impacts (above 20g) sustained various injuries including vertebral fractures and strains in vertebral discs. Since the present study is concerned with non-injurious neck motions, the reliability of the Mertz corridor questionable and will not be used in this study.

Thunnissen et al later proposed response corridors for both the head and neck link angle based on a revised analysis of the results achieved from sled tests performed many years earlier (Figure 6). The envelope represents the mean ± SD of a range of human tests reporting T1 acceleration, rotational, and linear kinematics of the head and neck for the given sled acceleration (Thunnissen, Wismans et al. 1995). These are the most widely used for validation of biofidelic neck forms and computer models of the head neck system.

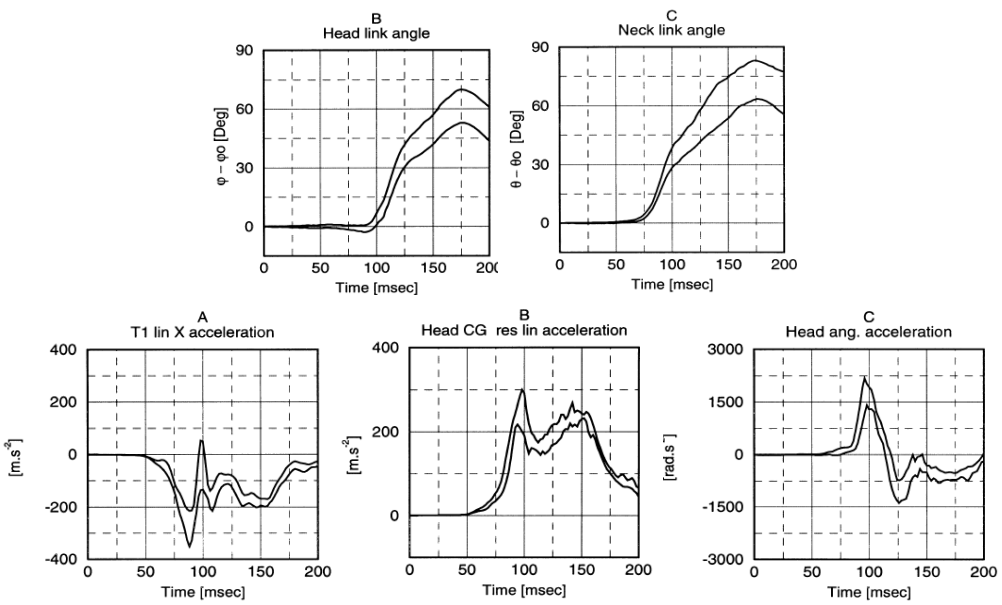

Figure 6: Response corridors for the acceleration input, accelerations and rotation angles for 9 volunteer experiments taken from (Thunnissen, Wismans et al. 1995)

The same study also compared the H3 head and neck response to that of the human corridor (Figure 7). The H3 neck was stiffer than the human neck, shown by lower peak rotation of the head. In 2009, Arbogast et al examined the head and neck response to low speed frontal impacts representative of those used in bumper cars. Maximum acceleration was limited to 4.5g, lower than what was used in previous studies. The adult average head rotation was 13.6 – 38.2° relative to the sled coordinate system (Arbogast, Balasubramanian et al. 2009). The authors of this study reported maximum head rotations of 0.2 – 13.4° relative to the T1 coordinate system (Table 8). This means that a large amount of torso motion was observed, and as such the acceleration at the T1 vertebra was different to that of the sled system. Due to the allowable motion of the T1 vertebral region during testing, Ewing et al reported peak T1 accelerations 2 – 3 times higher than those of the sled (Ewing, Thomas et al. 1978). Wismans et al report similar differences between the sled acceleration and the peak acceleration of the T1 vertebra. The authors of the latter study do not report the head rotation data with the T1 acceleration data, rather with the sled acceleration data (Wismans, van Oorschot et al. 1986). This is seen in almost every study that reports both input accelerations and measured T1 accelerations (Table 8).

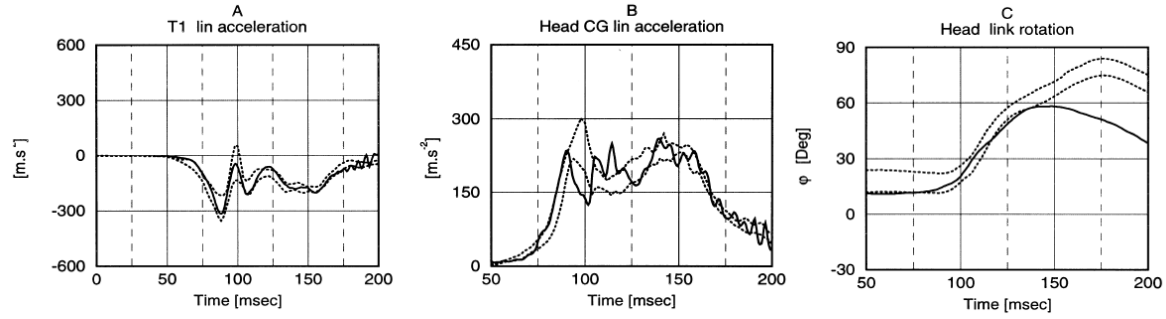

Figure 7: The applied T1 acceleration and the frontal H3 response (solid line) compared with proposed frontal performance requirements based on experimental data (dotted line) taken from (Thunnissen, Wismans et al. 1995)

A study by Walsh et al found clear differences in the behaviour of the H3 neck when compared to the human data and a newer more complex ATD neck called the BioRID neck. Due to the design of the neck, the H3 bends almost immediately on impact. The human neck, in comparison, initially translates following the head until a limit is reached, upon which rotation of the neck occurs (Figure 8) (Walsh, Kendall et al. 2018).

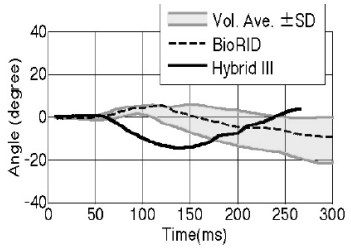

Fig. 11 HA-NA (ΔV=9.2km/h) Souse: Reference

Figure 8: Impact behaviour of the hybrid III neck compared to the BioRID and human corridor taken from (Walsh, Kendall et al. 2018)

Kallieris et al carried out frontal impact tests with cadavers, comparing the response to that of the H3 neck. The authors found the maximum cadaver head and neck flexion was about 30% greater than Hybrid III extension. The maximum bending angle occurred earlier with the dummy than the cadaver, similar to Figure 7. They also found the global kinematics of the Hybrid III dummy and cadaver are comparable, however there were temporal and spacial differences in head and neck motion. The magnitude of head and neck flexion is greater with the cadaver and maximum flexion occurs later than observed with the Hybrid III dummy. (Kallieris, Rizzetti et al. 1995). The same observations were made for rear end collisions above 25kph.

Until this point, all data reported has pertained to frontal impact conditions. Far fewer studies investigate living human head and neck dynamics for rear collisions. Those that do use methods that impede motion of the head, meaning the reliability and comparability for validation of the H3 neck is questionable.

Siegmund et al investigated the dynamic response of volunteers to low speed rear end collisions, however the speeds used were very slow (2 – 4kph). This meant peak input accelerations were also much lower than frontal studies (2.1 – 2.4g). Additionally, the participants were strapped into a car seat, with the headrest still attached limiting the motion of the head and neck. Nearly all participants contacted the headrest with the back of their head during the experiment (Siegmund, King et al. 1997). Kroonenberg et al used similar methods to investigate the rear end collision dynamics of volunteers. The same contact with the headrest was observed. This dictated the maximum neck extension angle (Van den Kroonenberg, Philippens et al. 1998). Methods such as these provide unfavourable results for comparison to the H3 neck, which is subjected to free, unrestrained motion during testing. The rationale behind the methods used in these two studies is obvious as allowing unrestrained movement of the volunteer head and neck in extension can easily lead to neck injuries. Due to this however, data presented by Siegmund and Kroonenberg should not be used for comparison to the H3 motion, which is unrestrained during testing.

Each study used slightly different parameters to generate head and neck motions. The most important of which are the T1 motions and the change in velocity during the acceleration event. Table 8 shows the data reported by each study discussed in this section. Lateral motion was not discussed as the methods are the same as those used for frontal flexion testing. The peak values presented in Table 3 were used to generate a validation criteria for the present study. The change in velocity was expected to have a large effect on the head and neck motions observed, however, this varies between studies. This is likely due to safety concerns as living volunteers cannot be subjected to the same extreme conditions that PMHS or ATD's can, especially in rear (extension) motion.

Table 3: Head and neck kinematics results reported in past studies

Study author	Impact direction	Test subjects	Change in velocity (m/s)	Input acceleration (g)	T1 acceleration (g)	Peak head angular acceleration (rad/s²)	Peak head angular velocity (rad/s)	Peak head angle (°)	Peak neck angle (°)
Ewing et al (1969)	frontal	Volunteer	-	2.8	4.9	-	9.6	37.0	-
Ewing et al (1978)	Lateral	Volunteer	3.1 – 5.7	3	5.6 – 10.0	295 – 560	9.4 – 17.2	-	-
			6.5 – 6.7	5	9.3 – 25.7	587 – 941	17.5 – 22.2		
			5.9 – 6.6	7	13.1 – 41.5	979 - 1614	23.8 – 28.0		
Wismans et al (1986)	Frontal	Volunteer	11.9 – 17.5	7.9 – 15.6	-	-	-	52.7 – 86.3	63 – 93
	oblique		10.9 – 14.9	7.0 – 14.0	-	-	-	33.7 – 78.0	47.7 – 101.0
	lateral		6.9 – 7.3	5.0 – 7.3	-	-	-	33.0 – 67.6	34.5 – 62.5
Wismans et al (1987)	Frontal	Volunteer	16.7 – 17.5	14.5 – 15.6	22.0 – 66.0	1500 – 2900	-	68.4 – 94.9	-
Thunnissen et al (1995)	Frontal	Volunteer	-	14.5 – 15.4	-	1200 – 2250	-	49.4 – 74	63 – 87
		PMHS				-		70.1 – 92.6	-
Siegmund et al (1997)	Rear	Volunteer	1.1	-	2.1 – 2.4	-407 – 240	-6.1 – 6.3	-5.2 – 9.9	-
			2.2		3 - 5	-909 – 524	-9.1 – 13.2	-10.1 – 12.0	
Kroonenberg et al (1998)	rear	volunteer	1.8 – 2.6	-	4.6 – 7.3	600	-	20 – 35	-
Arbogast et al (2009)	Frontal	volunteer	1.9	3.8	-	-	4.9	0.2 – 13.4	-

2 Experimental investigation into the potential of soft-shelled rugby headgear to reduce linear impact forces

2.1 Rugby headgear

Originally invented to stop players from getting “cauliflower ears’ during scrums, headgear has been a part of rugby since the 1920’s (sport 2019). It is mostly used to protect the head from cuts scrapes, abrasions and “cauliflower ears”. Headgear is only optional for players to use, unlike in other contact sports such as American football and ice hockey. Tight regulations are in place regarding the use of these headgear in all levels of rugby. Until recently, World Rugby (WR) permitted only certain types of headgear to be worn, with strict specifications imposed of 1cm max thickness and 45kg/m^3 maximum density (Rugby 2019). Headgear is to meet this to receive IRB approval and be deemed suitable for gameplay (Rugby 2019). Assumedly this is to prevent development of hard shelled rugby headgear, similar to what is seen in American football, such that the head could be used as a weapon during gameplay. This however, heavily limited the development of headgear with most using a lightweight closed cell foam. World rugby has long held the belief that players should self-regulate their own play to reduce injury, and only intervene by introducing rules around the gameplay to reduce the likelihood of injury. Due to the nature of the game and the culture surrounding it, this method has a limited effect. This has been shown in a review study of intervention strategies in American football such as rule changes, education, and training provided largely mixed results in terms of concussion reduction (Phillips and Crisco 2020).

Newer types of headgear are now being produced which are claiming potential concussion mitigation. The Npro headgear uses different materials to the earlier headgear designs for impact mitigation. Instead of a lightweight closed cell foam, the Npro headgear uses a higher density, open cell viscoelastic foam (Npro 2020). Similarly the Gamebreaker headgear uses a thin layer of viscoelastic foam, which is patented as their d30 impact absorbing material (Gamebreaker 2020). The impact attenuation properties of rugby headgear has been a subject of growing interest over the last two decades. Many researchers have endeavoured to find out if rugby headgear can reduce the likelihood of concussion through laboratory tests. However, until recently there hasn’t been an acceptable standard for testing rugby headgear for force mitigation. This has led to a range of methodologies within the literature, making comparisons between the studies difficult.

One study carried out in New South Wales tested headgear at a range of impact drop heights (0.2 – 0.6m), but omitted any tests above that as headgear performed poorly above this height (McIntosh and McCrory 2000). The study also only included two impact locations, however, tested at 3 temperatures: -10, 20 and 50°C and used two separate types of headform. One of these was the Hybrid III headform used in this study, and another was a fully rigid magnesium headform, both being dropped onto a steel anvil. A study of the Npro headgear alone used only a 300mm drop height, however used a pendulum impactor to investigate rotational accelerations and repetitive impact effects (Ganly and McMahon 2018). The headgear brands Npro is compared with in the study were not named. Similarly, a study of a novel headgear type utilises the same impact world rugby drop height, however uses a ½ inch MEP pad for the anvil, instead of a flat steel anvil (Knouse, Gould et al. 2003). This study

however, only reported the Gadd severity index (GSI or SI) of the impacts, which is far less commonly reported than the head impact criteria (HIC) severity measure within the literature. Another utilises drop heights of 0.2 – 0.6m, except when linear accelerations were too high for the 0.5 and 0.6m drops. This study however, uses a steel anvil instead of the standardised MEP pad (McIntosh, McCrory et al. 2004). Another study employs a 4G artificial grass surface, and a headform made from a resin to test impact performance of headgear (Frizzell, Arnold et al. 2018). This study also only records acceleration in one direction using a uniaxial accelerometer.

Using different impact surfaces affects the impact performance of the headgear. The MEP pad allows for longer impact durations than the steel anvil. This allows for impact durations that are closer to the average of 12ms measured during actual gameplay (King, Hume et al. 2015). The steel anvil creates a very short, high acceleration pulse, putting the laboratory measured accelerations well above those measured in real life. The studies conducted on headgear report peak linear accelerations of 100-1000g (McIntosh and McCrory 2000, Knouse, Gould et al. 2003, McIntosh, McCrory et al. 2004, Ganly and McMahon 2018). Additionally these studies all use different headgear and time between successive impacts for testing. Due to such a large variability in methodology, comparisons between the studies is difficult.

Despite the mounting literature suggesting headgear can reduce impact forces and potentially concussion risks (Knouse, Gould et al. 2003, McIntosh, McCrory et al. 2004, Frizzell, Arnold et al. 2018, Ganly and McMahon 2018), the use of rugby headgear is only optional with very few players actively wearing them due to an attitude that they "offer little increase in safety and interfere with gameplay, therefore are not worth the money" (Pettersen 2002). With Rugby Union being the second most popular sport in New Zealand for young people (NZSSSC 2017) and quickly gaining popularity worldwide (Rugby 2017), protecting players from the long term effects of concussion is imperative. Until recently, headgear only claimed to protect against cuts and scrapes. Now there are new types of headgear coming onto the market claiming impact force reduction (N-Pro, Gamebreaker) (Ganly and McMahon 2018, Gamebreaker 2019, Npro 2020) which have potential for concussion mitigation. This research therefore aimed to provide a coherent methodology to assess rugby headgear for its potential to reduce head impact accelerations critical for mitigation against concussions through reduction of accelerations. The need for clear data on whether or not headgear can make a difference in reducing head accelerations and associated injury risks is more important now than ever. Therefore, the aim of this study was to examine the effectiveness of soft-shelled rugby headgear to reduce the peak linear accelerations and the HIC score.

2.2 Drop test rig

A twin wire guided drop test rig was constructed to perform the headgear testing on (Figure 9). This simulates a free fall onto an impact surface. A drop test rig was chosen as these are common in impact testing of rugby headgear, and are specified for use in both World Rugby and NOCSAE standards(NOCSAE 2017, Rugby 2019). The impact surface was chosen to be a 1 inch MEP (modular elastomer programmer) pad manufactured by Cadex with a hardness of 60 ± 2 Shore A. This was chosen as it is a standardised rubber material which gives a longer

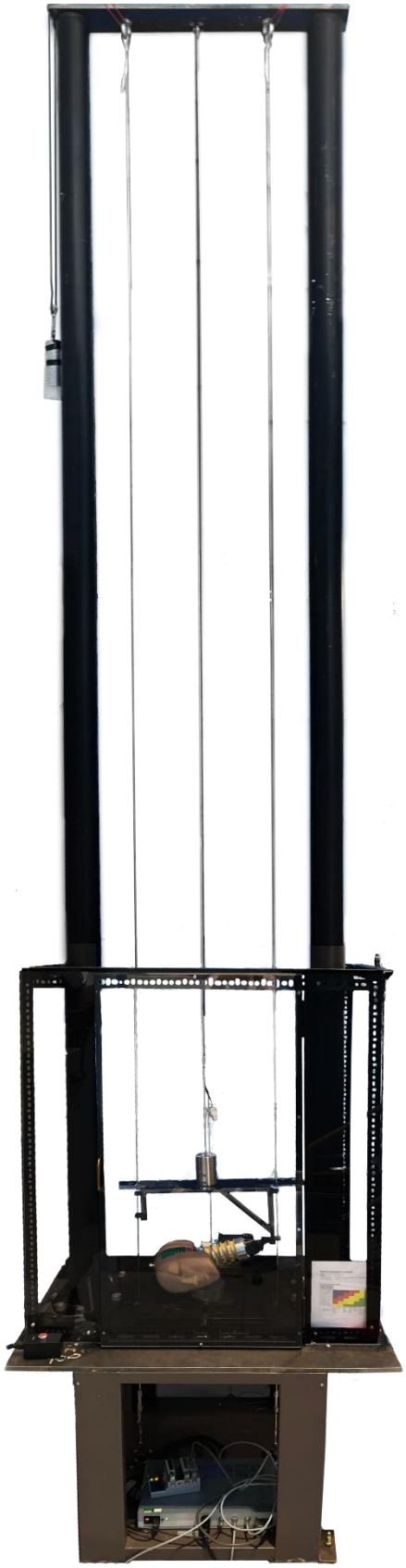

Figure 9 Drop test rig used in this study

duration impact than a steel anvil. This creates impact durations closer to those reported from in vivo impact measurements. The MEP pad is also used when testing to the NOCSAE headgear impact testing standards. The headform used for testing was a Hybrid III 50th percentile male headform manufactured by humanetics. This is a cast aluminium headform wrapped in a rubber skin to give a more realistic response to impact. These were developed for automotive crash testing, but have been widely used in sports impact testing. The properties of the headform are validated before being shipped from the manufacturer. This was chosen as it best represented the average male head size and weight, compared to other headforms on the market.

The headform was attached to a drop frame which held it in the specific orientations required for testing. The drop frame was made of thin (20x20x1.6mm) steel hollow section which could be lifted to the required heights by an electromagnet. This had an overall weight of 1kg (5.9kg total falling mass including headform). This electromagnet also allowed for instant release of the entire drop carriage, which is then guided by the wires in a 'free fall'. Nylon bushes were incorporated where the steel wires guided the drop frame to ensure a low friction contact. Impact velocities for drop testing are defined in the NOCSAE standard, therefore video verification of the impact speed was conducted and compared to the theoretical impact speed based on a free fall using kinematic equations. High speed imaging was used to capture the last 100mm of the fall. The impact velocity was taken as the maximum velocity before the headform touched the MEP pad. This was carried out at 0.1 – 1.5m in increments of 0.2m (Table 4). The impact energy was calculated from the measured impact velocity and compared to the theoretical energy based on free fall from the drop height. Each drop height was filmed 5 times to ensure accuracy and repeatability.

Table 4	Validation values taken using high speed imaging for the test rig					
	Kinematic (theoretical) values		Measured values		Errors	
Drop height (m)	Impact velocity (m/s)	Impact energy (J)	Impact velocity (m/s)	Impact energy (J)	Impact speed error (%)	Impact energy error (%)
0.1	1.40	6.72	1.44	6.12	2.77	5.47
0.3	2.43	20.16	2.45	17.75	1.08	2.16
0.5	3.13	33.60	3.11	28.59	0.60	1.21
0.7	3.71	47.04	3.70	40.29	0.28	0.56
0.9	4.20	60.48	4.17	51.19	0.88	1.76
1	4.43	67.20	4.43	57.90	0.01	0.03
1.2	4.85	80.64	4.87	70.10	0.46	0.92
1.4	5.24	94.08	5.31	83.31	1.37	2.74
1.5	5.42	100.80	5.40	86.13	0.40	0.80

The measured velocities agreed closely with the theoretical. At the lowest drop height there was an error of 2.8% for impact speed, and 5.5% for impact energy. This error reduced to a maximum of 1.4% and 2.7% for impact velocity and energy respectively. This was considered close enough to the theoretical to calculate the drop heights for the specified velocities and impact energies directly from the kinematic equations.

2.3 Headgear drop testing methods

Six models of headgear were chosen: CCC Ventilator, Kukri, 2nd Skull, N-Pro and a medium and large sized Gamebreaker Pro (Figure 10) (herein referred to as headgear 1-6 respectively) with all units in medium size except headgear 6. Headgear 1 and 3 use light weight (≤ 45kg/m^3) polyethylene foam arranged in cells around the headgear to provide padding. Headgear 1 uses honeycomb shaped cells while headgear 3 uses cells replicating the shape of the logo. Headgear 2 uses a light weight (≤ 45kg/m^3) ethylene vinyl acetate (EVA) foam arranged in cells similar to headgear 1. Headgear 4 uses a thicker, higher density (≥ 45kg/m^3) open cell polyurethane foam in square cells of varied size (Ganly and McMahon 2018). Headgear 5 and 6 use EVA foam and a layer of impact absorbing foam developed by D3O® (≥ 45kg/m^3) (Gamebreaker 2020). Headgears 4 – 6 all use foams that are viscoelastic and open celled compared to headgears 1 – 3 which all use closed cell foams. Headgear 5 and 6 were the thickest samples (15 – 20mm max thickness), compared to headgear 4 (12 – 13mm max thickness) and headgears 1 – 3 (8 – 10mm max thickness). All headgear fit tightly on the headform with no slippage ensuring a consistent impact region throughout testing. All headgear was new and in unused condition before testing began. Headgears 1 – 3 and recently headgear 4 have all been World Rugby approved and are allowed to be used during gameplay, however, headgear 5 and 6 have not. It should be noted that World Rugby approved headgear (prior to the law 4 trial approval process) is not designed to mitigate risks of brain injury or skull fracture. Approved headgear is, however, often purchased by parents to help protect their children from head injuries. Additionally, this headgear serves as an appropriate baseline for comparing to newer models of headgear with potential to lower concussion risk.

Testing of headgear was carried out using a twin wire guided, gravity induced drop test rig. A 50th percentile male headform (Humanetics Innovative Solutions Inc.) was used to simulate a player's head, on which the headgear was mounted (Figure 10 and 11). The headform was instrumented with a three axis accelerometer (MEAS 53-0500, ±500g, 10kHz sampling rate) held at the centre of gravity of the headform. The headform and sensors were calibrated using

the protocol set by the code of Federal Regulations (CFR) (1997). A 1 inch (25mm) Modular Elastomer Programmer (MEP) pad by Cadex Inc. served as an impact surface (Figure 11). The pad was calibrated at an independent laboratory by Cadex Inc.

Impact locations were determined using the NOCSAE (NOCSAE 2017) and World Rugby standards (Rugby 2014) for impact testing of sporting headgear (Figure 11). The top of the head (crown) was excluded from testing as preliminary impacts showed similar PLA and HIC reduction to other areas. Additionally, of the impact locations described in the standard, the crown is the least commonly impacted area during gameplay (King, Hume et al. 2015, King, Hume et al. 2016, King, Hume et al. 2018). The headform was dropped from 4 different heights, corresponding to 13.8J impact energy, specified by world rugby (Rugby 2014), 300mm drop height specified by World Rugby and common in previous studies (Knouse, Gould et al. 2003, Rugby 2014, Ganly and McMahon 2018, Rugby 2019), and heights providing impact velocities of 3.46 and 4.23m/s specified by NOCSAE (NOCSAE 2017). These are summarised in Table 5.

Figure 10 headgear included in the testing, from top left to bottom right: CCC Ventilator, Kukri, 2nd Skull, Gamebreaker blue, Gamebreaker Black, Npro

The impact energy was determined for the total falling mass of 5.9kg including the drop frame (Figure 11). Five repeats for each orientation and drop height were performed with 60 seconds between successive drops as required by NOCSAE (NOCSAE 2017). It should be noted that this study does not intend to exactly recreate either the World Rugby or NOCSAE standards, but uses them as a base from which to extend the investigation of headgear behaviour. This study did not test headgear for world rugby approval, but assessed and compared the impact attenuation behaviours of selected headgear.

Table 5	**Details of the drop heights used**		
Drop height (mm)	Impact velocity (m/s)	Impact energy (J)	Authority
238	2.16	13.76	World Rugby
300	2.43	17.24	World Rugby
610	3.46	35.32	NOCSAE
912	4.23	52.78	NOCSAE

Linear impact accelerations were measured for each drop. These were recorded 5ms before a 10g threshold was reached and continued recording for 50ms thereafter. Initial trials found this to encapsulate the entire acceleration-time curve for the longest impact times recorded. Data was then processed in a custom MATLAB code to find the peak acceleration and maximum HIC value for each of the five repeats.

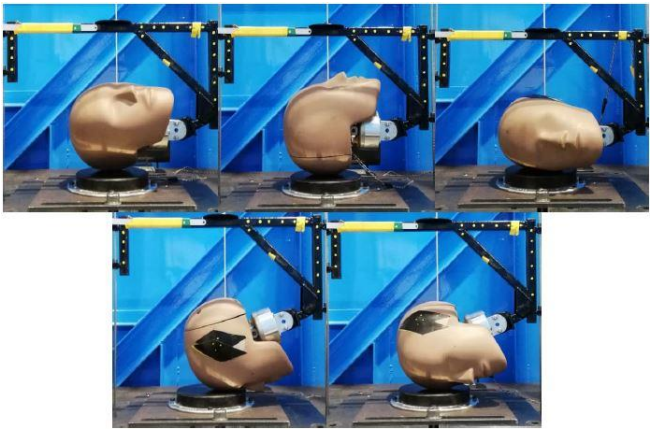

Figure 11 Impact locations, and locations on the MEP pad. From top left to bottom right: rear boss, rear, side, front, front boss

A post hoc analysis of the results was performed using IBM SPSS® Statistics with the mean peak linear acceleration (PLA) and HIC values calculated for each headgear at three drop heights (238mm, 610mm and 912mm) in each orientation. 300mm was excluded as there was little difference in impact forces between 238mm and 300mm. Composite averages were taken as the average PLA and HIC across all orientations for each height and headgear. The data was then analysed with a mixed design analysis of variance (ANOVA) to find statistically significant differences in the PLA and HIC measured for the headgear drops. A p-value <0.05 was considered statistically significant. 300mm drop height was excluded from the composite statistical analysis, as 238mm and 300mm impact behaviour follow the same trend and display extremely similar PLA and HIC values. 300mm drop height was included in location specific analyses of the data however.

2.4 Headgear drop testing results

2.4.1 Composite behaviour

All headgear significantly reduced both the PLA and HIC values (Table 6 and 7) compared to no headgear at all heights ($p < 0.05$). There were no significant differences in PLA between headgears 1 – 3 at any of the three heights. Headgear 4 significantly reduced PLA and HIC when compared to headgears 1 – 3 at all three drop heights. Headgear 5 and 6 reduced PLA significantly more than headgears 1 – 4 across all heights ($p < 0.05$). Headgear 6 produced significant PLA reduction when compared to headgear 5 at 238mm drop height ($p < 0.05$). At all heights above this, neither 5 nor 6 significantly reduced PLA more than the other, however they consistently reduced PLA compared to headgears 1 – 4.

Table 6	Mean (SD) composite percentage reduction values compared to no headgear					
	PLA Reduction (%)			HIC Reduction (%)		
	238mm	610mm	912mm	238mm	610mm	912mm
CCC	18.5(2.2)	7.2(2.2)	6.5(1.2)	32.4(3.7)	13.3(2.4)	12.4(2.2)
Kukri	17.8(1.9)	7.9(2.2)	7.2(1.5)	29.7(3.3)	14.7(2.4)	12.5(2.8)
2nd Skull	16.2(3.0)	7.8(2.9)	5.6(1.8)	29.2(4.8)	14.9(3.5)	11.7(2.4)
Gamebreaker Blue	39.7(3.1)	31.7(3.5)	29.9(2.7)	57.3(4.0)	49.6(4.5)	47.4(3.8)
Gamebreaker Black	45.3(2.6)	33.6(3.3)	32.4(2.4)	62.7(3.1)	51.6(3.9)	50.9(2.9)
N-Pro	32.6(2.7)	21.5(3.4)	19.9(3.1)	50.0(4.0)	34.7(3.9)	33.9(4.6)

Following a similar trend to PLA, all headgear significantly reduced HIC when compared with no headgear at all heights ($p < 0.05$) (Table 7). At 238mm drop height, headgear 1 reduced HIC significantly more than headgear 2 and 3. No significant difference in HIC reduction between headgears 1 – 3 was seen at any other height (Table 7). Following the trend of PLA reduction, headgear 4 significantly reduced HIC compared to headgears 1 – 3 while both 5 and 6 significantly reduced HIC compared to all other headgear including headgear 4. At 238mm, headgear 6 reduced HIC significantly more than headgear 5. This was not observed at any other heights.

Table 7	Mean (SD) values for the composite behavior of the headgear compared to no headgear					
	Peak Acceleration (g)			HIC Score		
	238mm	610mm	912mm	238mm	610mm	912mm
No Headgear	71(0.2)	142.6(2.0)	198.1(0.8)	100.8 (0.6)	424.5(4.3)	853.1 (8.3)
CCC	58.2(1.4)	132.8(1.6)	184.4(0.9)	67.8 (2.9)	372.8 (5.8)	743.7 (9.4)
Kukri	58.8(1.0)	131.4(1.4)	183.2(2.0)	70.9 (1.6)	363.3 (3.5)	741.9 (13.6)
2nd Skull	60.0 (1.9)	132.1 (2.5)	186.5(2.8)	71.6 (4.0)	371.7 (11.1)	751.5 (15.2)
Gamebreaker Red	42.9(1.7)	96.2 (3.8)	136.8 (4.3)	42.9 (2.7)	209.7 (13.7)	435.8 (26.3)
Gamebreaker Blue	39.0(1.7)	93.8(3.3)	132.4 (4.2)	37.4 (2.3)	201.8 (11.3)	412.1 (19.3)
N-Pro	48.3(1.8)	111.7(3.7)	158.6 (6.1)	50.4(3.2)	280.3 (11.4)	572.8 (32.4)

2.4.2 Location specific behaviour

All headgear reduced average PLA and HIC to some extent. The average PLA (Figure 12) and HIC values (Figure 13) were highest for rear impacts across all headgear at all heights. Side impact locations showed higher average PLA and HIC scores than the forehead, front boss and rear boss locations. Forehead and rear boss impact locations showed similar average PLA and HIC values across all heights while both giving consistently lower values than side and rear impacts. Front boss impacts gave the lowest PLA and HIC across all heights and headgear units. All trends were followed when no headgear was present. Headgear 4 showed much higher mean PLA and HIC values than headgear 5 and 6 in rear impacts, but still lower than headgears 1 – 3.

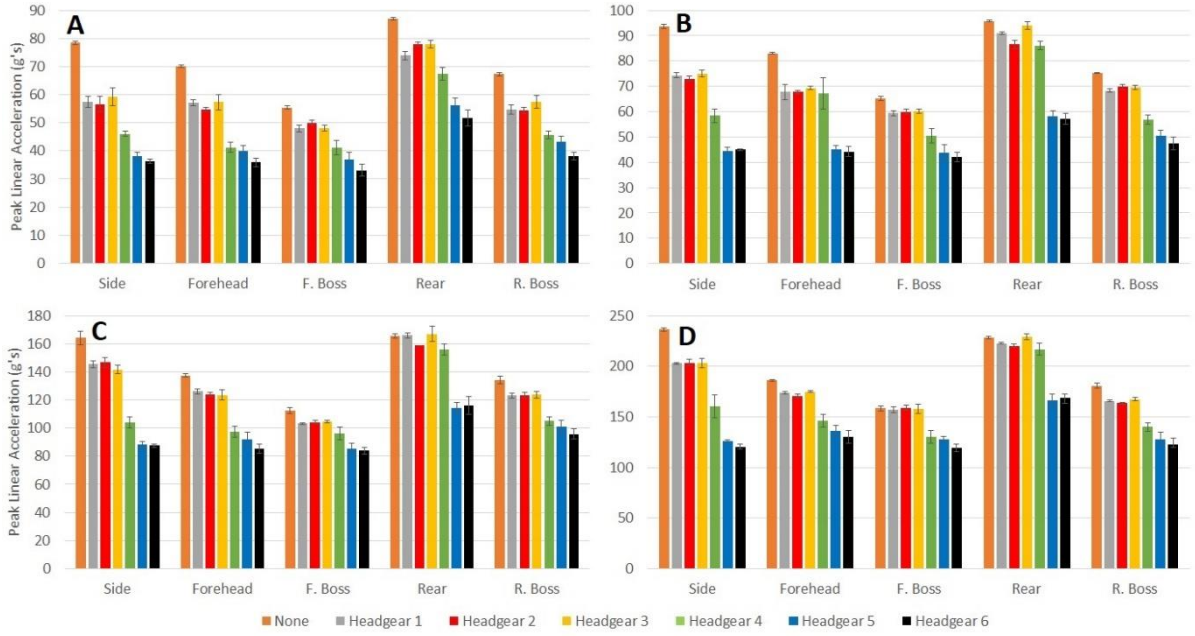

Figure 12 Mean (SD) peak linear acceleration for each headgear unit in each orientation at A. 238mm, B. 300mm, C. 610mm and D. 912mm

Table 8 displays the average percentage PLA and HIC reduction across all four drop heights for each orientation. For headgears 1, 3, and 4, the least PLA and HIC reduction occurred in the rear orientation, whilst the remaining headgear displayed the least PLA and HIC reduction in the front boss orientation. It should be noted that the difference in PLA and HIC reduction between the rear and front boss impact locations is minimal for all headgear with exception to headgear 4. All headgear displayed the highest PLA and HIC reductions in side, forehead, and then rear boss orientations. Headgears 4 – 6 consistently display larger PLA and HIC reductions across all positions compared to headgears 1 - 3.

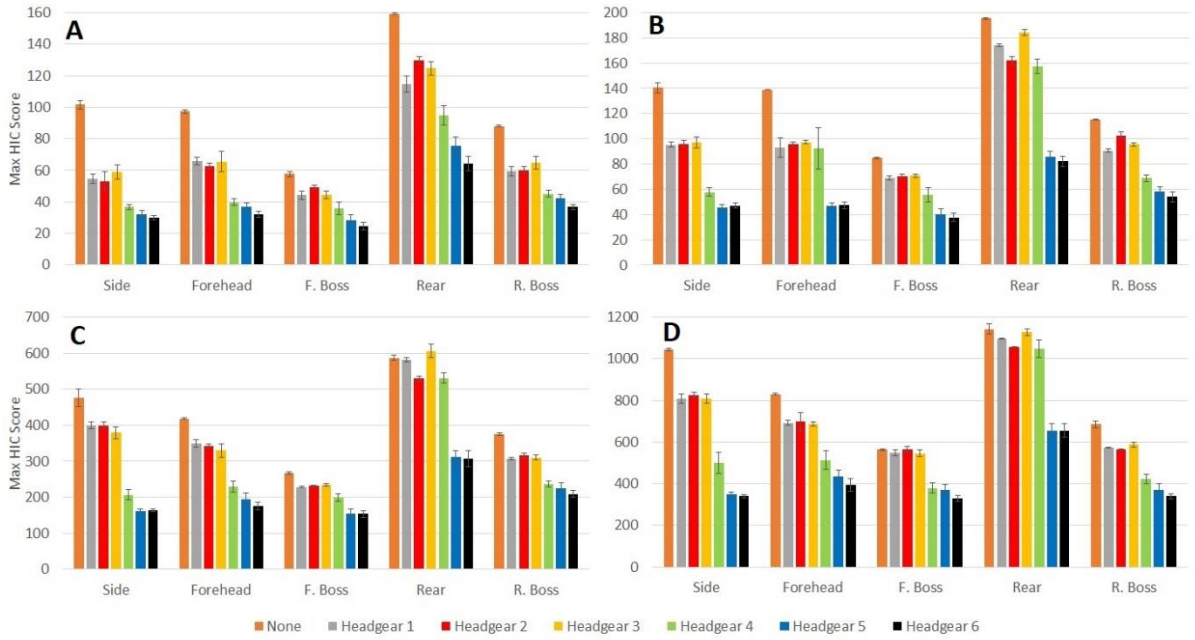

Figure 13 Mean (SD) max HIC scores for all headgear units in each orientation from drop heights of A. 238mm, B. 300mm, C. 610mm and D. 912mm

Both Gamebreaker and N-Pro units followed similar tends to those observed in the CCC, Kukri and 2nd Skull units with the maximum HIC reduction occurring at the lowest drop height and consistently decreasing as height increased. Maximum HIC reduction for Gamebreaker blue, black and N-Pro occurred in the side orientation (68.5% ± 4.0, 70.7% ± 3.4, 64.2% ± 3.5 respectively). The rear impact showed the lowest reduction in HIC for N-Pro headgear, however the headgear in this orientation performed vastly better in both Gamebreaker samples (Figure 13).

Table 8 **Mean (SD) percentage reduction values averaged across all four drop heights for each orientation**

	PLA					HIC				
Headgear	Side	Forehead	F. boss	Rear	R. boss	Side	Forehead	F. boss	Rear	R. boss
1	18.2(5.4)	12.9(5.6)	7.8(3.5)	5.7(4.7)	11.1(3.8)	29.3(9.9)	24.6(8.0)	14.7(6.2)	11.0(8.5)	22.1(5.1)
2	18.6(6.3)	14.6(5.6)	6.3(3.0)	7.0(3.1)	10.9(4.1)	29.1(10.6)	25.2(8.1)	11.3(5.4)	13.4(4.6)	19.1(6.4)
3	18(4.1)	12.7(4.7)	7.0(3.4)	3.3(3.6)	9.3(2.7)	29.0(7.5)	25.2(6.1)	13.6(6.0)	8.0(6.9)	18.9(3.8)
4	36.9(2.6)	27.7(7.4)	20.2(4.0)	11.0(5.8)	25.2(3.4)	57.9(3.6)	44.0(8.2)	32.5(3.6)	19.5(10.6)	41.1(3.8)
5	49.2(2.7)	37.1(7.2)	27.4(5.7)	33.2(4.1)	30.6(3.8)	67.2(0.7)	57.3(6.9)	44.7(6.8)	49.7(4.9)	46.9(4.0)
6	50.4(2.5)	40.8(7.0)	31.4(6.4)	34.2(6.3)	35.2(4.9)	67.5(1.6)	60.9(5.6)	49.2(7.3)	52.0(6.8)	51.5(4.2)

At 912mm drop height the range of HIC reduction over all orientations was 66.7-34.1%, 67.4-41.5% and 52.1-8.2% for Gamebreaker blue, black and N-Pro respectively. All positions in the Gamebreaker and N-Pro units performed better in all orientations than the CCC, Kukri and 2nd Skull units.

2.5 Discussion

All headgear reduced PLA and HIC compared to no headgear ($p < 0.05$). This is expected as the presence of foam padding will extend the time of total deceleration, thereby decreasing the peak acceleration. Headgear performance was clearly split into two groups; headgears 1 – 3, and headgears 4 – 6. Headgears 1 – 3 all use a lightweight (≤ 45kg/m^3) closed cell foam (CCC 2017, Skull 2019), which measured between 8 and 10mm max thickness, to provide impact attenuation. All three incorporate very similar materials, at similar thicknesses, in similar cell structure arrangements around the headgear. This is likely why all three display similar impact attenuation behaviour. Headgear 4 utilises a high density, viscoelastic, open cell polyurethane foam (Ganly and McMahon 2018) while headgear 5 and 6 samples use a layer of EVA foam (Gamebreaker 2019) and a layer of impact absorbing, viscoelastic foam developed by D3O® (Gamebreaker 2019). Headgears 4 – 6 each have a higher total thickness than headgears 1 – 3. Headgears 4 – 6 lowered PLA and HIC significantly more than headgears 1 – 3 across all impacts, however headgear 5 and 6 significantly lowered PLA and HIC more than headgear 4 across all impacts ($p < 0.05$). The difference between headgears 4, 5, and 6 can likely be attributed to the difference in thickness, as headgear 5 and 6 had a much greater thickness than headgear 4.

Side impacts showed the highest PLA and HIC reduction for all headgear as the side of the headgear had the greatest area of foam involved in the impact of all locations tested. Headgears 1 – 4 showed the lowest impact attenuation in the rear orientation. All of these headgear have laces at the back to ensure a tight fit when worn, therefore there is little padding in that area. Headgear 4 has a higher thickness of material than the other lace up

types, therefore reduced PLA and HIC slightly more than headgear 1 – 3 in the rear orientation. Headgear 5 and 6 use a large elastic pad with a foam insert instead of laces, giving much higher impact attenuation than all other headgear in the rear orientation. Front and rear boss impact positions performed better than rear impacts, but not as well as the side or forehead due to having lower amounts of foam involved in the impact compared to side and forehead, but more than the rear.

Studies of impact locations during gameplay all report the side of the head as the most commonly impacted region, followed by the front and back (with similar impact frequencies), and lastly the top of the head (crown) (King, Hume et al. 2015, King, Hume et al. 2016, King, Hume et al. 2018). It is unknown if the higher impact attenuation behaviour of the side impact location is intentionally designed into the headgear from results of previous field investigations or simply a consequence of the curvature of the head allowing for a flatter impact surface (therefore larger foam area involved in impact). Despite the back of the head being the second most common impact location, there is little padding at the back. The reason for this is likely that many of the impacts marked as rear impacts in studies are actually offset from the centre of the back of the head (i.e. rear boss). Rear boss impacts had significant PLA and HIC reduction across all headgear, similar to the forehead (Table 4). Impacts directly to the back of the head are still a concern, and one which is only addressed by headgear 5 and 6 with the foam and elastic backing of the headgear.

Headgear 6 (large) consistently performed better than the headgear 5 (medium). The medium size fit very tightly on the headform. Some amount of pre-crushing of the foam would have been present on the medium headgear, therefore reducing the amount of deformation the foam can undergo during the impact. Additionally, the larger sized headgear may have had a greater area of foam involved in the impact, therefore increasing the amount of energy absorbed in each impact. These differences were consistent, but non-significant at heights above 238mm.

All headgear showed a lowering of attenuation effectiveness as drop height increased. The foams used in headgear can only absorb a certain amount of energy through deformation. This amount of energy depends on a range of structural properties intrinsic to the material involved as well as the thickness of such materials. As the impact energy increases, the foam dissipates a lower percentage of the total energy involved, therefore is less effective at high impact energies. The higher density, viscoelastic, open cell foams used in headgear 4 – 6 were observed to dissipate a much greater proportion of the impact energy than the lower density closed cell foams used in headgear 1 – 3. Closed cell foams are made up of many tiny pockets of air trapped within cells made of the foam polymer. Energy is absorbed through compression of the air pockets inside, and deformation of the cell walls giving the foams their ‘springy’ feel when compressed. In open cell foams, cells are not fully closed off, allowing air to move through the material. In these, energy is absorbed through deformation of the polymer structure. As this happens, air is pushed through the cellular structure, offering some resistance to deformation, leading to the ‘memory foam’ properties of these foams. Open cell

foams are far less stiff than the equivalent density closed cell foams, therefore, much higher density foams can be used in 'soft-shelled' headgear than what is possible for closed cell foams. This increased foam density, and increased viscoelastic nature of the open cell foams, likely accounts for most of the difference in impact attenuation behaviour between the two foam types.

The headgear using closed cell foam experienced significant degradation in areas when subjected to the highest energy impacts. This was likely due to a bursting of the cell walls encapsulating the air pockets. Degradation was limited to headgears 1 – 3 and only occurred in the forehead and front boss areas, where there was low amounts of foam involved in the impacts. This was not observed at any other heights or on any other headgear.

World Rugby have designed the approval standards in a way that limits overprotection of players. World Rugby states that the specifications for padded clothing and headgear are intended to encourage players to protect themselves rather than provide equipment that would materially provide injury protection. The standard also explicitly states that headgear approved by world rugby is not intended to protect against any form of mild traumatic brain injury or skull fractures. It makes sense therefore, that headgear 1 – 3 which have received World Rugby approval, do not reduce PLA or HIC to the same extent as headgears 4 – 6. Headgear 4 has received World Rugby approval, however not through the same standards that headgears 1 – 3 have. Headgear 4 has been approved through the newer Law 4 assessment trial, for headgear designed to achieve specific, quantifiable medical benefits.

Headgear has potential to reduce the risk of concussive head injuries. If the accelerations seen in an impact can be lowered to a safer level, the concussive injury risk can potentially be reduced. It is, however, not well understood what exactly causes concussion and what are the underlying mechanisms in the brain, although the link between high intensity head impacts and concussions is recognised. The results of this study show that the headgear tested can lower the impact accelerations by up to 50%, indicating there is a potential they can make a difference on the field. Further testing of headgear performance on the field is required before any definite conclusions can be drawn on their protective performance. Additionally, the effect of the fit of the headgear should be investigated with regards to the impact attenuation behaviour. This study was limited to linear accelerations. Further investigation is needed investigating rotational accelerations, and their role in concussive injuries. Some researchers have proposed rotational accelerations to be more damaging to the brain than linear (King, Yang et al. 2003, Graham, Rivara et al. 2014). At present, however, no single widely used method exists to quantify the rotational injury risk. Some researchers have put forward metrics similar to HIC which integrate the rotational and linear acceleration (King, Yang et al. 2003, Gardner, Iverson et al. 2014), however, validation standards do not yet exist for verification, unlike HIC. Further investigation needs to take place into the metrics quantifying injury risk using both rotational and linear acceleration.

2.6 Conclusion

This study provides further evidence that rugby headgear can reduce the peak linear accelerations and HIC from an impact. All headgear significantly reduced the PLA and HIC of an impact. The newer types of headgear reduced PLA and HIC significantly more than the World Rugby approved headgear. All except headgear 5 and 6 showed little reduction in PLA and HIC in rear impact, and all headgear showed a reduction in effectiveness at higher drop heights. Further investigation is required into rotational accelerations, how headgear can mitigate these, whilst establishing standards for quantification of rotational injury risk.

3 Developing a biofidelic alternative to the Hybrid III ATD neck

3.1 Development of a neckform validation criteria

The H3 neck is validated by Humanetics using methods set in the code of federal regulations (Administration 1997). This specifies a pendulum be used, with neck and headform attached at the base, to create impact accelerations (Figure 14). The pendulum is to be released from stationary and allowed to free fall from a height such that tangential velocity at the pendulum accelerometer centreline at the instance of contact with the honeycomb is 7.01 ± 0.12m/s for flexion testing, and 6.07m/s ± 0.12m/s for extension testing (Administration 1997). These velocities correspond to initial heights of 2.5m and 1.9m respectively at the accelerometer. The pendulum is required to impact a block of honeycomb with 28.8 kg/m^3 density such that pendulum deceleration fits within the ranges in Table 9. The specifications for the pendulum itself are shown in Figure 14 (Administration 1997).

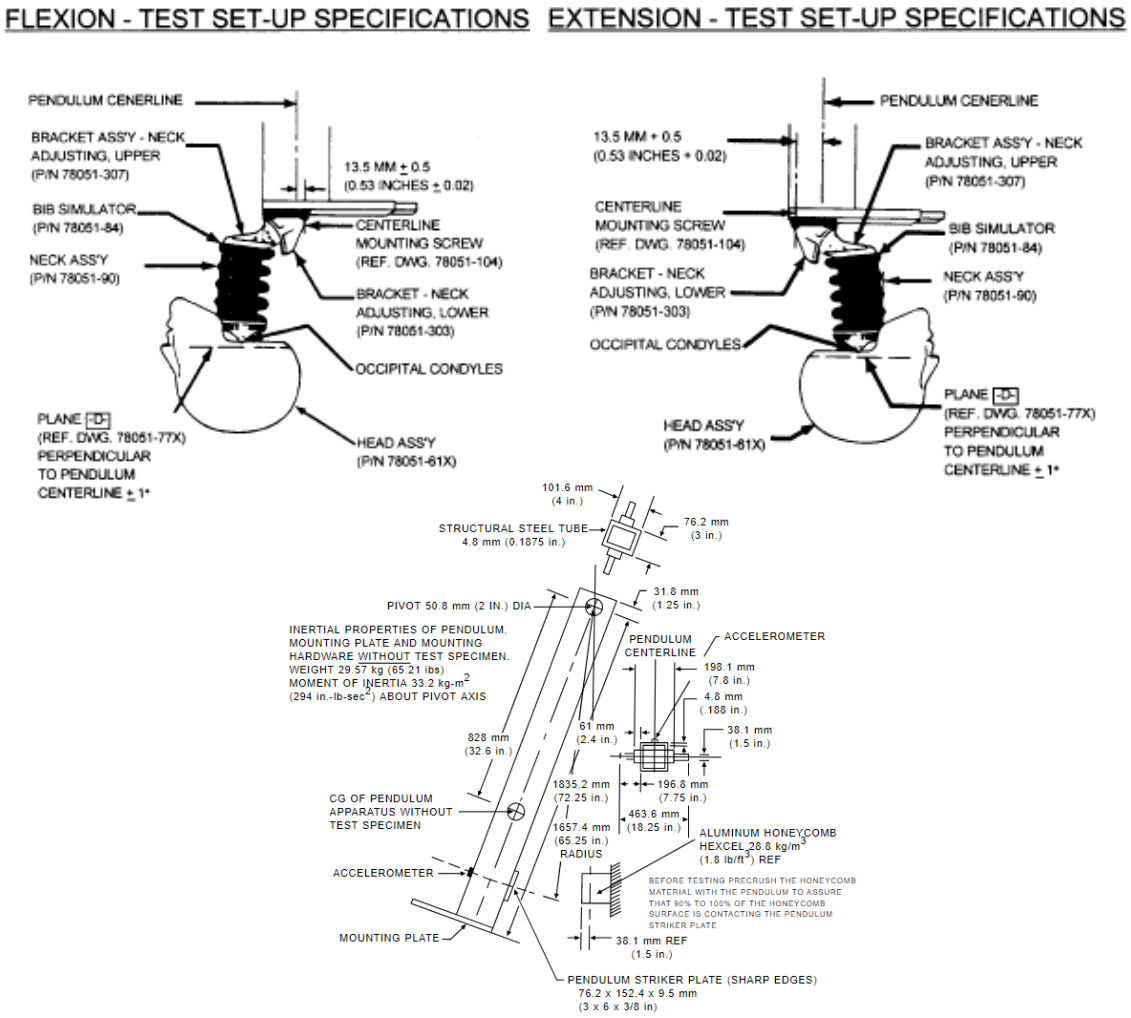

Figure 14: test setup showing head and neck orientation for flexion testing (top left) and extension testing (top right). Pendulum dimensions and requirements for the neck validation (bottom), taken from (Administration 1997)

Table 9	Pendulum deceleration curve values for flexion and extension testing	
Time (ms)	Flexion deceleration level (g)	Extension deceleration level (g)
10	22.5 – 27.5	17.2 – 21.2
20	17.6 – 22.6	14.0 – 19.0
30	12.5 – 18.5	11.0 – 16.0
> 30ms	29 maximum	22 maximum

The rotation of the head is measured at the line shown in Figure 14 denoting plane D (shown as a dashed line at the base of the head). Similar to the pendulum acceleration, a range is given for the rotation angle of plane D at certain times following the onset of impact. These are given in Table 10. Any H3 neck must fit within the ranges given to be considered validated.

Table 10	Plane D rotation for validation of the Hybrid III 50th percentile neck		
Flexion		Extension	
Time (ms)	Angle of rotation (°)	**Time (ms)**	Angle of rotation (°)
57 - 64	64 - 78	**72 – 82**	81 – 106
113 - 128	Rebound past 0°	**147 - 174**	Rebound past 0°

These acceleration values fit well within the ranges that have been seen for T1 accelerations across past studies despite seeming somewhat at the higher end (Figure 15). Mertz and Patrick subjected human volunteers to frontal accelerations ranging from 2 to 9.6g. Neck pain was experienced at any acceleration level higher than 8g (Mertz and Patrick 1971). T1 accelerations were not reported. From the data in Table 8, it is safe to assume the accelerations seen would have been 2 – 3 times as high as the sled acceleration.

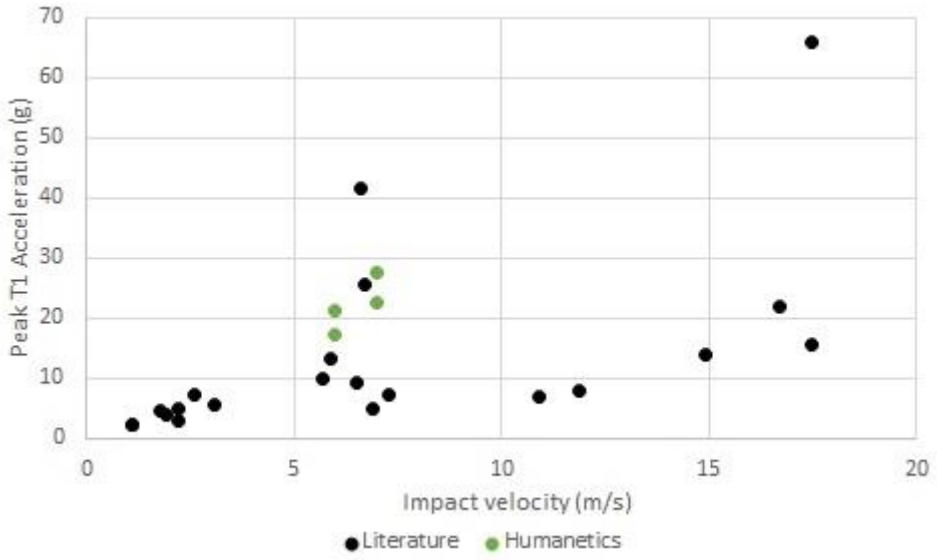

Figure 15 Humanetics Hybrid III T1 accelerations compared to those used in the literature (Ewing, Thomas et al. 1969, Ewing, Thomas et al. 1978, Thunnissen, Wismans et al. 1995) (Wismans, van Oorschot et al. 1986, Wismans, Philippens et al. 1987, Van den Kroonenberg, Philippens et al. 1998)

For this study, a combination of the humanetics validation and a comparison to the published data for human volunteers was used as a validation standard for the neck. Using the maximum and minimum values for head angle, neck angle, and head rotational acceleration and velocity, a set of validation corridors were created (Figure 16). These are largely based on the values presented in Table 3. This method of developing a validation corridor was chosen as it encapsulates all of the measured data that has been captured in human neck trials. Figure 16 A shows the peak head angles reported in the literature. Data points not used for creating the corridor were included to show how the data fits within the corridor. Figure 16 B, C, and D show the peak neck angle, head rotational velocity, and head rotational acceleration corridors respectively, similarly to Figure 16 A. Far less data was available for the rotational velocity and acceleration of the head, therefore data was not available to display relative to the validation corridor.

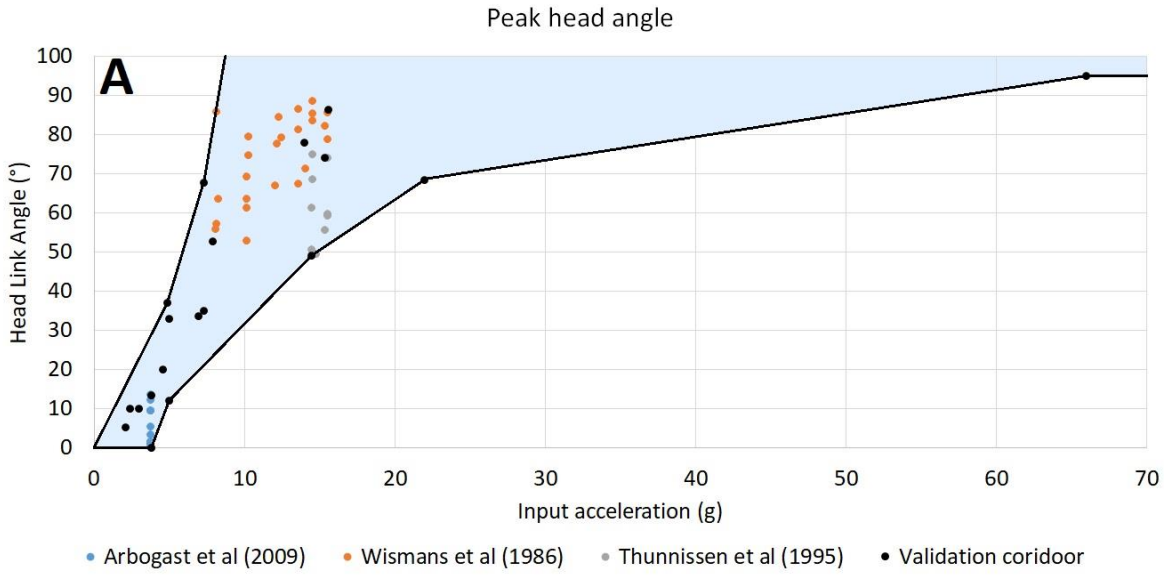

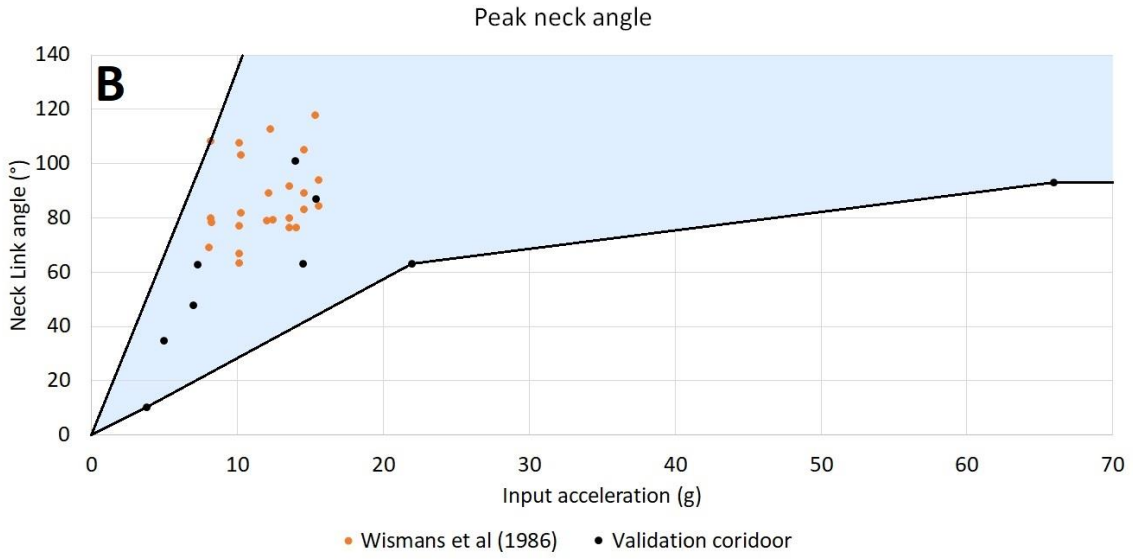

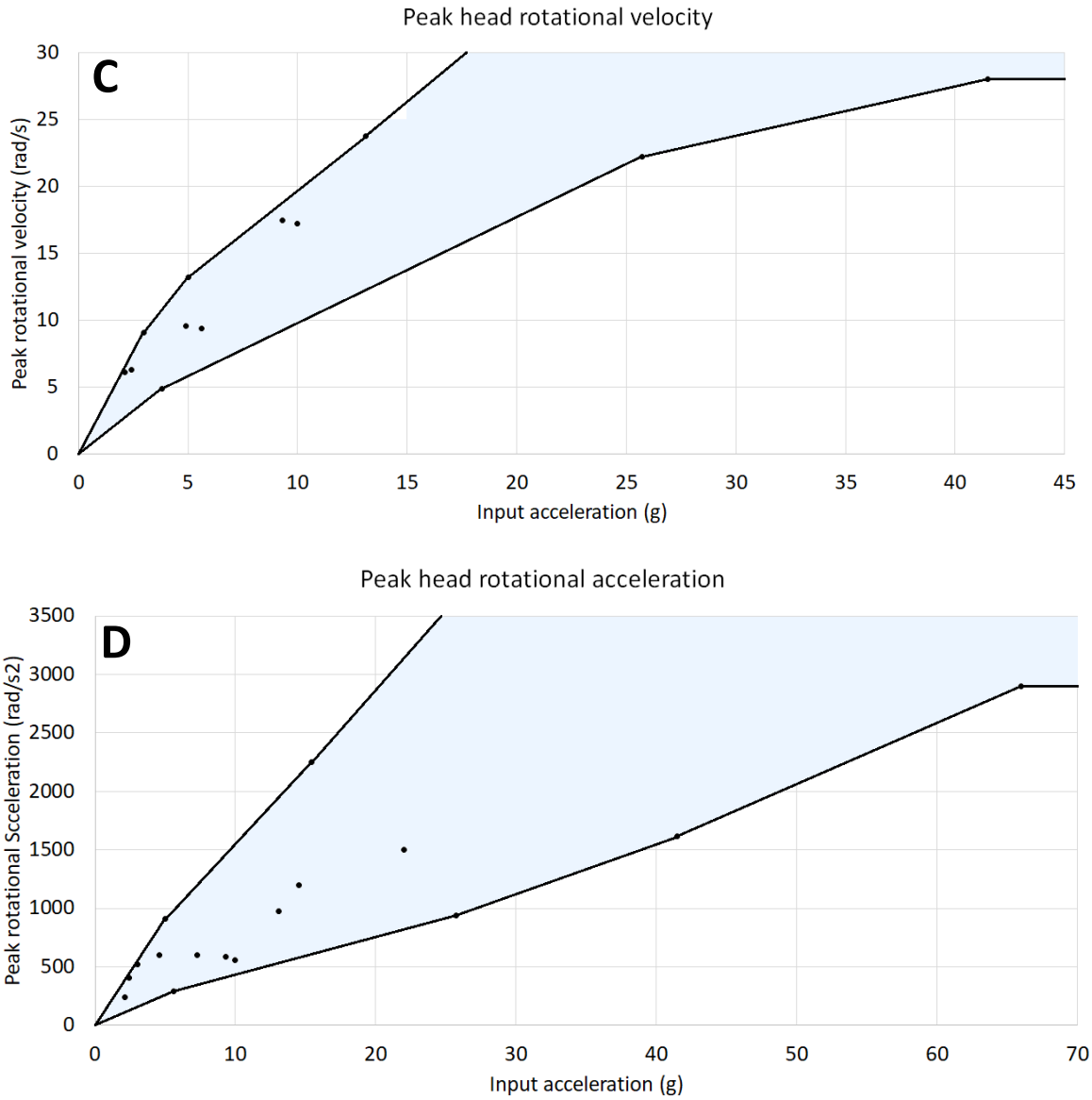

Figure 16 A - D: Validation corridors created using the published data (Ewing, Thomas et al. 1969, Ewing, Thomas et al. 1978, Thunnissen, Wismans et al. 1995) (Wismans, van Oorschot et al. 1986, Wismans, Philippens et al. 1987, Van den Kroonenberg, Philippens et al. 1998)

3.2 Neckform impact testing method

Impact velocities used across previous human trials sit in the range of 3.1 – 17.5 m/s for frontal testing with peak T1 accelerations of 4.9 – 66 g. The Humanetics impact velocities are 7 and 6m/s for flexion and extension with peak accelerations of 27.5 and 21.2 respectively, created by allowing the pendulum impact a block of aluminium honeycomb with a density of 28.8 kg/m^3. The specific type of aluminium honeycomb was not available and manufacturers for this this are limited in New Zealand. This meant 28.8 kg/m^3 density honeycomb was effectively unavailable. Therefore, a new method of creating input accelerations and durations was established, then compared to the literature.

The decision was made to replicate, as closely as possible, the accelerations and velocity changes reported for human volunteers. In doing so, it was assumed that the humanetics pendulum parameters would be easily replicated in the process. The first step was recreating

the range of accelerations over range of velocities used to develop the validation corridors in Figure 16. Initially, two different samples of aluminium honey comb were used as an impact surface for the pendulum. These had the densities of 48 and 95kg/m^3 with thicknesses of 30 and 50mm respectively.

Through preliminary trials, it was found these did not recreate the desired accelerations as they were far too thin, and far too dense. The accelerations were only recorded for the 95kg/m^3 honeycomb, oriented with the length of the honeycomb cells perpendicular to the pendulum impact direction. If honeycomb was oriented with the length of the cells in the direction of pendulum travel, accelerations were far too high for the given impact velocity. The perpendicular orientation, however, was only offering amortisation up to ~2.8m/s impact velocity. Above this, the honeycomb fully compressed and accelerations increased drastically. This is seen in Figure 17 as a sharp increase of the linear slope of the velocity vs T1 acceleration data.

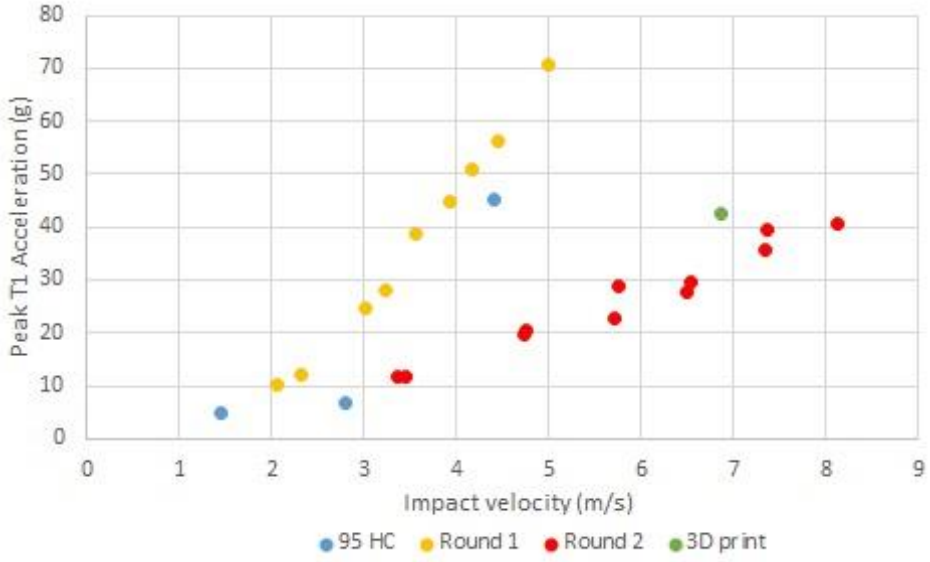

Figure 17 Peak accelerations at the base of the neck for the impact velocities measured

The second preliminary trial (labelled 3D print in Figure 17) used a 3D printed cellular structure with properties tailored to approximate the impact conditions required. This produced the resultant impact accelerations, but showed the closest match to the Humanetics impact conditions. This also led to another problem; failure of the neck (Figure 21). Considering each 3D print structure block required at least 24 hours continuous printing to create, it was deemed unsuitable for continued use.

The first round of measured and processed trials began (labelled as Round 1 in Figure 17), this time using foam slabs as the impact surface. Alternating layers of viscoelastic open cell polyurethane foams were used (Figure 17). These were the Confor green (13mm thickness, manufactured by Trelleborg) and the Sunmate (13mm thickness, manufactured by Dynamic systems Inc.), with the Confor green being far stiffer and denser than the Sunmate. 2 – 3 layers of the foam combination were used with one layer being one piece of each of the foams (Figure 18). Trials were carried out with the head and neck attached to the pendulum, and

data was recorded for both frontal flexion and rear extension. The pendulum was released from heights of 0.2 – 1m in steps of 0.2m. This distance was measured from the ground to a fixed point at the base of the neck. The pendulum acceleration results (Figure 17) show the material bottoming out at around 2.5m/s impact velocity (20 – 40cm drop height). Following this, accelerations rose sharply, until failure of the neck occurred.

More foam slabs were added to avoid bottoming out (Figure 18), and a fourth set of impacts were carried out (labelled as Round 2 in Figure 17). All foam pieces were inspected manually for signs of degradation, however none were present. Impact heights were 0.4 – 2m in steps of 0.4m. Figure 17 shows the foam did not bottom out at any of these heights. Additionally, the foam gave a much shallower increase in acceleration as the impact velocity increased, closer to that reported in the literature.

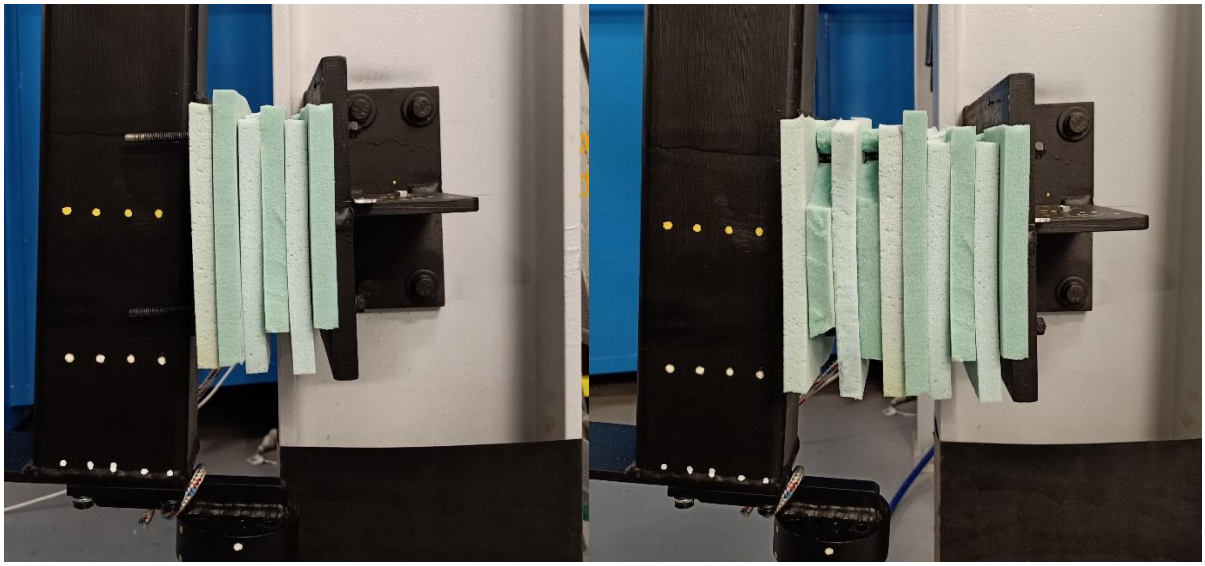

Figure 18 impact surface for the pendulum showing the alternating foam slabs with those on the left associated with testing Round 1, and those on the right for Round 2

3.3 Data collection and processing

Video analysis was used to evaluate the impact speed and acceleration of the pendulum (T1) as well as the rotational kinematics of the head and neck. A Photron SA-X1 camera was pointed at the impact area, filming at 1000fps and 1/8000s shutter speed. Higher frame rates were found to produce significant noise during post processing due to the smaller movements between each frame. Slower shutter speeds resulted in image blur, whilst shorter speeds excessively darkened the image.

All areas of interest were painted matte black, with an array of white tracer dots drawn over the top. This array was drawn such that at each location of interest, there was at least 4 points in a straight line. These dots were used for motion tracking in image processing software GOM Correlate (https://www.gom.com/3d-software/gom-correlate.html). The minimum radius for point identification was set to 1.5 pixels. Maximum residual grey value adjustment was set to 0.15, and minimum ellipse contract was 25 grey values. The scale of the image was set based on the white beam that the pendulum was attached to. This was 1.5 pixels/mm, and remained constant throughout testing as the camera never moved. Preliminary trials showed GOM

Correlate struggled to pick up on all points throughout the length of the impact and rotation of the head. This was due to the shape of the head and neck. Because using the high speed camera required using bright LED lights, reflections were created on the head and neck. These reflections often aligned themselves with the white points drawn on the head and whilst moving through their motions. This was not an issue for the flat surface of the pendulum itself.

To find the impact velocity of T1, identification points were created on the base of the neck (Figure 19). This was chosen as it was the last element rigidly fixed to the pendulum itself before the rubber neck elements. As many points as possible were selected to achieve reliable data output throughout the tests. This also allowed an average of many points to be taken, increasing the accuracy of the results.

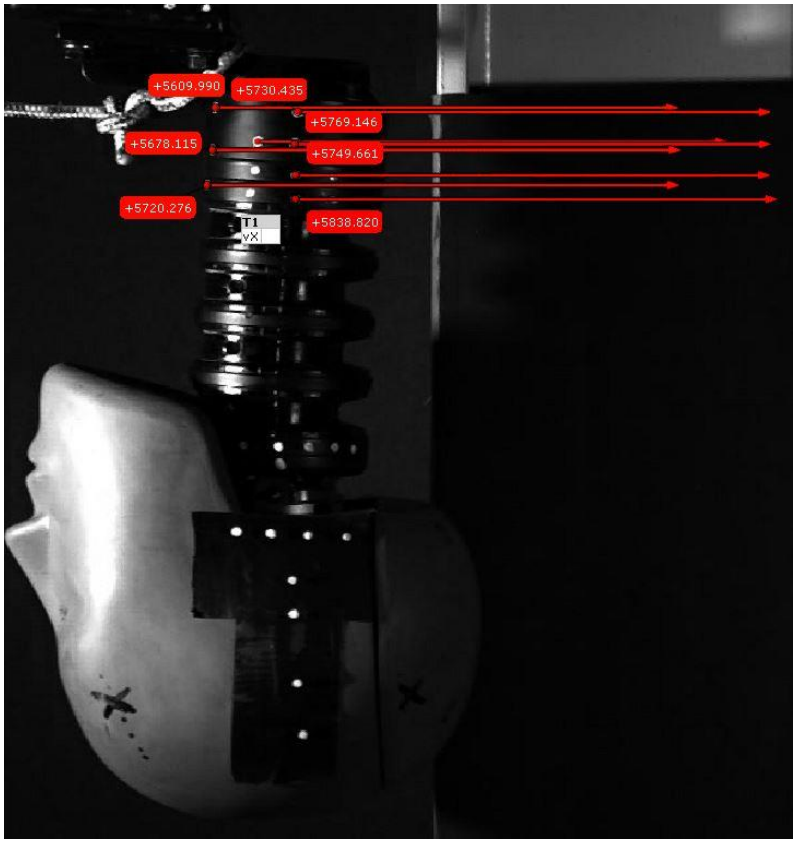

Figure 19 tracking dots on the base of the neck (T1) showing the horizontal velocity of each point

Following this, lines were created at T1, and also on the neck and head. The neck motion was assessed at the top of the neck near the occipital condyles joint. The head motion was evaluated both at plane D, and along the centre of gravity. To find angular motion, angles were created between the lines on rigid and moving areas (Figure 20). Multiple of these angles were created between each of the elements for the same reasons given previously. Only the velocity of the pendulum and the angular displacement of the head and neck were assessed in GOM Correlate. Differentiated data (linear acceleration, rotational velocity, and rotational acceleration) was not taken from GOM Correlate as it relied on the “smoothness” of the undifferentiated data. This data was not always smooth as reflections and errors in

tracking inhibited certain points from proper identification creating erratic data with large errors.

Data was collected into excel and any spurious data, such as data spikes up to 10 times greater than peak values, were removed. Data was then imported into MATLAB for continued processing. Pendulum velocity data had a moving average applied to it to smooth the data. This was then averaged to find the overall, continuous T1 velocity, then differentiated to find the T1 acceleration. This acceleration data had a subsequent moving average applied to it to further smooth the data. Due to the high number of data points, these moving averages did not affect the overall shape of the data, but rather removed much of the noise, revealing the underlying kinematics. A similar process for each of rotational velocity and acceleration was carried out, however it was found that a moving average did not smooth the data enough for reliable extraction of information.

The rotational displacement data was used to fit a curve using the Matlab “cftool” function. The head and neck rotation data was fitted with a sine curve of as many terms as needed to achieve the highest R^2 value. The lowest R^2 value used for fitting was 0.9978, which was considered valid based on visual inspection of the two data sets. The fitted curves were differentiated and used for finding maximum rotational velocity and acceleration, along with the times at which these occur. Many of the differences between the fitted curve and the measured data set was considered an error in the measured data set, and therefore maximal values for differentiated data was taken from these fitted curves.

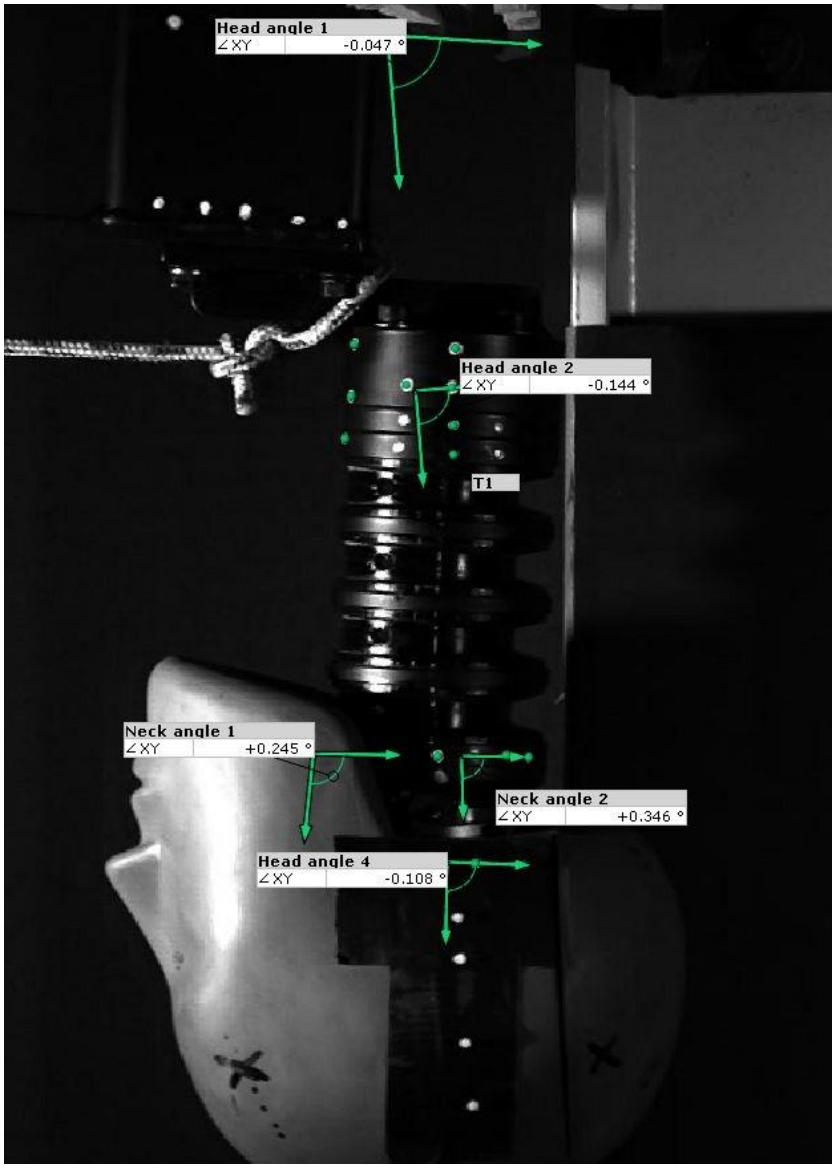

Figure 20 typical angle used for evaluation of the rotations of the head and neck

Errors were taken as the largest difference between the measured values of the data sets taken from GOM Correlate. These were propagated through the analysis and used as the uncertainties in the final data.

3.4 Neck design

3.4.1 First design

In keeping consistent with the H3 neck, an initial quote was sourced for casting the neck out of butyl rubber. Due to the asymmetric shape of the cast, this was quoted at over $3000 NZD. At the time this was not viable, therefore urethane rubber was chosen as the initial material as its mechanical properties were similar to that of the butyl. The urethane rubber, in a product named Task 16 by Smooth On Ltd., was used. It is a liquid part A and B mix which cures to a hardness of 80A shore hardness. The large rubber discs and nodding blocks were cast one at a time using a simple 3D printed mold (Figure 21), chosen due to the ease and cost efficiency of creating the difficult shape. Molding the rubber pieces one at a time meant the

whole assembly (Figure 21) consisted of separate parts held together with the centre tension cable.

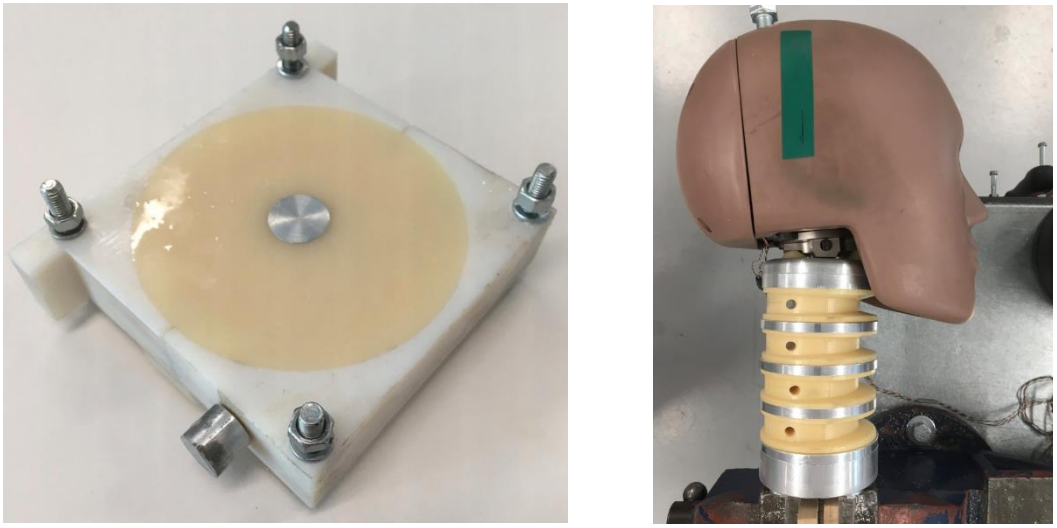

Figure 21: molding process for the individual pieces of the neck rubber (left). Complete first attempt of the neck (right)

This was tested in static loading and was found to fit into the biofidelic corridor proposed by Patrick and Mertz (Mertz and Patrick 1971). Static tests were completed outside of this project by the 2018 Final year projects team at the University of Canterbury (Adams, Stitt et al. 2018). This testing involved holding the base of the neck in a rigid clamp and applying weight to the top of the headform attached to the neck. This produced a measurable moment around the fixed point (representing the top of the thoracic spine (T1)) and the occipital condyles (OC), giving a rotation deflection of the neck and head. Further analysis of the methods used by Patrick and Mertz raised questions about the reliability and validity of the proposed method for the present study. This corridor was based on only one human subject and some post mortem data, therefore is of questionable reliability in itself. Additionally, Patrick and Mertz used dynamic loading instead of static loading. It was believed the neck would behave differently under a dynamic load.

Whilst carrying out these validation tests, high speed imaging revealed a problem with the design. Since all parts were molded separately, movement was permitted between the aluminium disks and the rubber inserts, despite being held together by the tension cable (Figure 22). In preliminary drop testing, the rubber and aluminium pieces moved significantly during each impact, leading to large repeatability errors.

It was found that the methods used by Humanetics to cast the neck was such that the rubber and aluminium did not separate during a bending event. In light of this finding the neck was secured differently. The same individual rubber and aluminium pieces were used, however the whole assembly was glued together using Maverick Bond, one of the strongest permanent bonding substances available suited for both urethane and aluminium. This however resulted in the glued neck assembly failing under impact load as shown in Figure 22. The first rubber insert (closest to the base of the neck) failed first, following which, the load was transferred fully through the tensioning cable. As a consequence, the tensioning cable also failed.

Based on this preliminary trial, a new set of design requirements were set for the neck:

1. The neck had to be manufactured without the need for adhesive use
2. Rubber inserts should not separate and move during validation impact testing or throughout drop testing thereafter

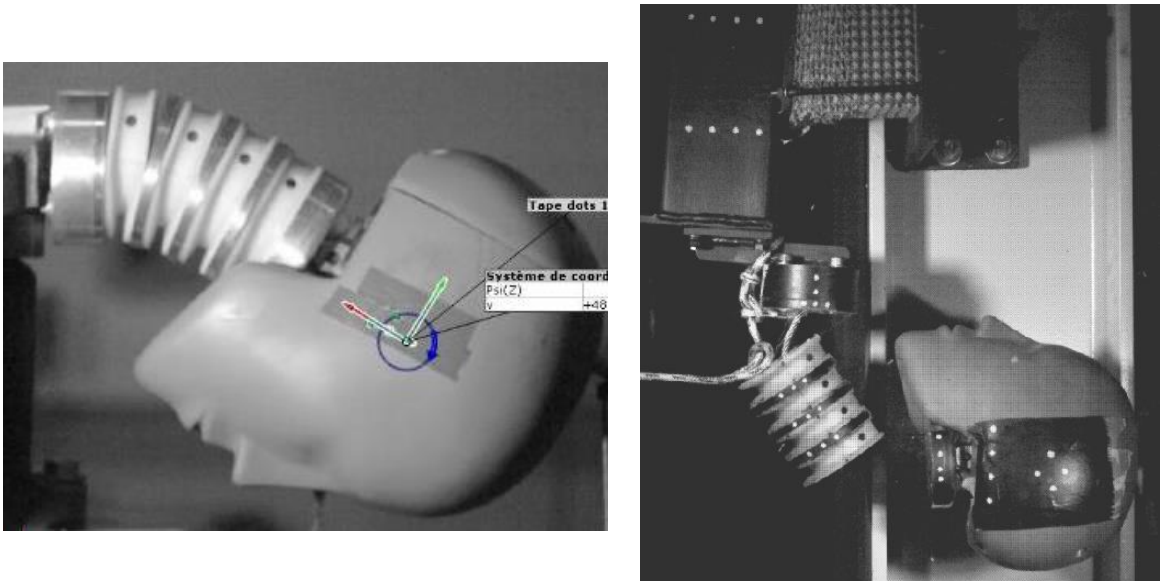

Figure 22: Video image of the validation carried out on the first neck showing the separation of the rubber and aluminium along the back of the neck (left). Second attempt at validating the neck showing failure of the neck internal cable and separation of the discs (right)

3.4.2 Improved neckform design

The second attempt required remanufacturing the aluminium pieces and rethinking the casting method. Instead of using flat and smooth aluminium inserts, each one had an undercut groove at the outer edge of where the urethane sits (Figure 23). This was undercut at an angle of 9° and a depth of 2.5mm ensuring the urethane did not peel away at the edges given a large bending event. In each downward facing groove air holes were drilled to release air bubbles that would get caught when pouring the urethane.

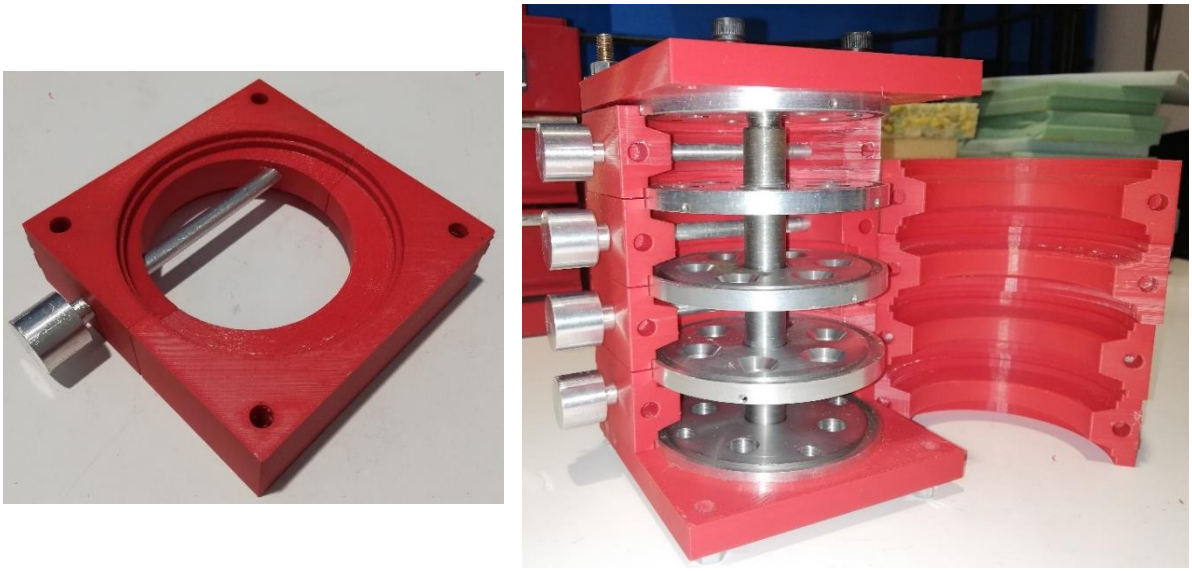

Figure 23: single layer of the mold showing the asymmetrical shape. Complete mold showing the inside cavity to be cast with urethane rubber (right)

In addition to this, 6 holes were drilled through each of the aluminium disks allowing the rubber pass through and cast as one single piece through all five disks. To cast the entire neck as one piece, a larger mold was constructed out of 3D printed blocks (Figure 23). The basic shape of each layer was the same as those used for the first design 3D printed molds. The urethane rubber was poured through the top of the mold until full, and left to set for 48 hours, until the material was fully cured.

Once this was completed, preliminary testing of the neck was carried out using the Humanetics pendulum methods. Failure of this neck occurred during extension testing (rear impacts). Similar to the first design, Figure 24 shows the failure of the base of the neck at the front. The rubber was pulled out of the undercut edges and peeled away at the first (lowest) insert. This is where most of the bending stress is concentrated as it is transferred through the front of the neck to the base. This occurred on the final impact, and data was collected for all impacts until failure occurred.

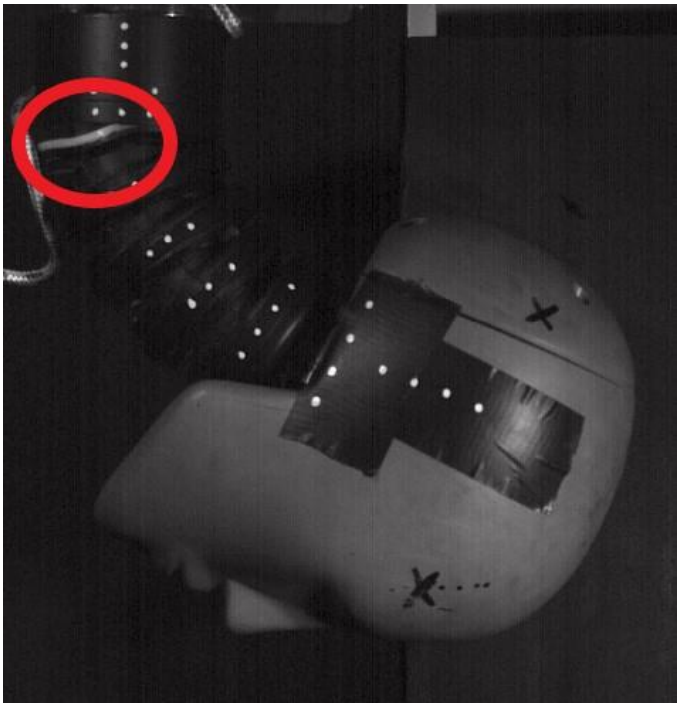

Figure 24 Second design of the neck showing the failure during rear end impacts

3.4.3 Further neckform design modifications

The second design of the neck yielded the results shown in Figure 27 – 30. Comparison to the validation corridors showed the neck was too stiff. There were two feasible explanations for this:

1. The neck materials were inherently too stiff.
2. The method of neck testing involved impact energies exceeding those in similar studies.

The first of these was addressed by attempting to cast the neck from silicone rubber. The aluminium discs were manufactured the same as the previous (second) design, however the silicone rubber had a far lower shore hardness, (45 A) therefore would allow greater rotation for the same applied force. This particular silicone rubber, whilst being far softer once fully cured, was far more viscous than the urethane rubber when first mixed. Additionally, the set time was shorter for the silicone than the urethane rubber. Due to these two properties, casting the neck with this material, in this particular way did not work. Figure 25 shows the final product using a silicone based rubber.

Figure 25 Attempt at casting the silicone neck

Only part of the mould filled with the rubber. As the rubber was being poured, the stream became thicker and wider as the rubber quickly set. This lead to the mold filling at the top and trapping large air pockets inside giving a false indication the mold was filled with rubber. This was allowed to set for 48 hours undisturbed.

To get a rough idea of its ability to withstand the validation testing, once set, the silicone neck was subject to manual bending. This was carried out by hand, imparting comparatively small amounts of force. The silicone rubber easily pulled out of the undercut grooves and was easily torn out of the aluminium holes. From this it was inferred that the silicone rubber was both too weak and required a different casting method to make its use a viable option.

3.4.4 Final neckform design

The fourth design used the same urethane rubber which produced the first and second designs. This time, however, greater impact energies were to be used. As noted earlier, the bending force is transferred from the head through each section of the neck, to the base, where the rubber had to hold the total bending force. With this in mind, all groves were cut with a more aggressive undercut angle (up to 13°), with the discs at either end of the neck having far deeper grooves cut. In addition to the deeper grooves, two M3 button head screws were added to the front of the base of the neck (point of maximum bending force and point of failure on previous designs). Figure 26 shows the neck during the maximum rotations achieved during testing.

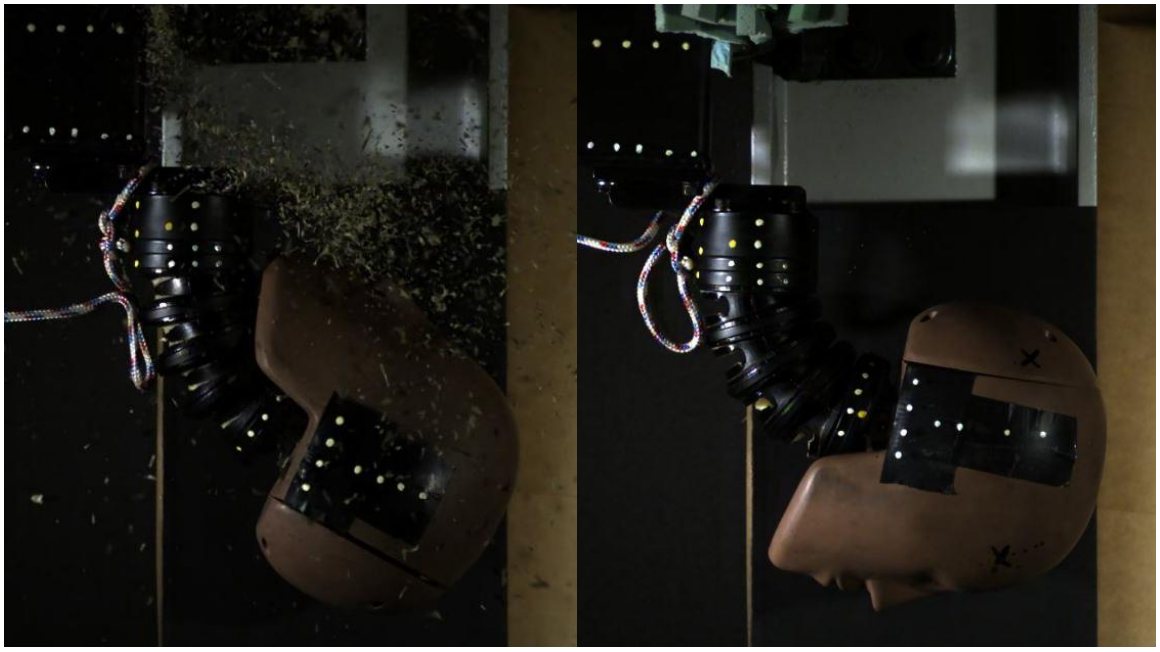

Figure 26 maximum rotation angle of the neck for flexion (left) and extension (right)

Despite the previous changes, the tensioning cable was kept the same as the cable was not the first component to fail on the first design, the glue was. The cable would not have experienced any issues had the glue not failed first, therefore this was not upgraded. This design was the first to withstand all the testing impacts. The results from this neck were the last recorded as time restrictions limited further development of the H3 replica neck.

3.5 Neckform impact test results

Figure 27 shows the head link angle for each impact measured. The majority of the data sits outside the validation envelope. The first round of testing (shown in red, displaying results for the second neck design) displays lower rotation angles for the same input acceleration than those measured in the second round of testing (yellow, final neck design). The first and second rounds pertain to the impact created with the conditions labelled round 1 and round 2 respectively (Figure 17 and 33). The differences between the two test runs was limited to the input velocity, and the amount of foam used as the impact surface. Both generated accelerations within the same range. This displays the importance of properly recreating the velocity and acceleration parameters when testing a model neck with comparison to human volunteer studies.

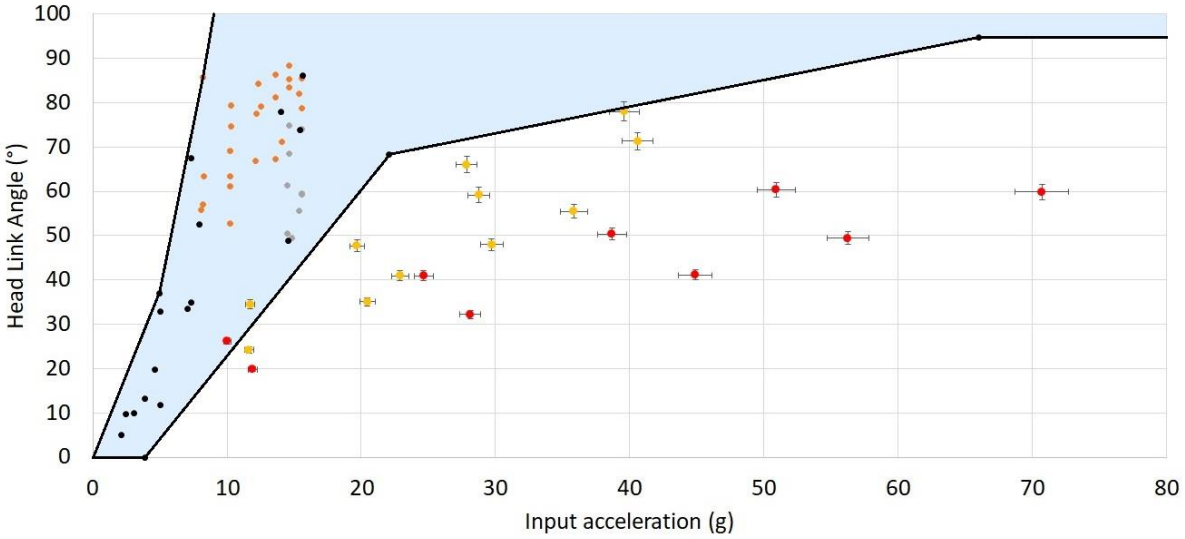

Figure 27 Peak head rotation angle with the first round of testing (round 1) shown in red and the second shown in yellow (round 2)

Figure 28 shows the peak neck rotation angle for all impacts. Similar to the head angle, almost all data sits outside the validation envelope. Additionally, there are visible differences between the first round of testing, and the second. Both Figure 27 and 28 show that the neck is stiffer than what has been reported for human volunteer necks. It is however, clear that the exact velocities and accelerations used in the literature were not recreated (Figure 33). What can be seen is an increase in the impact velocity results in a greater rotation of both neck and head for the same peak acceleration. This indicated that if impact conditions can more closely match those in the literature, the neck could potentially inhabit the validation envelope. Recreation of these conditions was not achievable with the current setup however, as there were physical size and range of motion constraints set by the location of the pendulum.

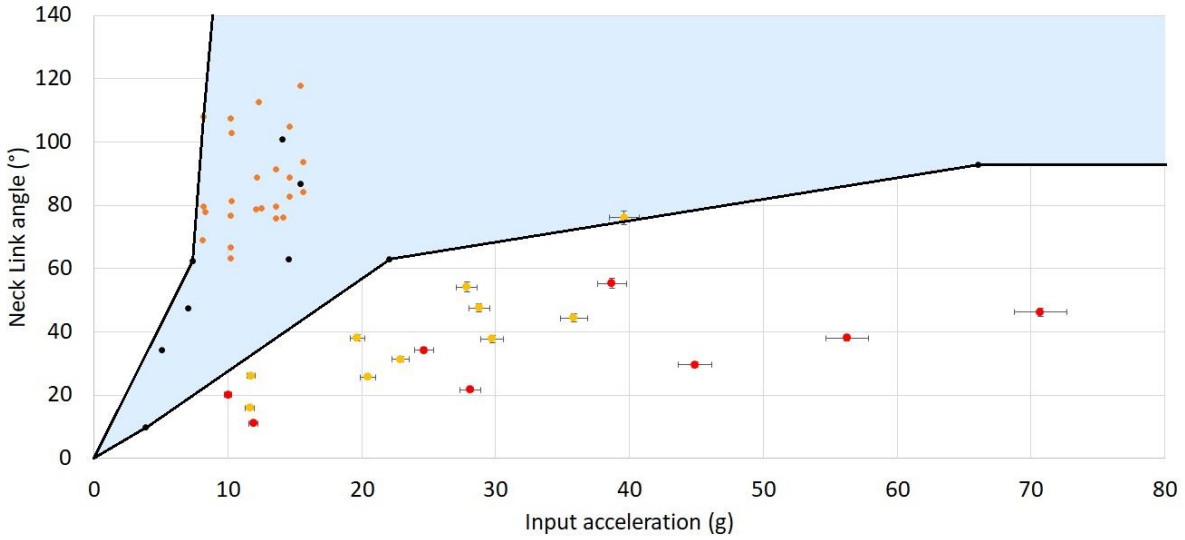

Figure 28 Peak neck rotation angle with the first round of testing shown in red and the second shown in yellow

Figure 29 shows the peak rotational velocity of the head for each impact. Much of the data sits comfortably within the validation envelope. Contrary to the results for rotation angle, the head displays higher rotational velocity for the second round of testing (shown in yellow).

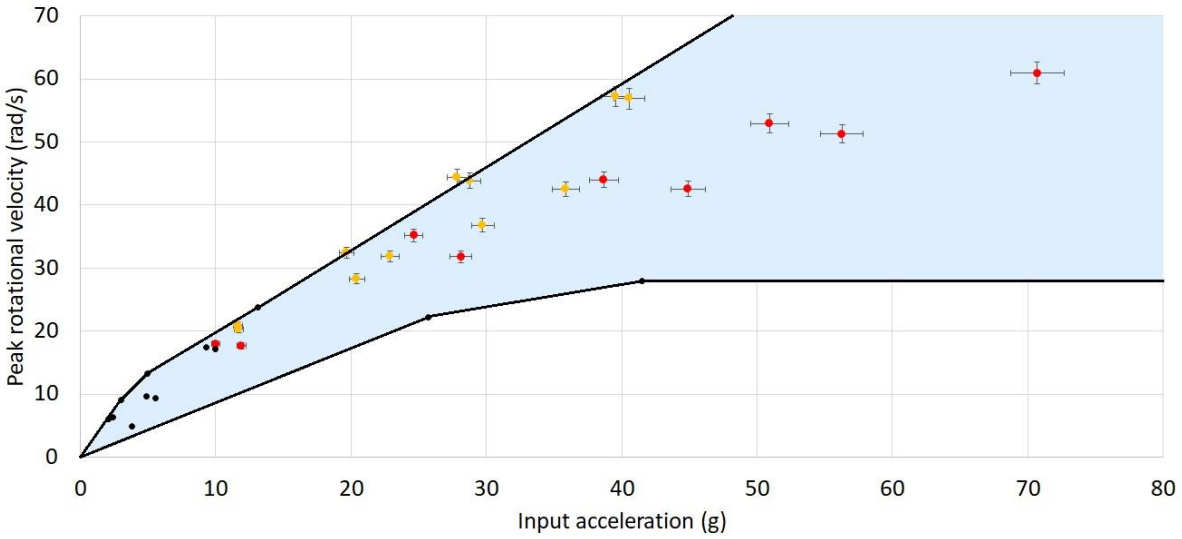

Figure 29 Peak rotational velocity of the head round of testing shown in red and the second shown in yellow

Figure 30 shows the peak rotational acceleration of the head. Similar to the peak rotational velocity, much of the measured data sits within the validation envelope. The data from the second round of testing sits further towards the middle of the envelope, and is lower than the data measured from the first round.

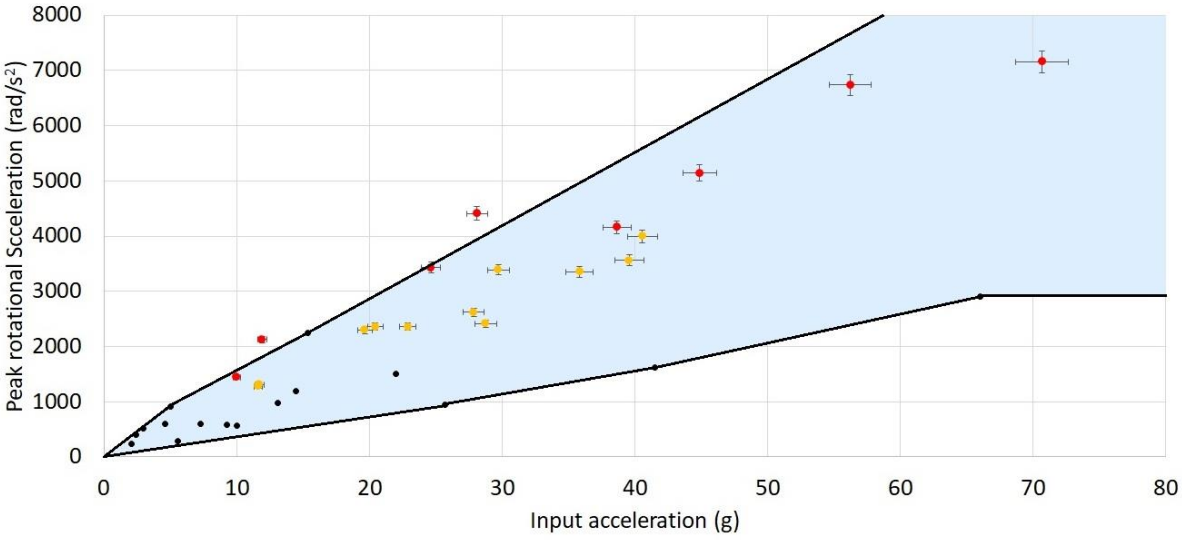

Figure 30 Peak rotational acceleration of the head round of testing shown in red and the second shown in yellow

Table 11 shows all of the data measured for each impact tested in both Round 1 and 2. It should be noted that the peak times are taken from the onset of impact, defined as the moment the horizontal velocity decreases on average for more than three frames. In general, the second round of testing had longer times to reach peak values.

Table 11	Mean (SD) peak values from neck testing														
Round 1 testing															
	T1 vel (m/s)	**T1 acc (g)**	**Time (ms)**	**Neck angle (°)**	**Time (ms)**	**Head angle (°)**	**Time (ms)**	**Neck RV (rad/s)**	**Time (ms)**	**Head RV (rad/s)**	**Time (ms)**	**Neck RA (rad/s²)**	**Time (ms)**	**Head RA (rad/s²)**	**Time (ms)**
Frontal	2.3 (0.1)	11.9 (0.4)	17	11.0 (0.3)	44	19.9 (0.6)	43	9.5 (0.3)	62	17.7 (0.5)	75	968.1 (28.1)	42	2125.4 (61.6)	39
	3.2 (0.1)	28.1 (0.8)	16	21.7 (0.6)	42	32.2 (0.9)	41	18.1 (0.5)	65	31.8 (0.9)	31	3165.4 (91.8)	40	4409.0 (127.9)	39
	3.9 (0.1)	44.9 (1.3)	14	29.6 (0.9)	41	41.2 (1.2)	40	25.3 (0.7)	33	42.6 (1.2)	31	5850.2 (169.7)	31	5143.8 (149.2)	35
	4.5 (0.1)	56.3 (1.6)	12	38.1 (1.1)	41	49.5 (1.4)	41	33.2 (1.0)	33	51.3 (1.5)	29	7037.5 (204.1)	30	6741.8 (195.5)	35
	5.0 (0.1)	70.7 (2.1)	11	46.3 (1.3)	42	59.8 (1.7)	41	39.7 (1.2)	31	60.9 (1.8)	29	7244.7 (210.1)	29	7156.0 (207.5)	39
Rear	2.1 (0.1)	10.0 (0.3)	19	20.1 (0.6)	59	26.2 (0.8)	55	9.6 (0.3)	107	18.0 (0.5)	35	2639.7 (76.6)	59	1442.7 (41.8)	47
	3.0 (0.1)	24.7 (0.7)	17	34.2 (1.0)	60	40.9 (1.2)	49	18.9 (0.5)	22	35.2 (1.0)	34	7725.1 (224.0)	25	3427.8 (99.4)	41
	3.6 (0.1)	38.7 (1.1)	14	-	-	50.4 (1.5)	47	-	-	44.0 (1.3)	33	-	-	4163.3 (120.7)	40
	4.2 (0.1)	50.9 (1.5)	13	55.3 (1.6)	59	60.4 (1.8)	66	34.1 (1.0)	37	52.9 (1.5)	30	8900.0 (258.1)	24	5057.0 (146.7)	42
Round 2 testing															
	T1 vel (m/s)	**T1 acc (g)**	**Time (ms)**	**Neck angle (°)**	**Time (ms)**	**Head angle (°)**	**Time (ms)**	**Neck RV (rad/s)**	**Time (ms)**	**Head RV (rad/s)**	**Time (ms)**	**Neck RA (rad/s²)**	**Time (ms)**	**Head RA (rad/s²)**	**Time (ms)**
Frontal	3.4 (0.1)	11.6 (0.3)	22	16.0 (0.5)	54	24.2 (0.7)	51	11.6 (0.3)	70	20.9 (0.6)	83	1049.3 (30.4)	55	1276.8 (37.0)	55
	4.8 (0.1)	20.5 (0.6)	22	25.7 (0.7)	50	35.1 (1.0)	48	18.3 (0.5)	68	28.3 (0.8)	81	1705.4 (49.5)	52	2356.0 (68.3)	45
	5.7 (0.2)	22.9 (0.7)	26	31.3 (0.9)	53	40.9 (1.2)	52	21.6 (0.6)	73	31.8 (0.9)	85	2001.9 (58.1)	55	2357.0 (67.0)	45
	6.5 (0.2)	29.7 (0.9)	25	37.8 (1.1)	53	48.0 (1.4)	52	26.3 (0.8)	72	36.8 (1.1)	37	2756.0 (79.9)	50	3390.0 (98.3)	49
	7.4 (0.2)	35.9 (1.0)	25	44.4 (1.3)	52	55.5 (1.6)	51	30.9 (0.9)	72	42.5 (1.2)	36	2986.2 (86.6)	50	3352.4 (97.2)	48
	8.1 (0.2)	40.6 (1.2)	19	-	-	71.3 (2.1)	49	-	-	56.8 (1.6)	83	-	-	3393.3 (115.8)	47
Rear	3.5 (0.1)	11.7 (0.3)	23	26.1 (0.8)	65	34.5 (1.0)	62	21.2 (0.6)	11	20.3 (0.6)	38	1220.8 (35.4)	128	1312.0 (38.0)	127
	4.7 (0.1)	19.7 (0.6)	24	38.1 (1.1)	64	47.6 (1.4)	64	20.1 (0.6)	43	32.4 (0.9)	38	1206.7 (35.0)	63	2300.0 (66.7)	48
	5.8 (0.2)	28.8 (0.8)	26	47.5 (1.4)	64	59.2 (1.7)	65	25.5 (0.7)	37	43.9 (1.3)	40	1397.2 (40.5)	59	2413.0 (70.0)	55
	6.5 (0.2)	27.9 (0.8)	26	54.2 (1.6)	65	66.0 (1.9)	64	28.3 (0.8)	39	44.4 (1.3)	38	1590.4 (46.1)	53	2623.2 (76.1)	263
	7.4 (0.2)	39.6 (1.1)	28	76.1 (2.2)	67	78.0 (2.3)	67	37.1 (1.1)	44	57.2 (1.7)	41	2729.1 (79.1)	65	3558.1 (103.2)	30

Figures 31 and 32 shows how the two closest velocity/acceleration tests matched the requirements of the Humanetics standard. Figure 31 shows the T1 acceleration for the flexion and extension impact. The acceleration of the pendulum takes far longer to peak and has a different shape to what is required by the standard. These two tests were carried out at ~5.7m/s impact velocity which is also lower than both flexion and extension requirements of 7 and 6m/s respectively.

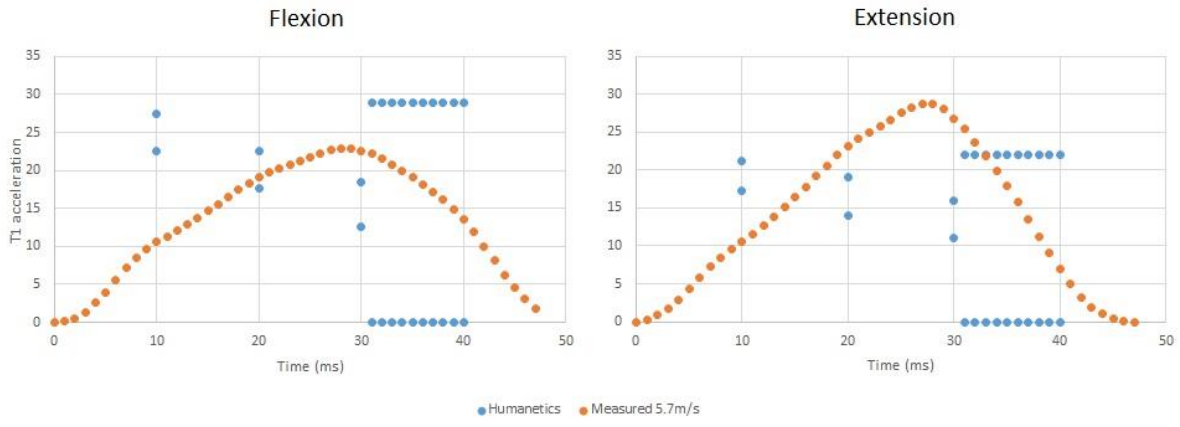

Figure 31 acceleration of the closest matching impact to the Humanetics standard compared to the requirements set in the standard

Figure 31 shows how the rotation angle of the head compared to the standard for the same two tests. The peak rotation is far lower than the requirements for both flexion and extension. The zero crossing also occurs much earlier for both tests, however, the peak rotation occurs close that of the standard.

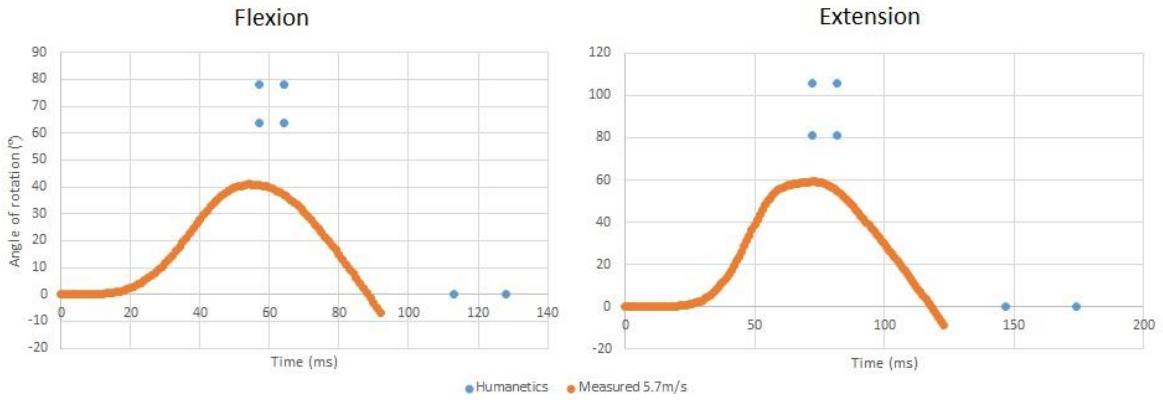

Figure 32 Head rotation for the two closest matching impact to the Humanetics standard compared to the requirements set in the standard

3.6 Discussion

3.6.1 Neck performance

Despite being cast from the same material, there were clear differences in the behaviour of the two neck designs tested (second and final neck designs). This is likely due to the differences caused by changing the impact conditions. The first round of testing showed high peak accelerations for the impact velocities measured. This was due to the amount of foam present for the pendulum to impact. Less foam meant less time for deceleration before bottoming out, therefore drop height (and corresponding velocity) was limited. Figure 33 shows the peak accelerations for the impact velocities measured compared to those used in the literature.

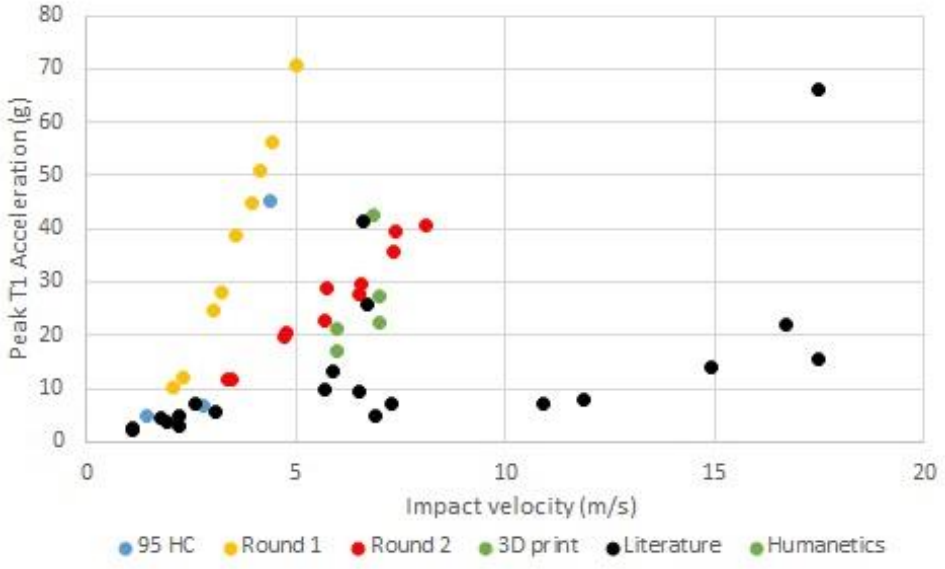

Figure 33 Peak accelerations of the pendulum during testing compared to those reported in past studies and those in the Humanetics validation standard (Ewing, Thomas et al. 1969, Ewing, Thomas et al. 1978, Thunnissen, Wismans et al. 1995) (Wismans, van Oorschot et al. 1986, Wismans, Philippens et al. 1987, Van den Kroonenberg, Philippens et al. 1998)

The second round of testing came closer than the first to recreating the impact conditions used in the literature. From Figure 33 however, it is debatable whether any of these were within the 'literature' range. Many of the tests in literature have a far lower peak acceleration

for the impact velocity than those measured in this investigation. As seen in Figures 27 - 30 as the impact velocity and acceleration get closer to that used in past studies, the head and neck kinematics get closer to the to that of the human head and neck. The higher the input velocity the greater rotation of both head and neck for any given acceleration. It is however, unknown whether given the appropriate impact conditions, the head and neck response would fit within the validation corridor. Despite the best efforts to recreate the impact conditions in the literature, there were some insurmountable differences inherently present using this experimental set up. The maximum height the pendulum could reach was 2.5m (120°, ~8m/s). This does not offer as large of a change in velocity as what is used in many of the studies which used upwards of 10m/s velocity change for testing frontal flexion.

In addition, the material of the rubber part of the neck, despite similar nominal stiffness, did not perform similarly to the butyl rubber used in the H3 neck. The H3 neck was noticeably softer than the final neck design. This difference in stiffness was not quantified, however was noticeable when bending the neck by hand. The difference in properties of the two materials lead to other differences in testing. The urethane rubber used for the new neck did not have the same damping properties as the rubber used for the H3 neck or the human neck data. This however was not investigated in any depth for the present study. Figures 31 and 32 displayed how the neck behaved when compared to the Humanetics standard. The two impacts chosen were those that most closely represented the accelerations and velocities in the standard. Both accelerations peaked much later than the standard requires. The foam used to create the accelerations behaves much differently to the aluminium honeycomb used in the standard. Aluminium honeycomb compresses with a constant force, whereas compression of the foam requires increasing force as the foam is crushed. This lead to a smaller acceleration initially, which increased as the pendulum crushed the foam.

The silicone neck could not be cast using the same methods as the urethane neck. The casting method relied on gravity to move the liquid material through the neck structure. The silicone was too viscous once mixed to flow through the structure properly. In an ideal case, this would be injected into the mould.

There were multiple difficulties associated with creating the validation criteria. There is a sufficient lack of reliable data on the behaviour of the human volunteer neck to acceleration events. The data that does exist is, for the most part, of questionable quality. The data for the rear impacts was performed with a head rest which limited head movement. Additionally, T1 movement was not always quantified, creating errors that prevented data from being used to create validation corridors. There is also a lack of published data for the torsion, flexural stiffness, static properties, and compressive strength of human necks. For a full validation of any neck model, these properties would need to be known. These were not investigated in this study as there was little to no published data for comparison. Another comparison not made in this study was that of the shapes of the response data for the neck against the human volunteer necks. Comparing the shapes of the rotational response curves would provide a great deal more information about how the neck form compares to human head and neck system.

3.6.2 Alternative solutions

Since the development of the H3 neck by Humanetics, there have been significant advancements made in the biofidelity of neck design. Some of the newer types are the THOR 50th percentile male, and the BioRID II neck. The THOR 50th male neck uses aluminium and rubber, however also incorporates spring tensioned steel cables for a varied stiffness along the different directions. The BioRID II uses a complex series of pin joined "vertebra" which use a cable to supply stiffness to flexion and extension bending directions. These have been shown to provide far greater biofidelity than the H3 neck design.

These newer neckforms, however, are far more complex in terms of manufacture than the H3 neck, creating their own subset of issues for use. There are multiple improvements that could be made to the design of the H3 style neck proposed in this study. Other casting materials such as Latex rubber that is available in NZ could be used to provide a lower stiffness.

3.7 Conclusion

The neck designed and built in this study did not meet the validation requirements. The testing methods could be the reason for this as the impact testing conditions were different from those used in previous studies. As the conditions approached those reported in the published data, the response of the head and neck became closer to that of the human neck. If further tests are to be completed, the material or joining method to the aluminium would need to be updated. The H3 neck is by far the easiest to manufacture out of the biofidelic neckforms and as such is the best candidate to be modified to better represent the human neck response to impact conditions.

4 Laboratory validation of instrumented mouthguard for use in sport

Concussion is an inherent risk of participating in contact, combat or collision sports. In an ideal case, assessment of injured players is facilitated by a certified athletic trainer, team physician, or other health care provider on the side line, however, the vast majority of young athletes practice and play in circumstances where trained personnel are not immediately available (Graham, Rivara et al. 2014). Currently there are guidelines imposed on New Zealand sporting organisations where players thought to have sustained a concussive injury are removed from play immediately and monitored for symptoms (ACC 2015). This method relies upon the player correctly reporting the immediate symptoms, which hinders effectiveness, as there is a tendency for athletes to underreport their symptoms (McCrea, Hammeke et al. 2004, Dziemianowicz, Kirschen et al. 2012, Anderson, Gittelman et al. 2016). One epidemiological study of traumatic brain injury (TBI) in the US estimated an economic burden of $60 billion annually (Daneshvar, Nowinski et al. 2011). While in New Zealand this number sits at $2 million annually (Gaffaney 2014).

Currently wearable sensor systems exist giving real time impact information. The most common types are helmet integrated sensors, patch sensors and mouthguard sensors all of which measure peak linear acceleration (PLA), rotational velocity (PRV) and rotational acceleration (PRA). The first of which is the head impact telemetry (HIT) system manufactured by Virginia tech and finds common use in studies of American football or ice hockey. The HIT system uses 12 accelerometers with 6DOF to find the linear and rotational components of the impacts (O'Connor, Rowson et al. 2017). The array is embedded rigidly in hard shelled helmets. and accuracy of the device depends on the fit of the helmet (Jadischke, Viano et al. 2013). The data recorded by these helmets have helped to better understand concussive injuries in sports. One study used the data from this in conjunction with medical reports for head injuries to propose an injury risk function for concussion (Funk, Rowson et al. 2012). These sensors however, can only be properly used in sports in which players wear a hard shelled helmet.

Patch, headband and mouthguard sensors, are a more recent addition, and have found common use in sports without helmets such as football or rugby. Patch sensors are secured onto the skin using adhesive or a headband. When attached using adhesive, the patch sensors are commonly placed over the mastoid process behind the ear (O'Connor, Rowson et al. 2017). They measure head impacts using 3 linear accelerometers and a triaxial angular rate sensor. The most common patch sensor is the X-Patch, which was manufactured by X2 Biosystems. Laboratory validation studies have found the patch and headband sensors to have large errors. One study conducted on the X-patch found an error rate of up to 50% for PLA and PAA (McCuen, Svaldi et al. 2015) with another finding the patch to underestimate PRA by more than 25% on average (Nevins, Smith et al. 2015). A study conducted in 2017 found the patch to have a combined direction RMSE of 34% for PLA, 2.8% for PRV and 23.4% for PRA (Schussler, Stark et al. 2017) while in 2018 it was found that the patch underpredicted linear and rotational acceleration (Tyson, Duma et al. 2018). The same study found an even lower correlation between the kinematic parameters of the SIM-G headband and reference sensor which heavily under predicted the linear acceleration and rotational velocity, but over predicted the rotational acceleration.

Validation studies performed in vivo show similar results. Wu *et al* showed that both patch and headband sensors to have large errors compared to mouthguard sensors as both of these sensors can slip over the skull with the skin, giving false acceleration values (Wu, Nangia et al. 2016). Video imaging in this study showed a movement of 2-4mm during impact for the patch sensors and 2-13mm for the headband sensor relative to a marker secured in the ear. Skin patch estimation of PLA and PRA were over-predicted by 15 ± 7g and 2500 ± 1200rad/s^2 respectively. Additionally, Video validation of in game head impacts confirmed the X-patch has a positive predictive value of 16.3% for head impacts (Press and Rowson 2017). The mouthguard sensor showed far less movement in this study (<1mm). In laboratory validation study, the X2 mouthguard showed a linear regression slope of 1.01 for PLA, 0.9 for PRA and 1.00 for PRV compared to the headform reference sensors (Camarillo, Shull et al. 2013). The average normalised RMS error for these tests was 9.9 ± 4.4% for linear acceleration and 9.7 ± 7% for rotational acceleration. Furthermore it was shown the X2 mouthguard detected 95.4% of the impacts as valid, however performed poorly when estimating the impact directions (Siegmund, Guskiewicz et al. 2016).

Now a new mouthguard sensor has been developed by HitIQ. This mouthguard differs from others as it uses 3 triaxial accelerometers and a gyroscope to estimate resultant linear and rotational acceleration components of the impacts. This is different from the single accelerometer design used previously by other manufacturers. This mouthguard design currently lacks proper validation in a laboratory setting. Mouthguards have been shown to produce lower errors than other sensor systems on the market, and have a better coupling to the head. Because of this, it is important to quantify the errors produced by this new mouthguard sensor before it becomes available for use on the market. The purpose of this study therefore, was to validate the HitIQ mouthguard in a laboratory setting. This was achieved by comparing the PLA, PRA and PRV values and the signal traces of the mouthguard to a reference accelerometer pack inside a 50th percentile male headform.

4.1 Mouthguard drop testing method

Testing of the mouthguards was carried out using a gravity induced drop test rig, based on proven models of twin wire drop test rigs. Impact locations were front, front boss, side, rear, rear boss described in the NOCSAE standard for impact testing of headgear (NOCSAE 2017). Figure 34 shows these impact locations. The headform used was based on a hybrid III 50th percentile male headform, modified to include a rigidly fastened top jaw (Figure 35). This headform was made of aluminium and did not have the skin cover that the hybrid III headform has. The headform was fitted with an array of 3-axis accelerometers around the centre of mass of the headform. There were at total of 4 triaxial accelerometers inside the headform. These were arranged orthogonally to each other. The neck used was a Hybrid III neck. The mouthguard used in the study was the HitIQ Nexus. The accelerometers sample at a rate of 3200Hz, and the gyro samples at 800Hz and are triggered when a threshold value of 10g is reached. Once the threshold value is reaches, the sensors capture data from 20ms before and 80ms post trigger time, however there is also a retrigger function which will allow the mouthguard to capture data for longer if the impact event exceeds this time. Two of these mouthguards were included in the analysis to see if there was any difference between them. Both of these mouthguards were molded specifically to fit the top jaw, ensuring no movement during impact.

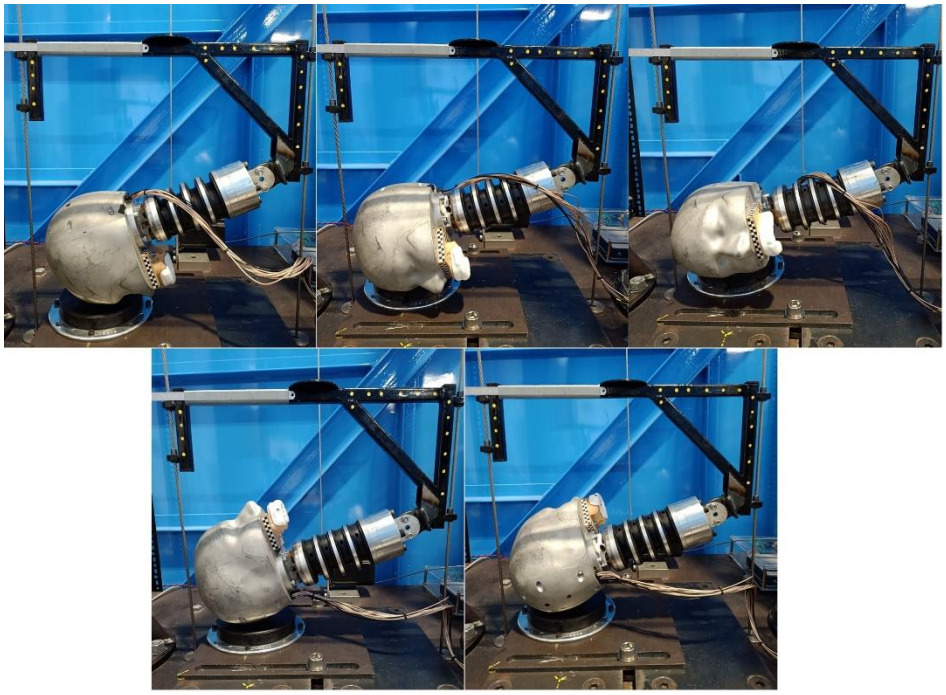

Figure 34: Impact locations from top left to bottom right: Front/Forehead, Front Boss, Side, Rear, and Rear Boss. The mouthguard and dentition are both shown rigidly fixed to the upper jaw of the ATD headform

The test positions available to use were limited by the test rig itself. Due to the extra adapters needed to mate the HitIQ head form and neck to the existing test rig components, a 90° angle (parallel to the ground) could not be achieved. The impact locations however are very close to those required, and due to the nature of the study, exact impact locations were not as important as the agreement between measures of the mouthguard and reference headform sensors.

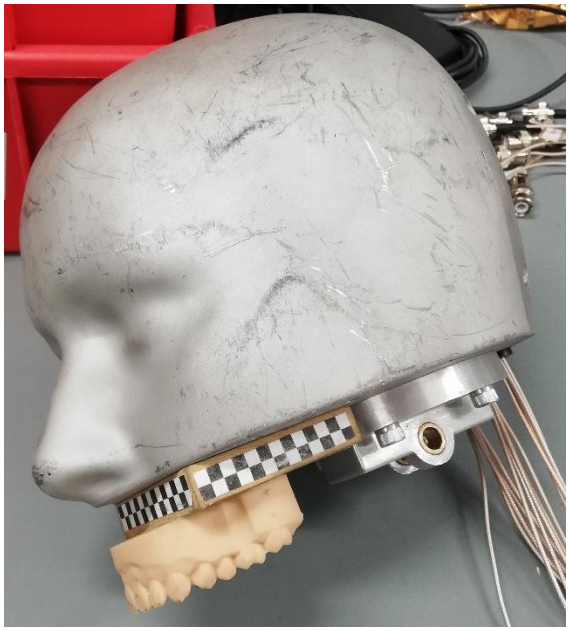

Figure 35: HitIQ headform with a rigidly mounted top jaw for the mouthguard to attach to through testing

Drop heights were chosen based on measured scenarios from gameplay. These were established to achieve PLA's of 20, 40 and 80g, chosen as they fall within the range of published data for sporting head impacts (King, Hume et al. 2009, King, Hume et al. 2015,

King, Hume et al. 2017, King, Hume et al. 2017, King, Hume et al. 2018, King, Hume et al. 2019, King, Hume et al. 2019). Three impact durations for the linear acceleration time-series traces were aimed for. These were 15, 30 and 60ms to represent short, medium and long duration head impacts (Table 12). Certain high energy impact scenarios were not performed due to likelihood of damaging components and not representing field conditions. Test Durations were taken from the onset of impact till the next local minimum in the resultant acceleration trace (Figure 36).

Table 12: Drop heights (m) and foam combination (A - L) for each impact scenario tested. Those unable to be tested are left blank

PLA (g)	Duration (ms)	Forehead	Front Boss	Side	Rear	Rear Boss
20g	15ms	0.05 (E)	0.11 (A)	0.08 (E)	0.06 (L)	0.08 (I)
	30ms	0.39 (C)	0.46 (C)	0.60 (C)	0.51 (C)	0.53 (C)
	60ms	1.16 (H)	1.04 (H)	-	-	-
40g	15ms	0.14 (F)	0.24 (B)	0.20 (F)	0.15 (L)	0.17 (F)
	30ms	0.64 (J)	1.60 (D)	-	-	-
80g	15ms	0.65 (G)	-	-	0.63 (K)	-

The headform was dropped onto a 1 inch MEP pad (Cadex), above which various combinations of foam were placed to achieve desired PLAs and durations. Foam combinations were coded A - L for ease of display and a detailed list can be found in supplementary table 1. Drop heights were taken from the top of the impact surface to the lowest point of the headform when attached to the drop carriage. Each impact scenario was repeated 5 times.

4.2 Data acquisition

The headform contained four tri-axial accelerometers (Analog Devices ADXL377, range: ± 200G, sensitivity: 6.5mV/g) for a total of 12 sensing axes. Accelerometers were configured in a standard "Nine Accelerometer Package" array (Padgaonkar, Krieger et al. 1975) with the three redundant sensing axes configured radially along each primary axis. The data were recorded using a NI9205 analog input module (National Instruments, sample rate: 20 kHz, 16 bit) and stored via a LabVIEW program. Accelerometer data were processed to find linear and rotational acceleration at the centre of mass of the headform, according to the standard NAP algorithm (Padgaonkar, Krieger et al. 1975). Once a kinematic solution was found, results were projected back to the location of each accelerometer and cross-checked with their actual reading, thereby allowing identification of capture errors such as misalignment and deformation.

The HitIQ Nexus A9 instrumented mouthguard contains three accelerometer devices (Analog Devices ADXL372, range: ± 200G, 12-bit) and a gyroscope (Bosch BMG260, ± 2000dps range, 16-bit). These were sampled at 3200Hz and 800Hz respectively, reflecting the different spectral components of on-field impacts, determined experimentally through field trials in Australian Rules, Rugby League and American Football. The circuit board and ancillary components such as a battery and antenna system were encapsulated in the mouthguard using HitIQ's proprietary process. A matching dentition was supplied by the manufacturer for attachment to the jaw section of the headform (Figure 35). A three-accelerometer array was selected to provide an estimate of angular acceleration independent of the gyroscope,

allowing for a cross-check to remove spurious readings, coming from actions like mouthguard deformation rather than head kinematics. The mouthguard had an indicative trigger level set at 10G and was set to record 20ms of data before the first trigger, and 80ms after the last trigger in the event. This re-trigger function allows for an impact event to contain complex kinematics, compared to a fixed-length window which can lose context during complex, multi impact events.

4.3 Post processing

Time series trace data for both Linear and rotational acceleration was collected into MATLAB, and used to find resultant linear and rotational accelerations. For each separate impact, PLA and PRA (Figure 36) were defined as the maximum values of the resultant time-series data for linear and rotational acceleration respectively. These were used for the regression and Bland Altman (BA) analysis. Similar to previous studies (Camarillo, Shull et al. 2013, Bartsch, Samorezov et al. 2014, Greybe, Jones et al. 2020), RMS error was calculated between the Reference and mouthguard traces for both linear and rotational acceleration. Signals were first temporally aligned such that minimal area existed between them, following which, RMS and normalised RMS (NRMS) were calculated. RMS were normalised by the peak values for their respective impact:

$$RMS = \sqrt{\frac{\sum_{i=1}^{n}(x_i^{mg} - x_i^{ref})^2}{n}}$$

$$NRMS = \frac{RMS}{max_{ref}} \times 100$$

With n being the number of measurements, x_i^{mg} and x_i^{ref} being the measurements made by the mouthguard and reference sensors respectively and max_{ref} being peak reference acceleration. Two methods of trimming data for RMS calculations were used. The first trimmed the data at a threshold acceleration of 20% of the peak either side of the peak of the reference time series trace, called 'Impact' RMS (figure 36a and c). The second trims the data to start at a threshold of 20% PLA pre linear peak, and ending at a threshold of 20% PRA post rotational peak, called 'Full' RMS (figure 36b and d). A 20% threshold was experimentally determined to include the necessary trajectories generated by the impact rig, whilst excluding largely noisy data pre and post impact. The 'Impact' period is expected to be the impact part associated with the highest risk of brain injury and is common in previous studies, however

fidelity of the 'Full' model may be required when investigating subconcussive impacts, where impact energy is spread over a larger time.

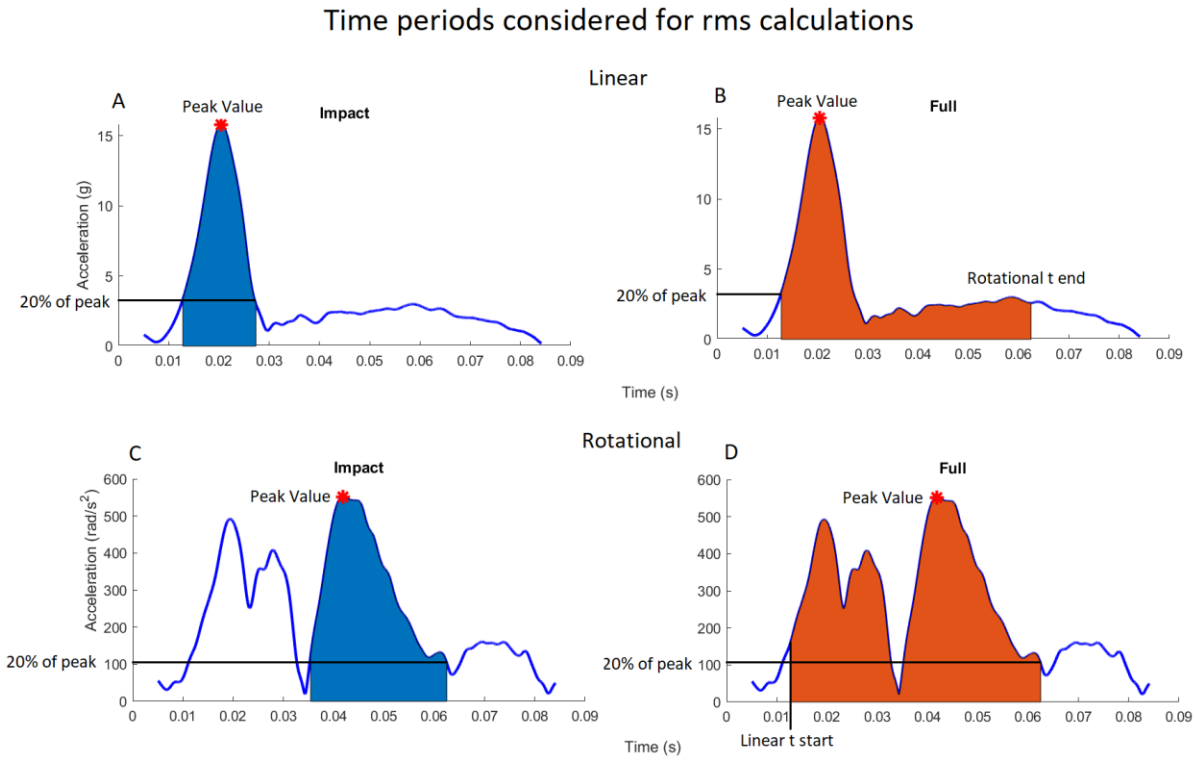

Figure 36: Time periods considered for RMS calculations with impact (A and C) defining a 20% of the peak threshold either side of the peak. Full (B and D) defines the same time duration for both based on linear and rotational 20% thresholds

4.4 Statistical analysis

Statistical analysis was carried out in MATLAB (R2019) with significance set to $p \leq 0.05$. Correlation between peak values was assessed using linear regression, finding coefficients of determination (r^2) for linear and rotational acceleration. BA analysis was used to find the systematic bias and 95% limits of agreement (LOA) of the measured PLA and PRA between the reference and mouthguard (Bland and Altman , Klein 2020). Lin's concordance correlation coefficient (LCCC), the intraclass correlation coefficient (ICC), and associated 95% confidence intervals were also calculated. Paired T tests were carried out on the rms values to assess statistically significant differences ($p \leq 0.05$) between the 'Impact' and 'Full' rms. Strength of agreement criteria for LCCC has been put forward in a research report by NIWA, with substantial agreement at LCCC = 0.95 - 0.99, and 'almost perfect' agreement at LCCC > 0.99 when compared to the lower one sided 95% CI (McBride 2005). An ICC value above 0.8 has been suggested as a minimum acceptable value for reliability and validity (Atkinson and Nevill 1998).

4.5 Mouthguard accuracy

No significant difference in peak value error was found between impact locations, therefore results were pooled together. The peak values measured by the mouthguard show strong positive correlation with those of the reference sensors. Figures 37 a-d display the correlation and BA scatter plots for PLA and PRA. Figure 37b shows a non-significant bias of -0.49% for PLA and Figure 37d shows a significant bias of 1% for PRA ($p < 0.05$). Figure 37 a and c both

show the strong correlation between the mouthguard and reference measures, having associated r^2 values of 0.996 and 0.994 for PLA and PRA respectively. Figure 37d shows one significant outlier, representing a rear boss 40g 15ms impact with a 13.1% mouthguard PRA underestimation.

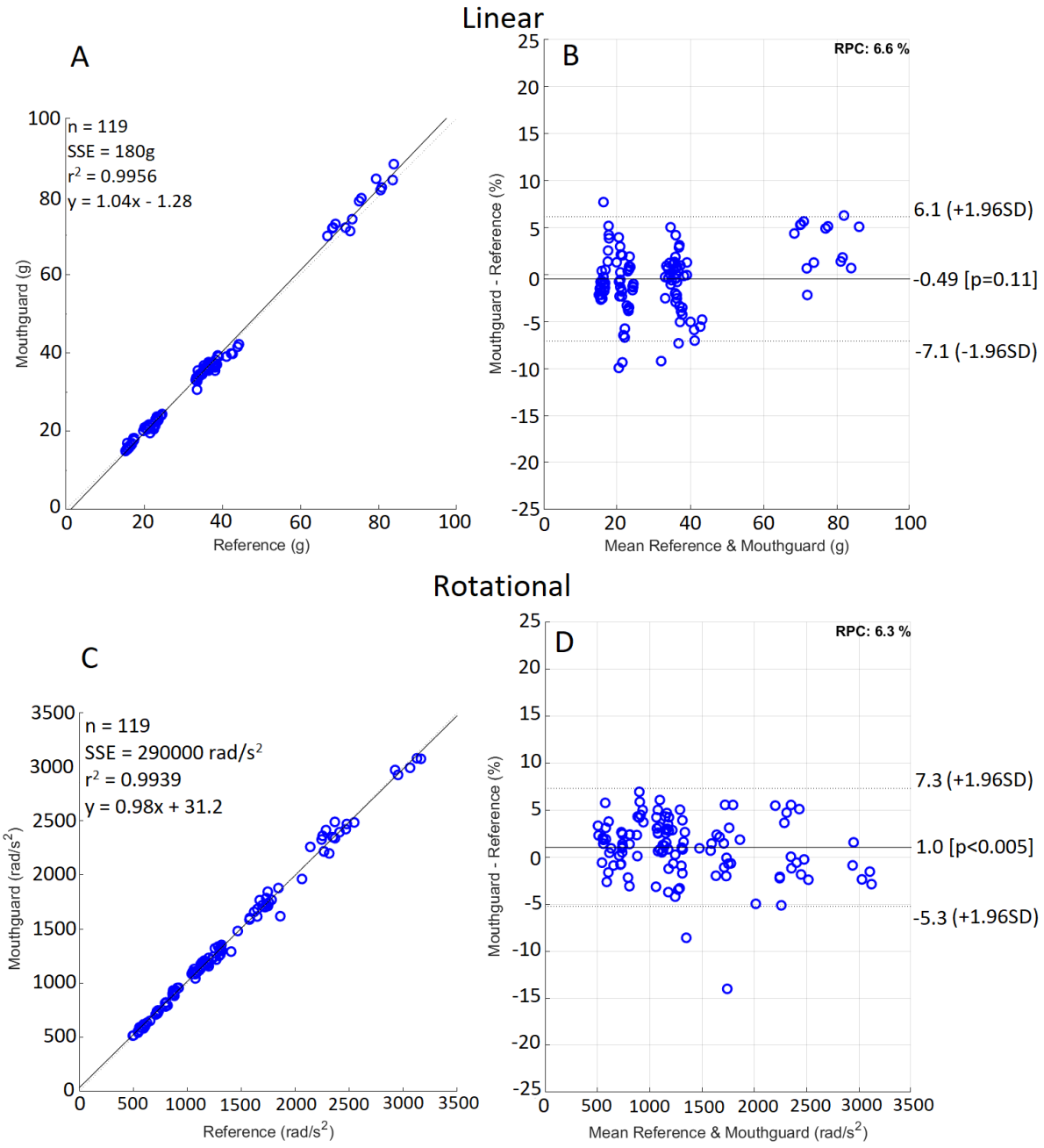

Figure 37: Correlation (A and C) and Bland-Altman (D and D) plots for PLA and PRA

Figures 38a – d show the 'Impact' and 'Full' NRMS errors across each impact location. In both cases for linear acceleration, one outlier was seen. The associated time series trace is shown in Figure 40. The two time periods over which the RMS and NRMS were calculated produced significantly different results with the 'full' RMS producing consistently higher RMS values for both linear and rotational acceleration. This is seen in Figure 38 when comparing the mean lines. A paired T test revealed mean differences between the two periods of 0.85% and 0.41%

NRMS for linear and rotational respectively. Figure 38 shows there was no increase in NRMS as the PLA increases. Additionally, NRMS showed no relationship with impact duration for either linear or rotational acceleration. Figure 39 shows histograms of the NRMS distribution produced in this study. Figure 39a-d all show similar distributions of NRMS errors with an increasing chance of NRMS error until the mean was reached, after which, the probability greatly reduces, indicating a low spread of NRMS errors across the range.

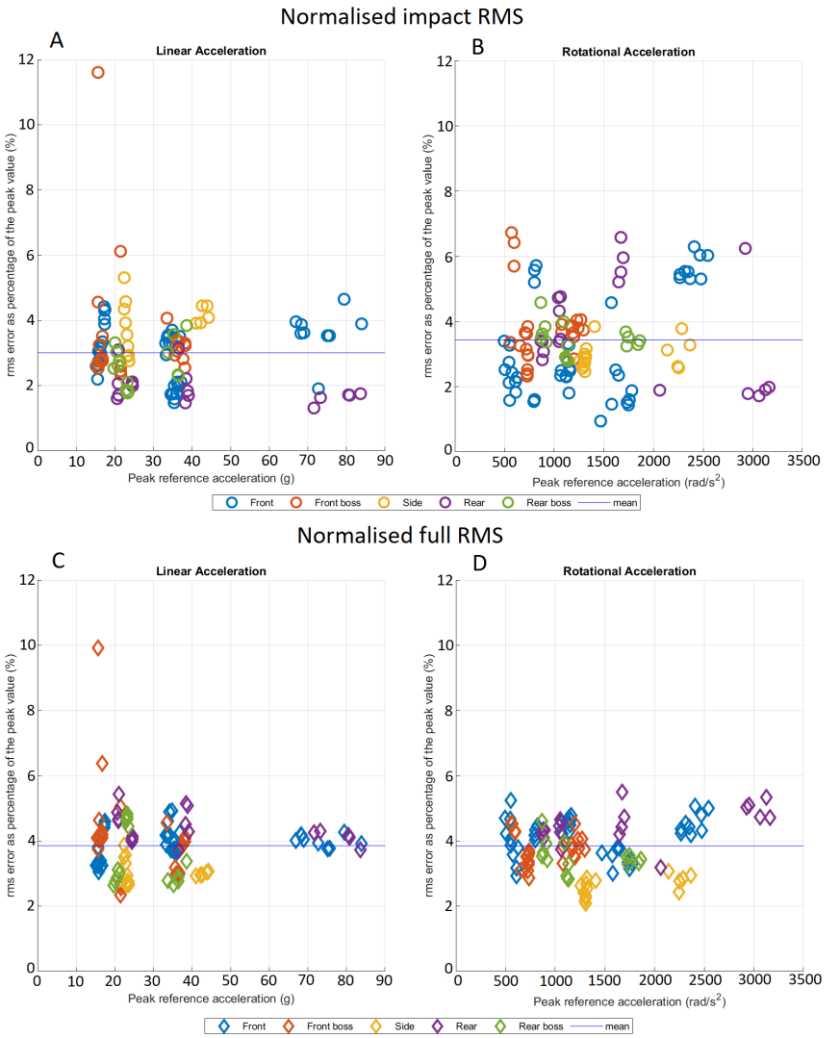

Figure 38: Normalised RMS values calculated over two different time periods for both linear and rotational acceleration.

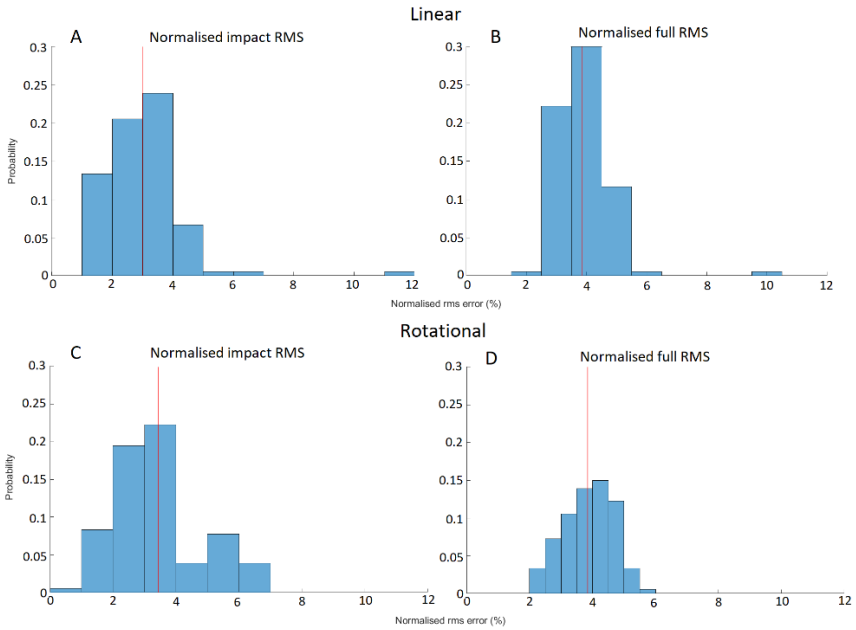

Figure 39: Probability of any single impact producing a NRMS error based on both rms durations used. The red line shows the mean NRMS error for each type of rms calculation

Figure 40 shows the NRMS outlier, a 20g 15ms front boss impact. This was the only outlying impact of the 5 recorded for that scenario. The high NRMS error was caused by the recognition of a second apparent impact after the initial peak likely due to a minor decoupling of the mouthguard from the dentition or a slippage of the foam impact surface. This was only displayed in the linear acceleration time-series trace, and not the rotational acceleration.

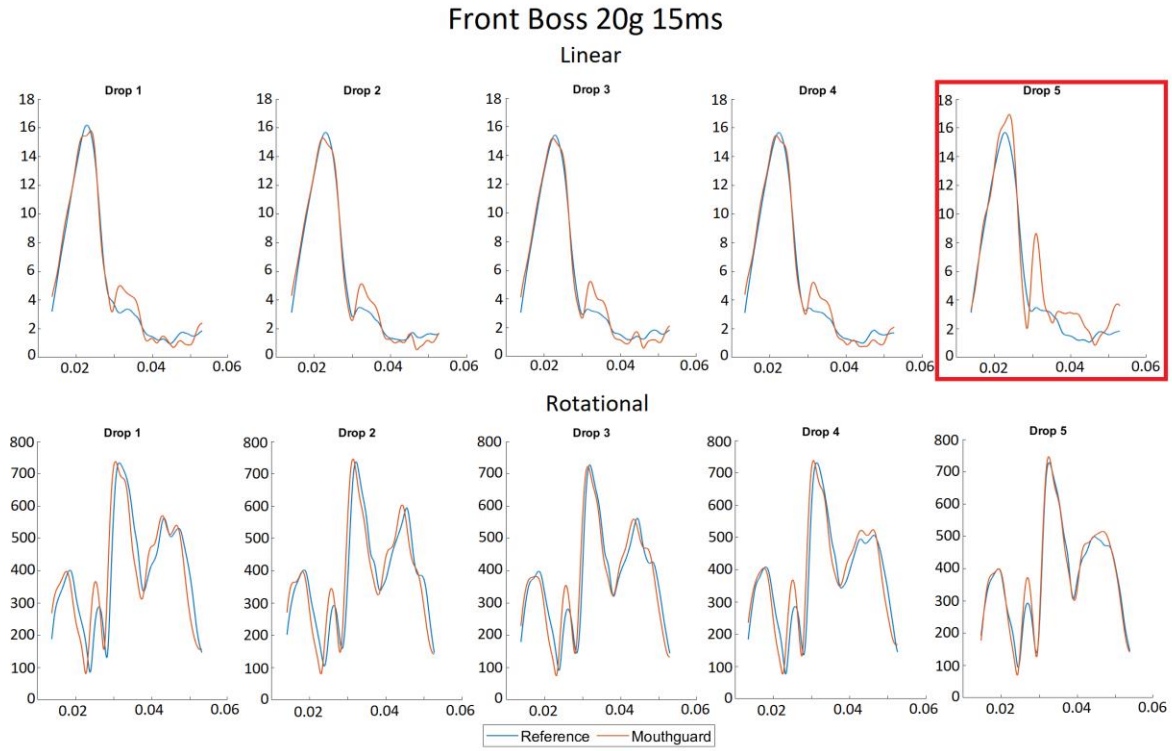

Figure 40: each impact in the 20g 15ms front boss scenario with the outlier marked

No significant difference was found between the LCCC or ICC of linear and rotational acceleration (Table 13). There was also no significant difference between the relative peak acceleration errors for linear and rotational acceleration, suggesting no significant difference in accuracy or reliability between the two measures made by the mouthguard. Table 13 also shows the mean values of peak and RMS errors. The rotational RMS error is substantially larger than the linear RMS errors due to the much higher values involved with rotational acceleration compared to linear acceleration.

Table 13: Measurement statistics

Metric	Measurement	Linear	Rotational
Lin's Concordance correlation Coefficient	Peak acceleration	0.997	0.997
LCCC 95% confidence interval	Peak acceleration	[0.996 0.998]	[0.995 0.998]
Pearson Correlation Coefficient	Peak acceleration	0.998	0.997
r^2 value	Peak acceleration	0.996	0.994
Intraclass correlation coefficient	Peak acceleration	0.997	0.997
ICC 95% confidence interval	Peak acceleration	[0.996 0.998]	[0.995 0.998]
Linear regression equation	Peak acceleration	1.04x – 1.28	0.98x + 31.2
Mean (SD)	Impact RMS	0.98 (0.64)	47.41 (34.99)
Mean (SD)	Impact NRMS	3.01 (1.22%)	3.44 (1.33%)
Mean (SD)	Full RMS	1.28 (0.75)	52.20 (31.60)
Mean (SD)	Full NRMS	3.85 (0.92%)	3.85 (0.76%)
Mean (SD) relative peak value error	Peak acceleration	2.56 (2.16%)	2.82 (2.54%)

4.6 Discussion

The results show strong agreement between the HitIQ mouthguard and headform reference sensors for both PLA and PRA with r^2 values of 0.996 and 0.994 respectively. Other correlation measures show strong correlations between reference and mouthguard of 0.997 for LCCC and ICC for both PLA and PRA. These results are comparable to previous studies on instrumented mouthguards. A study conducted by Greybe et al (Greybe, Jones et al. 2020) utilised a pendulum impactor producing PLAs of 7 – 102.5g, comparing an intelligent mouthguard to reference sensors inside a headform. The r^2 values were 0.93 for PLA and 0.99 for peak rotational velocity (PRV) whilst PRA was not investigated. An earlier mouthguard validation study by Bartsch et al (Bartsch, Samorezov et al. 2014) utilised both headform simulation and in vivo head impacts across a range of impact severities producing r^2 values of 0.99 for PLA, 0.99 for PRV and 0.98 for PRA. A third mouthguard validation study by Camarillo et al (Camarillo, Shull et al. 2013) reported r^2 values of 0.96 for PLA, 0.89 for PRA and 0.98 for PRV. Typically the strongest correlation on sporting head impact sensors are PRV values with most studies reporting r^2 values of 0.98 – 0.99 (Camarillo, Shull et al. 2013, Nevins, Smith et al. 2015, Schussler, Stark et al. 2017, Tyson, Duma et al. 2018), whilst PRA tends to have far weaker correlation with reference sensors.

BA analysis showed a non-significant bias of -0.49% with 95% LOA of [-7.1 6.1%] for PLA, and a statistically significant bias of 1% with 95% LOA of [-5.3 7.3%] for PRA ($p < 0.05$). The absolute BA analysis shows neither PLA nor PRA to have any statistically significant systematic bias. Neither Bartsch nor Camarillo display a BA analysis in their research. Greybe et al (Greybe, Jones et al. 2020) carried out a BA analysis, reporting systematic bias of 2.5g and -0.5 rad/s for PLA and PRV. Very few studies regarding sporting head impact sensors utilise BA analysis, with most going for only linear correlation instead. BA analysis is useful for studies such as these as it illustrates the measurement errors of the device being validated, whilst exposing any bias towards under or overestimation. Using only linear correlation heavily restricts the amount of information able to be gathered about the sensors performance.

The furthest outlier in the PRA BA analysis is due to an underestimation of the PRA by the mouthguard during a rear boss 40g 15ms impact. Unlike the outlier shown in Figure 38-40, the associated RMS error is low, indicating a close match of the shape of the time series trace between mouthguard and reference. RMS error is useful for investigating the shapes of the two time series traces. This is important as many of the metrics for determining the injury potential, such as HIC_{15}, HIT_{sp}, GSI and other kinematic injury predictors, rely on, and are sensitive to, the shape of the impact-acceleration trace. In previous studies, Camarillo et al (Camarillo, Shull et al. 2013) calculated the RMS over 25 data points (24.4ms) centred about the peak of the impact, assuming this to capture the entire impact. Greybe et al (Greybe, Jones et al. 2020) used similar methodology with RMS being taken over the duration of the 'impact part of the trace'. The longest impacts reported in this study were 23.5 ± 6.7ms, with the shortest at 12.1 ± 5.8ms, which are comparable with those achieved in the present study (9.7ms – 38ms). The time over which the PLA occurs does not encapsulate the time over which the PRA occurs, nor does it account for the total duration where a significant amount of excitation exists within the acceleration trace.

For comparison with other studies, 'impact' RMS values will be used due to the shorter duration and closer resemblance of durations used in other studies. Camarillo et al (Camarillo, Shull et al. 2013) reported average RMS, (NRMS) errors of 3.9 ± 2.1g, (9.9 ± 4.4%) and 202 ± 120rad/s^2, (9.7 ± 7%) for linear and rotational acceleration. Greybe et al (Greybe, Jones et al. 2020) found RMS, (NRMS) errors of 4.3 ± 3.5g, (13.1 ± 9.9%) for linear acceleration. Those found in the present study are smaller than those in previous literature with RMS, (NRMS) values of 1.0 ± 0.6g, (3.0 ± 1.2%) and 47.4 ± 35.0rad/s^2, (3.4 ± 1.3%) for linear and rotational acceleration respectively. When the 'full' time period was used for the RMS error calculation, a consistently higher result was achieved, reaching statistical significance for both linear and rotational acceleration. For linear acceleration this was likely due to the tail of the time series data trace having a much higher signal to noise ratio than what exists across the impact peak. For rotational acceleration however the difference is likely due to the increased amount of large numbers in the time series data trace across additional peaks either side of the maximal, rather than excess noise.

The small RMS errors and strong correlation between measurements made by the mouthguard and reference sensors demonstrate the high comparability of both linear and rotational acceleration time series traces between devices. This study, like those conducted

previously, has its limitations. This study was conducted in a controlled laboratory, on a rigid body headform. This differs from the conditions imposed on the mouthguard during use in sports, for example through relative motion of the mandible (Camarillo, Shull et al. 2013), decoupling from the upper jaw due to saliva lubrication, or noise from non-head impact events. The testing method only incorporated a limited amount of PLA values ranging from 15.2 – 83.9g with a visible break in continuous values from 40 – 80g (Figure 37) and far fewer impacts were carried out at the highest impact energy. Rigid coupling between the mouthguard and dentition were assumed during testing and was confirmed by visual inspection after every impact, however no movement was seen during testing. Future studies should investigate the effects of high energy, low duration impacts, as is seen with previous research (Camarillo, Shull et al. 2013, Bartsch, Samorezov et al. 2014, Greybe, Jones et al. 2020). Additionally a linear impactor could be employed instead of a drop test rig in order to replicate a greater range of impact positions and scenarios.

4.7 Conclusion

This study shows that the PLAs, PRAs and shapes of the time series acceleration data measured by the mouthguard closely match that measured by the reference sensors inside the headform. The methods for impact testing were limited as only certain impact locations could be tested under certain scenarios with longer impact durations. The results reported in this study only hold up under the assumption that the head is a rigid body. This however shows promising results for investigating impacts seen in a sporting context, with lower PLA, PRA and rms error than other intelligent mouthguards previously validated in a laboratory setting. The results show that this instrumented mouthguard is a valid tool for measuring head impact kinematics in the laboratory, and could serve as a reliable instrument for measuring and quantifying head impacts in vivo, whilst expanding the current understanding of concussive head injuries.

5 Conclusions and Future Work

From this body of research the linear acceleration attenuation performance of standard soft shelled rugby headgear has been investigated with comparison to a new rugby headgear potentially offering a reduction in risk of brain injury. This study provides further evidence that rugby headgear can reduce the peak linear accelerations and HIC from an impact. All headgear significantly reduced the PLA and HIC of an impact. The newer types of headgear reduced PLA and HIC significantly more than the World Rugby approved headgear. All headgear showed a reduction in effectiveness at higher drop heights. Further investigation is required into rotational accelerations, how headgear can mitigate these, whilst establishing standards for quantification of rotational injury risk.

The neck designed and built in this study did not meet the validation requirements. The testing methods could be the reason for this as the impact testing conditions were different from those used in previous studies. As impact conditions approached those reported in the published data, the response of the head and neck became closer to that of the human neck. If further tests are to be completed, the material or joining method to the aluminium would need to be updated.

This evaluation of the HitIQ Nexus A9 instrumented mouthguard shows that the PLAs, PRAs and shapes of the time series acceleration data measured by the mouthguard closely match those measured by the reference sensors. The results reported in this study only hold up under the assumption that the head is a rigid body. This however shows promising results for investigating impacts seen in a sporting context, with lower PLA, PRA and rms error than other intelligent mouthguards previously validated in a laboratory setting.

6 References

ACC (2015). Sport Concussion in New Zealand: ACC National Guidelines.

Adams, L., D. Stitt and C. Whitelaw (2018). End of year report, University of Canterbury.

Administration, N. H. T. S. (1997). Transportation. 49. E. C. o. F. regulations. Legal Information Institute, Legal Information Institute. **Subpart E**.

Agel, J., R. Dick, B. Nelson, S. W. Marshall and T. P. Dompier (2007). "Descriptive epidemiology of collegiate women's ice hockey injuries: National Collegiate Athletic Association Injury Surveillance System, 2000-2001 through 2003-2004." J Athl Train **42**(2): 249-254.

Agel, J., T. P. Dompier, R. Dick and S. W. Marshall (2007). "Descriptive epidemiology of collegiate men's ice hockey injuries: National Collegiate Athletic Association Injury Surveillance System, 1988-1989 through 2003-2004." J Athl Train **42**(2): 241-248.

Anderson, B. L., M. A. Gittelman, J. K. Mann, R. L. Cyriac and W. J. Pomerantz (2016). "High School Football Players' Knowledge and Attitudes About Concussions." Clinical Journal of Sport Medicine **26**(3).

Anderson, V., S. Brown, H. Newitt and H. Hoile (2009). "Educational, vocational, psychosocial, and quality-of-life outcomes for adult survivors of childhood traumatic brain injury." J Head Trauma Rehabil **24**(5): 303-312.

Arbogast, K. B., S. Balasubramanian, T. Seacrist, M. R. Maltese, J. F. Garcia-Espana, T. Hopely, E. Constans, F. J. Lopez-Valdes, R. W. Kent, H. Tanji and K. Higuchi (2009). "Comparison of kinematic responses of the head and spine for children and adults in low-speed frontal sled tests." Stapp Car Crash J **53**(1532-8546 (Print)): 329-372.

Atkinson, G. and A. M. Nevill (1998). "Statistical methods for assessing measurement error (reliability) in variables relevant to sports medicine." Sports Med **26**(4): 217-238.

Bailes, J. E., A. L. Petraglia, B. I. Omalu, E. Nauman and T. Talavage (2013). "Role of subconcussion in repetitive mild traumatic brain injury." J Neurosurg **119**(5): 1235-1245.

Baillargeon, A., M. Lassonde, S. Leclerc and D. Ellemberg (2012). "Neuropsychological and neurophysiological assessment of sport concussion in children, adolescents and adults." Brain Inj **26**(3): 211-220.

Barnes, S. (2020). The Crevical Spine. TeachMe Anatomy.

Bartsch, A., S. Samorezov, E. Benzel, C. Clinic, V. Miele and D. Brett (2014). Validation of an "Intelligent Mouthguard" Single Event Head Impact Dosimeter.

Best, J. P., A. S. McIntosh and T. N. Savage (2005). "Rugby World Cup 2003 injury surveillance project." Br J Sports Med **39**(11): 812-817.

Bland, J. M. and D. G. Altman (1986). "Statistical methods for assessing agreement between two methods of clinical measurement." Lancet **1**(0140-6736 (Print)): 307-310.

Bledsoe, G. H., G. Li and F. Levy (2005). "Injury risk in professional boxing." South Med J **98**(10): 994-998.

Britannica, T. E. o. E. (2018) "Neck."

Burman, E., J. Lysholm, P. Shahim, C. Malm and Y. Tegner (2016). "Concussed athletes are more prone to injury both before and after their index concussion: a data base analysis of 699 concussed contact sports athletes." BMJ Open Sport & Exercise Medicine **2**(1): e000092.

Buse, G. J. and R. M. Wood (2006). "Safety profile of amateur kickboxing among military and civilian competitors." Mil Med **171**(5): 443-447.

Camarillo, D. B., P. B. Shull, J. Mattson, R. Shultz and D. Garza (2013). "An instrumented mouthguard for measuring linear and angular head impact kinematics in American football." Ann Biomed Eng **41**(9): 1939-1949.

CCC. (2017). "Custom made ventilator rugby headgear." from https://www.canterburyofnz.com/head-protective-wear/headgear/custom-made/customised-headgear-ventilator.html.

Choe, M. C., T. Babikian, J. DiFiori, D. A. Hovda and C. C. Giza (2012). "A pediatric perspective on concussion pathophysiology." Curr Opin Pediatr **24**(6): 689-695.

Collins, C. L., L. J. Micheli, E. E. Yard and R. D. Comstock (2008). "Injuries sustained by high school rugby players in the United States, 2005-2006." Arch Pediatr Adolesc Med **162**(1): 49-54.
Collins, M. W., M. R. Lovell, G. L. Iverson, R. C. Cantu, J. C. Maroon and M. Field (2002). "Cumulative effects of concussion in high school athletes." Neurosurgery **51**(5): 1175-1179; discussion 1180-1171.
Cross, M., S. Kemp, A. Smith, G. Trewartha and K. Stokes (2016). "Professional Rugby Union players have a 60% greater risk of time loss injury after concussion: a 2-season prospective study of clinical outcomes." Br J Sports Med **50**(15): 926-931.
Cullen, D. K., J. P. Harris, K. D. Browne, J. A. Wolf, J. E. Duda, D. F. Meaney, S. S. Margulies and D. H. Smith (2016). A porcine model of traumatic brain injury via head rotational acceleration. Injury Models of the Central Nervous System, Springer**:** 289-324.
Daneshvar, D. H., C. J. Nowinski, A. C. McKee and R. C. Cantu (2011). "The epidemiology of sport-related concussion." Clin Sports Med **30**(1): 1-17, vii.
Davidsson, J., M. Angeria and M. Risling (2009). Injury threshold for sagittal plane rotational induced diffuse axonal injuries. International IRCOBI conference on the biomechanics of injury.
Denny-Brown, D. E. and W. R. Russell (1941). "Experimental Concussion: (Section of Neurology)." Proc R Soc Med **34**(11): 691-692.
Duhaime, A. C., J. G. Beckwith, A. C. Maerlender, T. W. McAllister, J. J. Crisco, S. M. Duma, P. G. Brolinson, S. Rowson, L. A. Flashman, J. J. Chu and R. M. Greenwald (2012). "Spectrum of acute clinical characteristics of diagnosed concussions in college athletes wearing instrumented helmets: clinical article." J Neurosurg **117**(6): 1092-1099.
Dziemianowicz, M. S., M. P. Kirschen, B. A. Pukenas, E. Laudano, L. J. Balcer and S. L. Galetta (2012). "Sports-related concussion testing." Curr Neurol Neurosci Rep **12**(5): 547-559.
Eisenberg, M. A., J. Andrea, W. Meehan and R. Mannix (2013). "Time interval between concussions and symptom duration." Pediatrics **132**(1): 8-17.
Estwanik, J. J., M. Boitano and N. Ari (2016). "Amateur Boxing Injuries at the 1981 and 1982 USA/ABF National Championships." The Physician and Sportsmedicine **12**(10): 123-128.
Ewing, C., D. Thomas, B. W, L. Patrick and D. Gillis (1969). "DYNAMIC RESPONSE OF THE HEAD AND NECK OF THE LIVING HUMAN TO -Gx IMPACT ACCELERATION. 1. EXPERIMENTAL DESIGN AND PRELIMINARY EXPERIMENTAL DATA." 24.
Ewing, C. L., D. J. Thomas, L. Lustick, W. H. Muzzy, G. C. Willems and P. Majewski (1978). Effect of Initial Position on the Human Head and Neck Response to +Y Impact Acceleration. SAE Technical Paper Series, SAE International.
Field, M., M. W. Collins, M. R. Lovell and J. Maroon (2003). "Does age play a role in recovery from sports-related concussion? A comparison of high school and collegiate athletes." J Pediatr **142**(5): 546-553.
Fortington, L. V., D. M. Twomey and C. F. Finch (2015). "Concussion in community Australian football - epidemiological monitoring of the causes and immediate impact on play." Inj Epidemiol **2**(1): 20.
Foster, J. K., J. O. Kortge and M. J. Wolanin (1977). Hybrid III-A Biomechanically-Based Crash Test Dummy. SAE Technical Paper Series, SAE International.
Frechede, B. and A. S. McIntosh (2009). "Numerical reconstruction of real-life concussive football impacts." Med Sci Sports Exerc **41**(2): 390-398.
Frizzell, E. R. A., G. P. Arnold, W. Wang, R. J. Abboud and T. S. Drew (2018). "Comparison of branded rugby headguards on their effectiveness in reducing impact on the head." BMJ Open Sport Exerc Med **4**(1): e000361.
Fuller, C. W., A. Taylor and M. Raftery (2017). "2016 Rio Olympics: an epidemiological study of the men's and women's Rugby-7s tournaments." Br J Sports Med **51**(17): 1272-1278.
Funk, J. R., S. Rowson, R. W. Daniel and S. M. Duma (2012). "Validation of concussion risk curves for collegiate football players derived from HITS data." Ann Biomed Eng **40**(1): 79-89.
Gadd, C. W. (1966). Use of a Weighted-Impulse Criterion for Estimating Injury Hazard. SAE Technical Paper Series, SAE International.
Gaffaney, C. (2014) "Counting the Cost of Concussion in Sport."

Gamebreaker. (2019). "Soft protective rugby scrum caps." from https://gamebreaker.com/sports/soft-padded-rugby-scrum-caps/.
Gamebreaker. (2020). "About D30." from https://gamebreaker.com/d3o/.
Ganly, M. and J. M. McMahon (2018). "New generation of headgear for rugby: impact reduction of linear and rotational forces by a viscoelastic material-based rugby head guard." BMJ Open Sport Exerc Med **4**(1): e000464.
Gardner, A., G. L. Iverson, C. R. Levi, P. W. Schofield, F. Kay-Lambkin, R. M. Kohler and P. Stanwell (2015). "A systematic review of concussion in rugby league." Br J Sports Med **49**(8): 495-498.
Gardner, A. J., G. L. Iverson, W. H. Williams, S. Baker and P. Stanwell (2014). "A systematic review and meta-analysis of concussion in rugby union." Sports Med **44**(12): 1717-1731.
Gavett, B. E., R. A. Stern and A. C. McKee (2011). "Chronic traumatic encephalopathy: a potential late effect of sport-related concussive and subconcussive head trauma." Clin Sports Med **30**(1): 179-188, xi.
Gennarelli, T. A. (1983). Head Injury in Man and Experimental Animals: Clinical Aspects, Vienna, Springer Vienna.
Gennarelli, T. A., L. E. Thibault, J. H. Adams, D. I. Graham, C. J. Thompson and R. P. Marcincin (1982). "Diffuse axonal injury and traumatic coma in the primate." Ann Neurol **12**(6): 564-574.
Gennarelli, T. A., L. E. Thibault and A. K. Ommaya (1972). Pathophysiologic Responses to Rotational and Translational Accelerations of the Head. SAE Technical Paper Series, SAE International.
Gessel, L. M., S. K. Fields, C. L. Collins, R. W. Dick and R. D. Comstock (2007). "Concussions among United States high school and collegiate athletes." J Athl Train **42**(4): 495-503.
Gough, C. (2019). Countries by number of registered ice hockey players in 2018/19. Statista.
Graham, R., F. P. Rivara, M. A. Ford, C. M. Spicer, Y. Committee on Sports-Related Concussions in, Y. Board on Children, Families, M. Institute of, C. National Research and R. Graham (2014). Sports-Related Concussions in Youth : Improving the Science, Changing the Culture. Washington, D.C., UNITED STATES, National Academies Press.
Greenwald, R. M., J. T. Gwin, J. J. Chu and J. J. Crisco (2008). "Head impact severity measures for evaluating mild traumatic brain injury risk exposure." Neurosurgery **62**(4): 789-798; discussion 798.
Greybe, D. G., C. M. Jones, M. R. Brown and E. M. P. Williams (2020). "Comparison of head impact measurements via an instrumented mouthguard and an anthropometric testing device." Sports Engineering **23**(1): 12.
Guskiewicz, K. M., S. W. Marshall, J. Bailes, M. McCrea, R. C. Cantu, C. Randolph and B. D. Jordan (2005). "Association between Recurrent Concussion and Late-Life Cognitive Impairment in Retired Professional Football Players." Neurosurgery **57**(4): 719-726.
Guskiewicz, K. M., S. W. Marshall, J. Bailes, M. McCrea, H. P. Harding, Jr., A. Matthews, J. R. Mihalik and R. C. Cantu (2007). "Recurrent concussion and risk of depression in retired professional football players." Med Sci Sports Exerc **39**(6): 903-909.
Harmon, K. G., J. A. Drezner, M. Gammons, K. M. Guskiewicz, M. Halstead, S. A. Herring, J. S. Kutcher, A. Pana, M. Putukian and W. O. Roberts (2013). "American Medical Society for Sports Medicine position statement: concussion in sport." Br J Sports Med **47**(1): 15-26.
Hecimovich, M., D. King, A. Dempsey and M. Murphy (2018). "Head Impact Exposure in Junior and Adult Australian Football Players." J Sports Med **1**: 8-16.
Hecimovich, M. D. and D. King (2017). "Prevalence of head injury and medically diagnosed concussion in junior-level community-based Australian Rules Football." J Paediatr Child Health **53**(3): 246-251.
Hendricks, S., E. Jordaan and M. Lambert (2012). "Attitude and behaviour of junior rugby union players towards tackling during training and match play." Safety Science **50**(2): 266-284.
High Jr, W. M., A. M. Sander, M. A. Struchen and K. A. Hart (2005). Rehabilitation for traumatic brain injury, Oxford University Press.
Hinton-Bayre, A. D., G. Geffen and P. Friis (2004). "Presentation and mechanisms of concussion in professional Rugby League Football." J Sci Med Sport **7**(3): 400-404.

Holbourn, A. (1943). "Mechanics of head injuries." The Lancet **242**(6267): 438-441.
Hosey, R. and Y. Liu (1980). "A homeomorphic finite element model of impact head and neck injury." CP of Finite Elements in Biomechanics **2**: 379-401.
Humanetics. (2019). "History of Crash Test Dummies." from https://www.humaneticsatd.com/about-us/dummy-history.
Hume, P., A. Theadom, G. N. Lewis, K. L. Quarrie, S. R. Brown, R. Hill and S. W. Marshall (2017). "Cognition in former rugby union players and impact of concussion history." Br J Sports Med **51**(4): 333-333.
Jadischke, R., D. C. Viano, N. Dau, A. I. King and J. McCarthy (2013). "On the accuracy of the Head Impact Telemetry (HIT) System used in football helmets." J Biomech **46**(1873-2380 (Electronic)): 2310-2315.
Jones, K. M., P. Prah, N. Starkey, A. Theadom, S. Barker-Collo, S. Ameratunga, V. L. Feigin and B. S. Group (2019). "Longitudinal patterns of behavior, cognition, and quality of life after mild traumatic brain injury in children: BIONIC study findings." Brain Inj **33**(7): 884-893.
Kallieris, D., A. Rizzetti and R. Mattern (1995). The biofidelity of Hybrid III dummies. International Research Council on Biomechanics of Injury (IRCOBI) Conference.
Kerr, H. A., C. Curtis, L. J. Micheli, M. S. Kocher, D. Zurakowski, S. P. Kemp and J. H. Brooks (2008). "Collegiate rugby union injury patterns in New England: a prospective cohort study." Br J Sports Med **42**(7): 595-603.
Kimpara, H. and M. Iwamoto (2012). "Mild traumatic brain injury predictors based on angular accelerations during impacts." Ann Biomed Eng **40**(1): 114-126.
King, A., K. Yang, L. Zhang and W. Hardy (2003). "Is Head Injury Caused by Linear or Angular Acceleration?" IRCOBI Conference.
King, D., Hume, C. Gissane, C. Cummins and T. Clark (2017). "Measurement of Head Impacts in a Senior Amateur Rugby League Team with an Instrumented Patch: Exploratory Analysis." ARC Journal of Research in Sports Medicine **2**(1): 9-20.
King, D., P. Hume, C. Cummins, A. Pearce, T. Clark, A. Foskett and M. Barnes (2019). "Match and Training Injuries in Women's Rugby Union: A Systematic Review of Published Studies." Sports Med **49**(10): 1559-1574.
King, D., P. Hume, C. Gissane, M. Brughelli and T. Clark (2016). "The Influence of Head Impact Threshold for Reporting Data in Contact and Collision Sports: Systematic Review and Original Data Analysis." Sports Med **46**(2): 151-169.
King, D., P. Hume, C. Gissane and T. Clark (2017). "Head impacts in a junior rugby league team measured with a wireless head impact sensor: an exploratory analysis." J Neurosurg Pediatr **19**(1): 13-23.
King, D., P. Hume, P. Milburn and S. Gianotti (2009). "Rugby league injuries in New Zealand: Variations in injury claims and costs by ethnicity, gender, age, district, body site, injury type and occupation." NZ J Sport Med **36**(2): 48-55.
King, D., P. A. Hume, M. Brughelli and C. Gissane (2015). "Instrumented mouthguard acceleration analyses for head impacts in amateur rugby union players over a season of matches." Am J Sports Med **43**(3): 614-624.
King, D., P. A. Hume, N. Hardaker, C. Cummins, T. Clark, A. J. Pearce and C. Gissane (2019). "Female rugby union injuries in New Zealand: A review of five years (2013-2017) of Accident Compensation Corporation moderate to severe claims and costs." J Sci Med Sport **22**(5): 532-537.
King, D. A., P. A. Hume, C. Gissane and T. N. Clark (2016). "Similar head impact acceleration measured using instrumented ear patches in a junior rugby union team during matches in comparison with other sports." Journal of Neurosurgery: Pediatrics **18**(1): 65-72.
King, D. A., P. A. Hume, C. Gissane, D. C. Kieser and T. N. Clark (2018). "Head impact exposure from match participation in women's rugby league over one season of domestic competition." J Sci Med Sport **21**(2): 139-146.
Klein, R. (2020). Bland-Altman and Correlation Plot. MATLAB Central File Exchange.

Knouse, C. L., T. E. Gould, S. V. Caswell and R. G. Deivert (2003). "Efficacy of Rugby Headgear in Attenuating Repetitive Linear Impact Forces." J Athl Train **38**(4): 330-335.
Kontos, A. P., R. J. Elbin, V. C. Fazio-Sumrock, S. Burkhart, H. Swindell, J. Maroon and M. W. Collins (2013). "Incidence of sports-related concussion among youth football players aged 8-12 years." J Pediatr **163**(3): 717-720.
Lange, D. (2019) "Number of people participating in boxing* in England from 2016 to 2019."
LeBlanc, D. (2016). "From 30 to 75%: Range of motion milestones." https://dpleblanc.wordpress.com/2016/03/12/from-30-to-75-range-of-motion-milestones/.
Lincoln, A. E., S. V. Caswell, J. L. Almquist, R. E. Dunn, J. B. Norris and R. Y. Hinton (2011). "Trends in concussion incidence in high school sports: a prospective 11-year study." Am J Sports Med **39**(5): 958-963.
Lock, S. (2018) "Number of participants in boxing in the United States from 2006 to 2017."
Lock, S. (2020) "Number of participants in tackle football in the United States from 2006 to 2018."
Ma, R., V. Lopez, Jr., M. G. Weinstein, J. L. Chen, C. M. Black, A. T. Gupta, J. D. Harbst, C. Victoria and A. A. Allen (2016). "Injury Profile of American Women's Rugby-7s." Med Sci Sports Exerc **48**(10): 1957-1966.
Makdissi, M., D. Darby, P. Maruff, A. Ugoni, P. Brukner and P. R. McCrory (2010). "Natural history of concussion in sport: markers of severity and implications for management." Am J Sports Med **38**(3): 464-471.
Margulies, S. S. and L. E. Thibault (1992). "A proposed tolerance criterion for diffuse axonal injury in man." J Biomech **25**(8): 917-923.
Marshall, S. W. and R. J. Spencer (2001). "Concussion in Rugby: The Hidden Epidemic." J Athl Train **36**(3): 334-338.
McBride, G. B. (2005). A Proposal for Strength of Agreement Criteria for Lin's Concordance Correlation Coefficient, Naitional Institute of Water and Atmospheric Research Ltd.
McClincy, M. P., M. R. Lovell, J. Pardini, M. W. Collins and M. K. Spore (2006). "Recovery from sports concussion in high school and collegiate athletes." Brain Inj **20**(1): 33-39.
McCrea, M., K. Guskiewicz, C. Randolph, W. B. Barr, T. A. Hammeke, S. W. Marshall and J. P. Kelly (2009). "Effects of a symptom-free waiting period on clinical outcome and risk of reinjury after sport-related concussion." Neurosurgery **65**(5): 876-882; discussion 882-873.
McCrea, M., K. Guskiewicz, C. Randolph, W. B. Barr, T. A. Hammeke, S. W. Marshall, M. R. Powell, K. Woo Ahn, Y. Wang and J. P. Kelly (2013). "Incidence, clinical course, and predictors of prolonged recovery time following sport-related concussion in high school and college athletes." J Int Neuropsychol Soc **19**(1): 22-33.
McCrea, M., T. Hammeke, G. Olsen, P. Leo and K. Guskiewicz (2004). "Unreported concussion in high school football players: implications for prevention." Clin J Sport Med **14**(1): 13-17.
McCrory, P., W. Meeuwisse, M. Aubry, B. Cantu, J. Dvorak, R. Echemendia, L. Engebretsen, K. Johnston, J. Kutcher, M. Raftery, A. Sills, B. Benson, G. Davis, R. Ellenbogen, K. Guskiewicz, S. A. Herring, G. Iverson, B. Jordan, J. Kissick, M. McCrea, A. McIntosh, D. Maddocks, M. Makdissi, L. Purcell, M. Putukian, K. Schneider, C. Tator and M. Turner (2013). "Consensus statement on Concussion in Sport--the 4th International Conference on Concussion in Sport held in Zurich, November 2012." J Sci Med Sport **16**(3): 178-189.
McCuen, E., D. Svaldi, K. Breedlove, N. Kraz, B. Cummiskey, E. L. Breedlove, J. Traver, K. F. Desmond, R. E. Hannemann, E. Zanath, A. Guerra, L. Leverenz, T. M. Talavage and E. A. Nauman (2015). "Collegiate women's soccer players suffer greater cumulative head impacts than their high school counterparts." J Biomech **43**(1873-2380 (Electronic)): 3720-3723.
McIntosh, A., P. McCrory and C. F. Finch (2004). "Performance enhanced headgear: a scientific approach to the development of protective headgear." Br J Sports Med **38**(1): 46-49.
McIntosh, A. S. and P. McCrory (2000). "Impact energy attenuation performance of football headgear." Br J Sports Med **34**(5): 337-341.

McKinlay, A., R. C. Grace, L. J. Horwood, D. M. Fergusson, E. M. Ridder and M. R. MacFarlane (2008). "Prevalence of traumatic brain injury among children, adolescents and young adults: prospective evidence from a birth cohort." Brain Inj **22**(2): 175-181.
Mertz, H. J. and L. M. Patrick (1971). Strength and Response of the Human Neck. SAE Technical Paper Series, SAE International.
Moore, I. S., C. Ranson and P. Mathema (2015). "Injury Risk in International Rugby Union: Three-Year Injury Surveillance of the Welsh National Team." Orthop J Sports Med **3**(7): 2325967115596194.
Namjoshi, D. R., C. Good, W. H. Cheng, W. Panenka, D. Richards, P. A. Cripton and C. L. Wellington (2013). "Towards clinical management of traumatic brain injury: a review of models and mechanisms from a biomechanical perspective." Dis Model Mech **6**(6): 1325-1338.
Nevins, D., L. Smith and J. Kensrud (2015). "Laboratory Evaluation of Wireless Head Impact Sensor." Procedia Engineering **112**: 175-179.
Newman, J. A. (1986). A generalized acceleration model for brain injury threshold (GAMBIT).
Newman, J. A., N. Shewchenko and E. Welbourne (2000). "A proposed new biomechanical head injury assessment function - the maximum power index." Stapp Car Crash J **44**(1532-8546 (Print)): 215-247.
NOCSAE (2017). Standard Performance Specification for Newly Manufactured Football Helmets. Impact Attenuation Tests.
Nordstrom, A., P. Nordstrom and J. Ekstrand (2014). "Sports-related concussion increases the risk of subsequent injury by about 50% in elite male football players." Br J Sports Med **48**(19): 1447-1450.
Npro. (2020). "Npro." from https://n-pro.com.au/.
NZSSSC (2017) "Representation Census."
O'Connor, K. L., S. Rowson, S. M. Duma and S. P. Broglio (2017). "Head-Impact-Measurement Devices: A Systematic Review." J Athl Train **52**(3): 206-227.
Ornstein, S. (2019). Cervical Strain Is A Common General Diagnosis That Can Be Related To Different Factors. Neck Solutions.
P McLellan, C. (2013). "Performance Analysis of Super 15 Rugby Match-Play Using Portable Micro-Technology." J Ath Enhanc **02**(05): 1-6.
Padgaonkar, A. J., K. W. Krieger and A. I. King (1975). "Measurement of Angular Acceleration of a Rigid Body Using Linear Accelerometers." Journal of Applied Mechanics **42**(3): 552-556.
Pettersen, J. A. (2002). "Does rugby headgear prevent concussion? Attitudes of Canadian players and coaches." Br J Sports Med **36**(1): 19-22.
Phillips, N. and J. J. Crisco (2020). "The Effectiveness of Regulations and Behavioral Interventions on Head Impacts and Concussions in Youth, High-School, and Collegiate Football: A Systematized Review." Ann Biomed Eng **48**(11): 2508-2530.
Porter, M. and M. O'Brien (1996). "Incidence and severity of injuries resulting from amateur boxing in Ireland." Clin J Sport Med **6**(2): 97-101.
Powell, J. W. and K. D. Barber-Foss (1999). "Traumatic brain injury in high school athletes." JAMA **282**(10): 958-963.
Press, J. N. and S. Rowson (2017). "Quantifying Head Impact Exposure in Collegiate Women's Soccer." Clin J Sport Med **27**(2): 104-110.
Ransohoff, J. (1970). "Impact Injury and Crash Protection." Archives of Neurology **23**(2): 188-189.
Rishiraj, N., R. Lloyd-Smith, T. Lorenz, B. Niven and M. Michel (2009). "University men's ice hockey: rates and risk of injuries over 6-years." J Sports Med Phys Fitness **49**(2): 159-166.
Rolf Eppinger, Emily Sun, Faris Bandak, Mark Haffner, Nopporn Khaewpong and M. Maltese (1998). "Development of Improved Injury Criteria for the Assessment of Advanced Automotive Restraint Systems - II." NHTSA.
Rowson, S., S. M. Duma, J. G. Beckwith, J. J. Chu, R. M. Greenwald, J. J. Crisco, P. G. Brolinson, A. C. Duhaime, T. W. McAllister and A. C. Maerlender (2012). "Rotational head kinematics in football impacts: an injury risk function for concussion." Ann Biomed Eng **40**(1): 1-13.

Rugby, W. (2014). Handbook. Specifications Relating to Players' Dress Law 4 - Players Clothing, World Rugby. **4**.
Rugby, W. (2017) "Global Rugby Participation."
Rugby, W. (2019). Headgear performance specification. 6. W. Rugby, World rugby. **6.3**.
Rugby, W. (2019). "World rugby law 4 headgear assessment trial." from https://playerwelfare.worldrugby.org/content/getfile.php?h=3a2d78ccb4e008771c7c5c75dd31e86d&p=pdfs/reg-22/Law-4-Headgear-Trial-Explanation_EN.pdf.
Sabesan, V., Z. Steffes, D. J. Lombardo, G. R. Petersen-Fitts and T. R. Jildeh (2016). "Epidemiology and location of rugby injuries treated in US emergency departments from 2004 to 2013." Open Access J Sports Med **7**(1179-1543 (Print)): 135-142.
Sanchez, G. M. and A. L. Burridge (2007). "Decision making in head injury management in the Edwin Smith Papyrus." Neurosurg Focus **23**(1): E5.
Schick, D. M. and W. H. Meeuwisse (2003). "Injury rates and profiles in female ice hockey players." Am J Sports Med **31**(1): 47-52.
Schick, D. M., M. G. Molloy and J. P. Wiley (2008). "Injuries during the 2006 Women's Rugby World Cup." Br J Sports Med **42**(6): 447-451.
Schulz, M. R., S. W. Marshall, F. O. Mueller, J. Yang, N. L. Weaver, W. D. Kalsbeek and J. M. Bowling (2004). "Incidence and risk factors for concussion in high school athletes, North Carolina, 1996-1999." Am J Epidemiol **160**(10): 937-944.
Schussler, E., D. Stark, J. H. Bolte, Y. S. Kang and J. A. Onate (2017). "Comparison of a Head Mounted Impact Measurement Device to the Hybrid Iii Anthropomorphic Testing Device in a Controlled Laboratory Setting." Int J Sports Phys Ther **12**(4): 592-600.
Scurlock, J. A. and B. Andersen (2005). Diagnoses in Assyrian and Babylonian medicine: ancient sources, translations, and modern medical analyses, University of Illinois Press.
Shrey, D. W., G. S. Griesbach and C. C. Giza (2011). "The pathophysiology of concussions in youth." Phys Med Rehabil Clin N Am **22**(4): 577-602, vii.
Shugar, T. A. and M. G. Katona (1975). "Development of finite element head injury model." Journal of the Engineering Mechanics Division **101**(3): 223-239.
Siegmund, G. P., K. M. Guskiewicz, S. W. Marshall, A. L. DeMarco and S. J. Bonin (2016). "Laboratory Validation of Two Wearable Sensor Systems for Measuring Head Impact Severity in Football Players." Ann Biomed Eng **44**(4): 1257-1274.
Siegmund, G. P., D. J. King, J. M. Lawrence, J. B. Wheeler, J. R. Brault and T. A. Smith (1997). "Head/neck kinematic response of human subjects in low-speed rear-end collisions." SAE transactions: 3877-3905.
Silver, D., N. Brown and C. Gissane (2018). "Reported concussion incidence in youth community Rugby Union and parental assessment of post head injury cognitive recovery using the King-Devick test." J Neurol Sci **388**: 40-46.
Skull, n. (2019). "Soft Shell Helmet." 2019, from https://2ndskull.com/products/2nd-skull-rugby-style-headgear.
Sosin, D. M., J. E. Sniezek and D. J. Thurman (1996). "Incidence of mild and moderate brain injury in the United States, 1991." Brain Inj **10**(1): 47-54.
Spiotta, A. M., J. H. Shin, A. J. Bartsch and E. C. Benzel (2011). "Subconcussive impact in sports: a new era of awareness." World Neurosurg **75**(2): 175-178.
sport, F. (2019). "What is the history of scrum caps?", from https://firepowersport.com/history-of-scrum-caps/.
Thunnissen, J., J. Wismans, C. L. Ewing and D. J. Thomas (1995). Human Volunteer Head-Neck Response in Frontal Flexion: A New Analysis. SAE Technical Paper Series, SAE International.
Tyson, A. M., S. M. Duma and S. Rowson (2018). "Laboratory Evaluation of Low-Cost Wearable Sensors for Measuring Head Impacts in Sports." J Appl Biomech **34**(4): 320-326.
Van den Kroonenberg, A., M. Philippens, H. Cappon, J. Wismans, W. Hell and K. Langwieder (1998). "Human head-neck response during low-speed rear end impacts." SAE transactions: 2836-2851.

Versace, J. (1971). A Review of the Severity Index. SAE Technical Paper Series, SAE International.
Walsh, E. S., M. Kendall, A. Post, A. Meehan and T. B. Hoshizaki (2018). "Comparative analysis of Hybrid III neckform and an unbiased neckform." Sports Engineering **21**(4): 479-485.
Ward, C., M. Chan and A. Nahum (1980). Intracranial Pressure–A Brain Injury Criterion. SAE Technical Paper Series, SAE International.
Williams, R. M., T. W. Puetz, C. C. Giza and S. P. Broglio (2015). "Concussion recovery time among high school and collegiate athletes: a systematic review and meta-analysis." Sports Med **45**(6): 893-903.
Willigenburg, N. W., J. R. Borchers, R. Quincy, C. C. Kaeding and T. E. Hewett (2016). "Comparison of Injuries in American Collegiate Football and Club Rugby: A Prospective Cohort Study." Am J Sports Med **44**(3): 753-760.
Wismans, J., M. Philippens, E. van Oorschot, D. Kallieris and R. Mattern (1987). Comparison of Human Volunteer and Cadaver Head-Neck Response in Frontal Flexion. SAE Technical Paper Series, SAE International.
Wismans, J., H. van Oorschot and H. J. Woltring (1986). Omni-Directional Human Head-Neck Response. SAE Technical Paper Series, SAE International.
Wu, L. C., V. Nangia, K. Bui, B. Hammoor, M. Kurt, F. Hernandez, C. Kuo and D. B. Camarillo (2016). "In Vivo Evaluation of Wearable Head Impact Sensors." Ann Biomed Eng **44**(4): 1234-1245.
Zazryn, T. R., C. F. Finch and P. McCrory (2003). "A 16 year study of injuries to professional boxers in the state of Victoria, Australia." Br J Sports Med **37**(4): 321-324.
Zazryn, T. R., C. F. Finch and P. McCrory (2003). "A 16 year study of injuries to professional kickboxers in the state of Victoria, Australia." Br J Sports Med **37**(5): 448-451.
Zhang, L., K. H. Yang, R. Dwarampudi, K. Omori, T. Li, K. Chang, W. N. Hardy, T. B. Khalil and A. I. King (2001). Recent advances in brain injury research: a new human head model development and validation, SAE Technical Paper.
Zhou, C., T. Khalil and A. King (1995). A 3D human finite element head for impact injury analyses. Symposium proc. of prevention through biomechanics.
Zuckerman, S. L., Y. M. Lee, M. J. Odom, G. S. Solomon, J. A. Forbes and A. K. Sills (2012). "Recovery from sports-related concussion: Days to return to neurocognitive baseline in adolescents versus young adults." Surg Neurol Int **3**: 130.